9-22-2020

Epoxy-functional thermoplastic copolymers and their incorporation into thermosetting resins

Kayla Rose Sweet
Rowan University

EPOXY-FUNCTIONAL THERMOPLASTIC COPOLYMERS AND THEIR INCORPORATION INTO THERMOSETTING RESINS

by
Kayla Rose Sweet

A Thesis

Submitted to the
Department of Chemical Engineering
Henry M. Rowan College of Engineering
In partial fulfillment of the requirements
For the degree of
Master of Science in Chemical Engineering
at
Rowan University
September 11, 2020

Thesis Chair: Joseph F. Stanzione, III, Ph.D.

Dedication

For my parents

Acknowledgements

I would like to recognize and thank my advisor, Dr. Joseph F. Stanzione, III for his support and guidance. His support began in my undergraduate degree, and through working in his laboratory I found my love for chemistry and chemical engineering. Without his continual encouragement and mentorship, I would not have been able to foresee this path for myself. I have him to thank for this work.

Thank you to all of my colleagues in the laboratory for your support, whether I needed your expertise or your emotional support. I would particularly like to thank Alexander Bassett, Ph.D. for teaching me along every stage of the journey, including being my mentor throughout my undergraduate degree. I would also like to thank the group that helped begin this work, Amy Honnig, Claire Breyta, and Julia Reilly, for showing me what a great team could accomplish. Thank you to Silvio Curia, Ph.D. for acting as both a colleague and professor of mine. And a big thank you to my cohort Alexandra Chong, Maggie Gillian, Kelli Hambleton, John Chea, Tristan Bacha, and Jasmin Vasquez for making the work in and out of the classroom more enjoyable daily. I could not have asked for a more positive environment in which to complete this work.

Thank you to the support from the Rowan University Chemical Engineering and Chemistry Departments and to my committee. I would like to acknowledge express gratitude to the U.S. Army CCDC-ARL for their support via Cooperative Agreements W911NF 14-2-0086 and W911NF 16-2-0225.

Lastly, I would like to thank my entire family for guiding and supporting me throughout my life. Mom, Dad, Eliza, and Ray, thank you for being my emotional support system throughout this process. You have made this all possible.

Abstract

Kayla R. Sweet
EPOXY-FUNCTIONAL THERMOPLASTIC COPOLYMERS AND THEIR INCORPORATION INTO THERMOSETTING RESINS
2019-2020
Joseph F. Stanzione, III, Ph.D.
Master of Science in Chemical Engineering

While polymers have secured a place in the consumer, industrial, and military markets over the last seventy years, the next generation of polymers must become more renewable, more adaptive, and higher performing to bridge industrial needs and environmental gaps. To this end, unique network configurations of copolymers and interpenetrating polymer networks (IPNs) have been employed to combine features of two or more polymers into a single material that surpasses the sum of its parts. The customization of polymer networks can be made possible via dual-functional monomers, molecules characterized by two different reactive substituents that allow for versatile methods of polymerization. This thesis expands the applications of such materials by investigating bio-based, aromatic, dual-functional monomers, vanillyl alcohol epoxy-methacrylate (VAEM) and gastrodigenin epoxy-methacrylate (GDEM), as alternatives to glycidyl methacrylate (GMA) in thermoplastic copolymers with methyl methacrylate (MMA). Additionally, low molecular weight epoxy-functional thermoplastic copolymers poly(VAEM-co-MMA) and poly(GMA-co-MMA) were prepared via reversible addition-fragmentation chain transfer (RAFT) polymerization, blended at 5 wt% into an epoxy resin system containing EPON® Resin 828 and EPIKURE™ W Curing Agent, and cured thermally. The resulting IPNs were compared to the neat resin and evaluated for thermal and mechanical properties, where maintained thermal properties and marginal enhancements of stiffness and toughness were demonstrated.

Table of Contents

Table of Contents (Continued)

Table of Contents (Continued)

List of Figures

List of Figures (Continued)

Figure Page

List of Tables

Chapter 1

Introduction

Text and figures are reproduced and adapted with permission from A. W. Bassett, K. R. Sweet, R. M. O'Dea, A. E. Honnig, C. M. Breyta, J. H. Reilly, J. J. La Scala, T. H. Epps, III, and J. F. Stanzione, III, reference [1].

1.1 Overview

Over the past seventy years, synthetic polymers have gone from a novelty material to one of the most common products in our homes today, jumping from a global annual production of 2 Mt in 1950 to 380 Mt in 2015 [2]. While polymers surpass other materials in chemical and electrical resistance, ease of use, and economic advantages, researchers are still looking for ways to improve properties. This includes pushing the current materials to become more renewable, more adaptive, and higher performing, as well as creating new polymers to bridge the gaps in the existing market [3]. Currently, many researchers are taking advantage of unique network configurations, such as copolymers and interpenetrating polymer networks (IPNs), to combine the best features of two or more polymers into a single material. The resulting polymers are making advances in the biomedical, automotive, aerospace, computer, and additive manufacturing industries as well as for military applications. This work seeks to expand the applications of known polymeric materials by investigating and characterizing bio-based, aromatic, epoxy-functional monomers as an alternative to glycidyl methacrylate (GMA) in thermoplastic copolymers. Additionally, this work focuses on blending the resulting copolymers into epoxy resin formulations to create thermosetting IPNs for

maintained or enhanced thermal properties and significantly increased mechanical properties.

The following chapter provides an overview of the species and concepts used within this work, beginning with dual-functional, epoxy-methacrylate monomers and bio-based, aromatic, epoxy-methacrylate monomers. There is a description of thermoplastic polymers and the importance and background of reversible addition-fragmentation chain transfer (RAFT) polymerization, an overview of thermosetting epoxy resins, and a description of common types of IPNs and their uses as they relate to this work. Finally, a brief summary of the remainder of this thesis is provided.

1.2 Dual-Functional, Epoxy-Methacrylate Monomers

Dual-functional monomers are characterized by two different reactive substituents that allow for multiple and versatile methods of chemical modification and/or monomer polymerization, permitting customization of linear polymers and polymer networks [4]. Creating a monomer with both epoxy and methacrylate functionality facilitates unique polymer network formation via reactive sites for covalent bonding or inter-connected, interpenetrating polymer network formation [5]. Currently, glycidyl methacrylate (GMA) is the main commercially available, dual-functional monomer with both epoxy and methacrylate functionalities. Multi-functional vinyl ester monomers can be prepared via the reaction of a polyepoxide with less than stoichiometric amount of methacrylic acid; however, this approach does not follow the same structural motif as GMA and yields relatively large molecules with high viscosities that make processing difficult [6].

Kim et al. have presented a dual-functional monomer with both epoxy and methacrylate functionalities for holographic recording from 2-(oxiranylmethoxy)ethyl 2-

methyl-2-propenoate [7]. This dual-functional monomer was efficient for holographic recording with high photosensitivity and low shrinkage for unique optical properties [7]. However, synthesized monomers that include both epoxy and methacrylate functional groups are uncommon despite their appeal.

Additionally, epoxy-functional thermoplastic polymers are highly desired for their tunable properties for consumer plastic goods, coatings, and adhesives [8, 9]. GMA has been homopolymerized and copolymerized with many other (meth)acrylate monomers to produce polymers with pendant oxirane rings [10]. These pendant groups enable further modifications through various chemistries, including ring-opening reactions with nucleophiles, and facilitating the robust attachment of films to surfaces [11]. Poly(glycyidyl methacrylate), poly(GMA), is known for biocompatibility and versatility as previous research has found utility for poly(GMA) and its copolymers in gene delivery, polymer scaffolds, and self-healing materials [12, 13]. Poly(GMA) has additional uses in industrial and consumer settings including automotive coatings, protective finishes, adhesives, and electrical laminates. While GMA and poly(GMA) have been well researched, GMA has no commercial complements with similar functionality which could broaden and diversify the applications of epoxy-functional materials [9].

1.3 Bio-Based, Aromatic, Epoxy-Methacrylate Monomers

Vanillyl alcohol (VA), a lignin-based aromatic diol and product of lignin depolymerization, and gastrodigenin (GD), a bio-based aromatic diol found in the Chinese *Gastrodia elata* Blume herb and *Coelogossum* orchid, are suitable platform chemicals for the preparation of unique, aromatic GMA complements [14-19]. While

these compounds have been previously investigated for thermosetting resins, their use as dual-functional monomers has only recently been explored [1, 16, 20, 21]. The natural asymmetry and differences in reactivity of the aromatic and aliphatic hydroxyls enable the facile, selective synthesis of dual-functional, epoxy-methacrylate monomers [1].

VA and GD bear aromatic and aliphatic hydroxyls, with the aromatic hydroxyl being more acidic and more reactive towards epichlorohydrin [16, 20]. Previous studies preparing diglycidyl ethers of VA and GD have reported moderate to low yields of monoglycidyl ethers as byproducts due to this slight difference in acidity [16, 20]. Intentional synthesis of monoglycidyl ethers of these compounds as intermediate building blocks for other modifications can be prepared as well [1, 20]. The monoepoxidized intermediate can be produced as the major product, in which the aliphatic hydroxyl is unreacted. The unreacted aliphatic hydroxyl can then be esterified with methacryloyl chloride to prepare the dual-functional monomers vanillyl alcohol epoxy-methacrylate (VAEM) and gastrodigenin epoxy-methacrylate (GDEM). Excess triethylamine is utilized in the synthesis to ensure the rapid trapping of hydrochloric acid that is formed during the reaction, thus preventing epoxy ring opening [1]. The dual-functional monomers used within this study are VAEM, GDEM, and the commercially available GMA, shown in Figure 1.

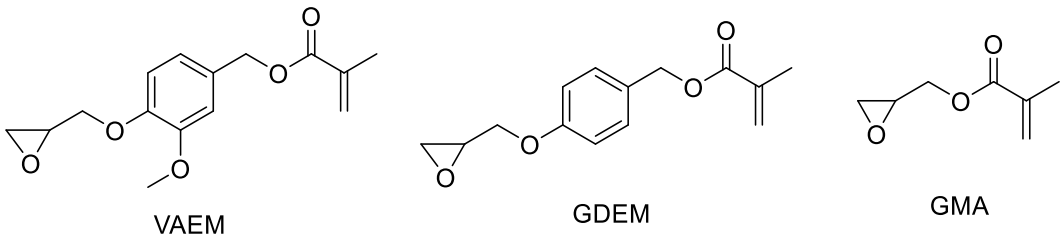

Figure 1. Chemical structures of aromatic, dual-functional monomers used in this study.

These bio-based monomers have been shown to exhibit substantially higher thermal stabilities and comparable surface energies when polymerized via solution polymerization relative to the structurally similar poly(GMA), leading to potential for use in high temperature applications including coatings and adhesives [1]. Additionally, VAEM and GDEM are solids at room temperature, potentially increasing storage stability and reducing volatility relative to GMA [1].

1.4 Thermoplastic Polymers and RAFT Polymerization

Thermoplastic polymers are one of the most widely used class of materials globally, largely due to their ease of use and processability. Among plastics, thermoplastics make up approximately 80% of the total market shares [22]. Structurally, thermoplastics consist of linear chains of monomers chemically bound together. The lack of crosslinking between chains allows thermoplastics to be softened or melted when heated and reformed into a variety of shapes which are maintained when cooled. The uses for thermoplastic polymers range from commodity goods, such as polystyrene (Styrofoam) cups and polyethylene plastic bags, to targeted uses in medical and high-tech applications [22].

Thermoplastic polymers have a widespread range of thermomechanical properties, which are dependent on chemical structure, processing, and molecular weight. Thermoplastics are often mixed with additives that stabilize, plasticize, color, or reinforce the polymer, all of which can impact the polymer properties. This allows thermoplastics to be used as coatings and paints, rigid containers, clothing, automotive parts, electrical components, and insulations, among many other applications. Like all polymers, thermoplastics have environmental constraints that need to be addressed, including potential toxicity and pollution. Due to their inherent ability to be heated and reformed into different shapes, thermoplastics can be recycled; however, when different types or grades of thermoplastics are mixed during recycling, the material properties are altered. Additionally, thermoplastic polymers are traditionally formed from petroleum based monomers and often use toxic reactants and initiators such as formaldehyde, heavy metals, halogens, and excess solvents. In an effort to create more sustainable, safer polymers and polymer processes, thermoplastics have been formed from renewable resources including vegetable oil, starches, sugars, (hemi)cellulose and lignin [22].

While thermoplastics gained wide adoption in consumer goods during the mid and late twentieth century, researchers have also sought to enhance the capabilities of thermoplastic polymers for engineered applications. One method for creating advanced materials, reversible addition-fragmentation chain transfer (RAFT) polymerization, was discovered in 1998 by researchers at CSIRO Molecular Science and greatly expanded the versatility of controlled free-radical polymerization [23-26]. RAFT polymerization is one type of reversible-deactivation or “living” radical polymerizations (RDRP), which rely on an equilibrium between active and dormant chains to control the polymerization [27].

RDRP includes most notably nitroxide mediated polymerization (NMP), atom transfer radical polymerization (ATRP), and RAFT polymerization [26, 27]. During RDRP, the active sites continue to propagate until all of the monomer is consumed, and if additional monomer is added the chains will continue to grow [28]. Ideally, in a living polymerization all polymer chains are initiated rapidly with respect to propagation, yielding a very narrow molecular weight distribution that can be altered by changing reaction conditions [28, 29]. A typical molecular weight distribution of RDRP is shown in Figure 2 [29].

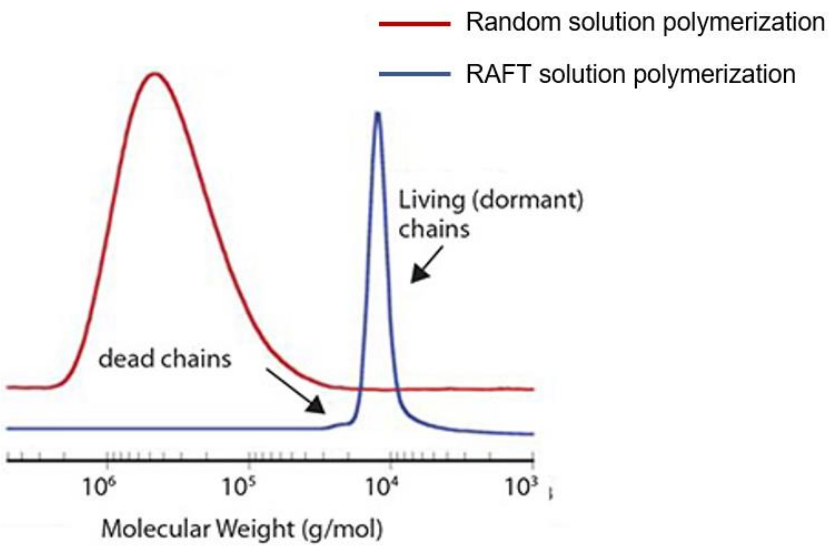

Figure 2. Molecular weight distributions of a conventional and a RAFT polymerization of styrene.

The theoretical number average molecular weight (M_n) for RAFT polymerization is given by Equation 1 [27]. The initial monomer, chain transfer agent (CTA), and initiator concentrations are given by $[M]_0$, $[CTA]_0$, and $[I]_0$, respectively. The monomer conversion is given by p, the initiator efficiency is given by f, k_d is the decomposition rate

of the initiator, f_c is the coupling factor, and M_M and M_{CTA} are the molar masses of monomer and chain transfer agent, respectively. Equation 1 can be simplified to the more commonly used Equation 2 when the k_d is assumed to be 0 [27].

$$M_{n,th} = \frac{[M]_0 p M_M}{[CTA]_0 + 2f[I]_0(1 - e^{-k_d t})\left(1 - \frac{f_c}{2}\right)} + M_{CTA} \quad (1)$$

$$M_{n,th} = \frac{[M]_0 p M_M}{[CTA]_0} + M_{CTA} \quad (2)$$

Unlike other RDPR reactions, RAFT operates through the use of degenerative chain transfer [24, 25, 27]. There is no change in the overall number of radicals in the reaction process without an addition of a radical source, typically an initiator [24, 27]. RAFT polymerizations include all the steps of a typical radical polymerization (initiation, propagation, and termination), with the addition of a CTA that allows for the equilibrium between active and dormant chains [27, 28]. The RAFT mechanism is depicted in Figure 3, adapted from references [24, 27, 28]. The propagating radical is given as $P_n\bullet$ and $P_m\bullet$ is a secondary propagating radical. The process begins with addition (I), followed by the initiation of a monomer (II), then the addition of the radical species to the RAFT agent or CTA where an equilibrium between active and dormant species is established (steps III and V). The final step results in radical termination (VI). It should be noted that bimolecular termination can still occur although it is not shown in the mechanism [28].

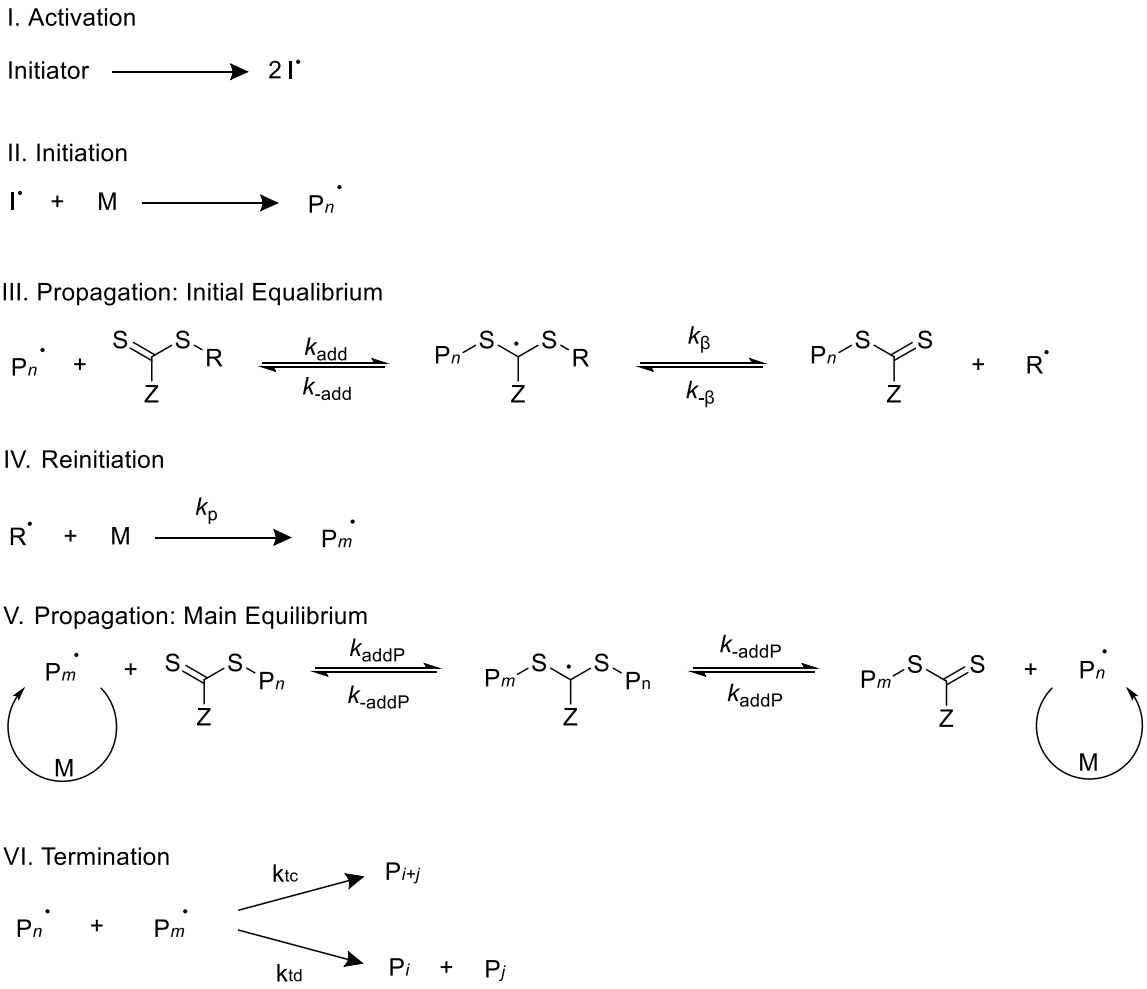

Figure 3. Proposed mechanism for RAFT polymerization.

While the mechanism of RAFT presented is widely accepted, the kinetics of the reaction are not fully understood [28, 30, 31]. As long as the RAFT equilibria are sufficiently fast, they have no direct effect on the rate of polymerization [28, 31]. However, there are potential causes of retardation in RAFT that manifest as an initially slow rate of polymerization [28, 31]. This can be the case if the "R" group is a poor initiator (step IV), poor choice of initiator, impurities in the CTA or solution, and/or ineffective degassing [31]. Other theories suggest that the highly stable intermediate adduct radicals in steps III and V slow down the reaction sufficiently enough to cause

retardation or undergo bimolecular radical coupling, leading to termination and a subsequent reduction in the rate of polymerization [28, 30-32].

The selection of an appropriate CTA is key to the RAFT polymerization process [25, 28]. The reactivity of the Z and R groups affect the efficiency of the chain transfer and the likelihood of retardation [25]. The R group is chosen to be a good leaving group with respect to the propagating radical P_n• and must also be able to reinitiate polymerization efficiently, whereas the Z group modifies the rate of addition of P_n• [25]. General guidelines for selecting the appropriate Z and R groups based on the monomer class are available. The monomers are considered either "more activated" monomers (MAMs) or "less activated" monomers (LAMs). MAMs include monomers where the double bond is conjugated next to an aromatic ring (e.g. styrene, vinylpyridine), a carbonyl group (e.g. methyl methacrylate, methyl acrylate, acrylamide), or a nitrile (e.g. acrylonitrile) [25]. LAMs include monomers with a double bond adjacent to a saturated carbon (e.g. diallyldimethylammoniom chloride), an oxygen or nitrogen lone pair (e.g. vinyl acetate, N-vinylpyrrolidone), or a heteroatom of a heteroaromatic ring (e.g. N-vinylcarbazole) [25].

The basic structure of the major classes of RAFT agents are shown in Figure 4 [29]. Dithioesters and trithiocarbonates with a carbon or sulfur adjacent to the thiocarbonylthio group are the most reactive RAFT agents, whereas RAFT agents with a lone pair on a nitrogen or oxygen adjacent to the thiocarbonyl group have much lower reactivity [3]. Dithiobenzoates are prone to hydrolysis and may cause retardation when used in high concentrations, whereas trithiocarbonates are more hydrolytically stable than dithiobenzoates and cause less retardation [29]. Both dithiobenzoates and

trithiocarbonates are used with MAM polymerizations and actively inhibit LAM polymerizations [29]. Dithiocarbamates have variable activity and are effective with electron-rich LAMs [29]. Xanthates have the lowest transfer constants, but can be more effective with LAMs [29].

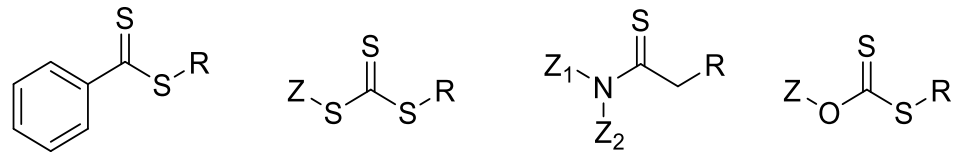

Figure 4. Common RAFT agent classes.

Due to the nature of RAFT polymerization, the thiocarbonylthio group of the CTA remains as an end group on the polymer chains. These end groups impart a pink (dithiobenzoates) or a yellow (trithiocarbonates, xanthates, and dithiocarbamates) color onto the final polymers [27]. Thiocarbonylthio groups can also impact the thermal and chemical stability of the polymers [27]. Thiocarbonylthio groups can be exploited as a functional group itself or can be reduced down to a thiol [27]. When the thiocarbonylthio group is left on the polymer chain, a polymer is a so-called "macroRAFT agent" that can be extended or used to create block copolymers by adding additional monomer [27]. If removal of the thiocarbonylthio is needed, thermolysis or radical-induced transformation can be used [27].

RAFT polymerization is currently utilized at over 100 companies and features in over 1,000 patents in applications including microelectronics, lubricants, paints,

adhesives, cosmetics, polymer therapeutics, and biosensors. The ability to produce a narrow distribution of molecular weight allows for more homogenous properties within and between reactions [27]. Because it is a simple modification of free radical polymerization, it is easily adoptable into existing production setups, and RAFT agents are commercially available in large quantities [27, 29]. RAFT polymerization is a useful tool that both the industrial and academic communities are employing to create unique and impactful materials.

1.5 Thermosetting Epoxy Resins

Epoxy resins fall under the broader group of polymers known as thermosetting resins, or thermosets, which include all cross-linking polymers. The crosslinks of thermosets form a network of covalent bonds, which upon formation prevent melting. Thermosets are typically amorphous and can possess high tensile strengths and modulus, high thermal resistances, and long-term stabilities. Epoxy resins are characterized by their oxirane rings, which are reacted with a curing agent to form thermosetting resins [33].

Oxirane rings are highly reactive and may react with nucleophilic or electrophilic reagents. This versatility allows for a wide range of curing agents including amines, phenols, carboxylic acids, thiols, and anhydrides, among others. Depending on the desired applications, the curing agent can be chosen to modify mechanical, chemical, and thermal properties of the resulting polymer network. Primary and secondary amines are among the most popular curing agents due to their ability to impart elevated temperature performance, chemical resistance, and long pot life [33].

The diverse range of properties of epoxy resin systems allow for their use in high performance applications in the military and commercial manufacturing sectors.

Traditionally, the resin systems are cured thermally; however, their ability to cure via ultra-violet (UV) and visible light allows for their use in additive manufacturing (AM), or 3D printing [34, 35]. While adopted widely by hobbyists from its beginnings, recent work has sought to utilize the ability of additive manufacturing (AM) to rapidly print complex, material-efficient parts in higher-performance spaces [36]. Epoxy resins exhibit low shrinkage and can produce highly accurate geometries, factors that have led to their wide adoption in AM resin formulations [34]. The relative newness of the AM field has left much to explore, including formulating epoxy resins that can provide the balance of properties needed for the expansion of AM into high performance industries.

One challenge of epoxy resins is that although they are characterized by their thermal and chemical resistance, advantageous thermomechanical properties, and adhesion abilities, epoxy resins are often also brittle after cure [33, 37]. Toughening agents such as liquid rubbers, rubber particles, and thermoplastic polymers have been blended into epoxy resins, however this can also affect other characteristics such as thermomechanical properties [33, 37, 38]. Recent advances have used hyperbranched polymers, nanotubes, and block copolymers in an attempt to toughen epoxy resins. Despite these efforts, there still exists a need for modifiers that provide a balance of toughening effects without significantly impacting the advantageous properties inherent to epoxy resins [39, 40].

1.6 Interpenetrating Polymer Networks (IPNs)

Interpenetrating polymer networks (IPNs) are a combination of two or more polymers in network formation that are synthesized in the presence of the other. Often IPNs provide a combination of the characteristics inherent to the polymers within the

system, allowing for tunable thermal and mechanical properties based on the desired application [41]. The history of IPNs begins in 1914 when researcher J. W. Aylsworth toughened phenol formaldehyde with natural rubber to produce a material for phonograph records. There were a few more patents on IPNs in the following decades, but the term interpenetrating polymer network only began to be used in 1960 when John Millar coined the term in reference to his work with styrene IPNs. In recent decades, IPNs have been employed in a growing number of industries including the biomedical, electrical, and automotive sectors [41]. Due to the variety of compositions of IPNs, the applications extend from sound and vibration dampening to artificial teeth and ion-exchange resins [42].

IPNs are distinguished from one another based on the mechanism of network formation, leading to a multitude of subsets. Some of the most common IPNs include sequential IPNs, simultaneous interpenetrating networks (SINs), thermoplastic IPNs, and semi-IPNs [41]. In sequential IPNs, one polymer is formed and then swollen or mixed with a second polymer and its respective crosslinker and activator. The second polymer is cured in situ, forming a second network in the material. SINs are prepared by mixing two or more polymers with their crosslinkers and activators and curing the entire system via noninterfering reactions. Thermoplastic IPNs utilize physical entanglement of two or more polymers, usually made by blending polymer chains. Semi-IPNs are polymer networks in which one or more crosslinked polymer is interspersed with a linear or branched polymer [41].

Grafted IPNs are another type of IPN where the two polymer networks are also connected to one another at graft sites. Grafting is to be expected in most IPNs, but

typically is neglected if the number of crosslinks greatly exceeds the number of graft sites and the morphology is relatively unaffected by the graft sites. However, some researchers induce grafting through manipulation of side reactions between the networks during cure, post-polymerization modifications, condensation reactions between the networks, or introduction of a monomer reactive with both networks. Grafted IPNs resemble AB-crosslinked polymers (ABCP), in which polymer I is grafted to polymer II at either end or polymer I and polymer II are formed across one another to create tetrafunctional graft linkages. Both grafted IPNs and ABCPs can form similar topological morphologies. A representation of an IPN, a semi-IPN, and an ABCP can be found in Figure 5 [43].

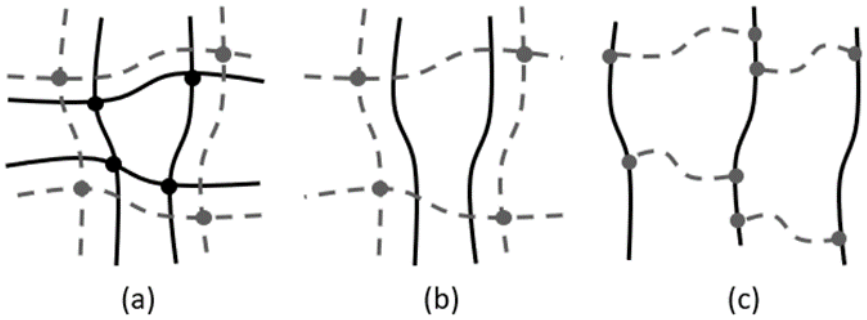

Figure 5. Common crosslinked two-polymer systems, where (a) represents an IPN, (b) represents a semi-IPN, and (c) represents an AB-crosslinked copolymer.

One of the major intrigues of IPNs is their compelling morphology differences. IPNs have the ability to form single or multiphase regions within a material. The phase domain size is dependent on the length of the chains between crosslinks, where short links usually result in small domains and large links usually result in large domains. This corresponds to the overall miscibility of the system, where small domains generally

decrease the miscibility of the system and large domains increase the miscibility of the system [5]. For the multiphase systems, each phase will exhibit its own glass transition, which may be broadened or moved towards each other depending on the crosslinks. Phase morphology can be observed under electron microscopy, and phase diagrams have been developed for several IPNs [41]. The presence of multiphase systems in IPNs can provide toughening effects and impact resistance, which can change depending on the size and shapes of the domains [43].

IPNs have been formed using many different systems, however epoxy systems are a common choice for the crosslinking portion of many IPNs for the reasons explored earlier in section 1.5. Researchers have explored the combination of epoxy thermosets, varying crosslinkers, and thermoplastic polymers of many types to form specialized semi-IPNs and grafted IPNs [44]. Popular epoxy resins for these studies include diglycidyl ether of bisphenol A (DGEBA), tetraglycidyl diamino diphenyl methane (TGDDM), and triglycidyl *p*-aminophenol (TGAP) with a wide range of amine crosslinkers and thermoplastics [44].

Several research groups have used the polymerization induced phase separation (PIPS) inherent to many thermoset-thermoplastic blends to form complex shapes such as nano-scale tubes, spheres, and particles [40, 45, 46]. Luo et al. made thermoset-thermoplastic blends that exhibit thermal self-mending and adhesion properties [13]. Other researchers have investigated the influence of multiblock copolymers and thermoplastic chain length on epoxy systems, results of which vary widely based on the monomers used [38, 44, 47-49]. GMA has been used as an end group on thermoplastic chains to utilize the oxirane group to create grafted IPNs in epoxy systems [50]. Each of

these studies prioritized specific properties of the final IPN, but thermoplastics are typically considered a toughening agent for epoxy resins [44]. Although the topic has been explored by many groups, the complexity and range of IPNs and the ever-present need for epoxy resin modifications leaves room for further studies on the impact of thermoplastic polymers on thermosetting resins.

1.7 Summary

This work investigates the influence of the copolymers of the dual-functional, epoxy-methacrylates GMA, VAEM and GDEM with methyl methacrylate (MMA) and the impact of their structural differences on thermoplastic polymers and thermosetting resin formulations, building upon the work and concepts discussed in Chapter 1. The thesis hypothesizes that epoxy-functional thermoplastic copolymers can be synthesized and incorporated into polymer networks for maintained or enhanced thermal properties and significantly increased mechanical toughness. Chapter 2 explores the analytical techniques and instrumental methods used within this work. Chapter 3 delves into the materials and experimental methods used to create and characterize the polymers in this work. A discussion of the results including the thermal, mechanical, and analytical properties of the synthesized polymers are presented in Chapter 4. Chapter 5 gives conclusions and recommendations for future work beyond this thesis.

Chapter 2

Characterization Methods

2.1 Introduction

This chapter serves as a brief introduction to the fundamental characterization techniques used within this body of work. The sections include information on nuclear magnetic resonance (NMR) spectroscopy, size exclusion chromatography (SEC), thermogravimetric analysis (TGA), differential scanning calorimetry (DSC), Fourier transform infrared spectroscopy (FT-IR), dynamic mechanical analysis (DMA), and fracture toughness. The general concepts, theories, and history for each method are discussed within their respective sections. The descriptions of instrumentation and their uses are to serve as a background to their importance and uses in the field of polymers, materials science, and engineering, in general. Experimental methods specific to this work are explored in subsequent chapters for each technique.

2.2 Nuclear Magnetic Resonance (NMR) Spectroscopy

Nuclear magnetic resonance (NMR) spectroscopy was first introduced in 1946 by the independent work of physicists researching resonance at Stanford University and Harvard University [51]. Two of the researchers, Bloch and Purcell, later won the Nobel Prize in Physics in 1952 for the significance of the technology [51]. NMR spectroscopy utilizes measured changes in the magnetic resonance of atomic nuclei to indicate proximity to other magnetic nuclei, electronegative atoms, and double bonds [51, 52]. The structure of organic molecules can be determined through the interpretation of the magnetic resonance information. Chemists realized the importance of this technology and by 1953 the first 60 MHz NMR instrument was released on the market [51, 52]. With the

integration of superconducting magnets and liquid helium cooling systems in the 1970s, NMR instruments rapidly improved for greater resolution [51, 52]. Currently, NMR instruments use a frequency of 60-1020 MHz, which provides for varying resolution [52, 53]. The tool has become one of the most powerful techniques for analyzing chemical structures used by chemists, physicists, biochemists, and engineers [52]. The technique is also the basis of Magnetic Resonance Imaging (MRI), which is used by medical professionals for disease detection and diagnosis [52, 54].

Several types of nucleus, including ^{13}C, ^{19}F, ^{31}P, and ^{1}H, spin in a manner that creates a magnetic dipole along the axis of rotation [51, 52]. The spinning nuclei are each assigned spin quantum numbers, *I*, indicating the possible spin orientations. For example, ^{1}H has $I = 1/2$, signifying there are two possible spin orientations [52]. As a result of the change in atomic mass, different isotopes of the same element have different quantum numbers. The quantum numbers can be calculated based on the mass and atomic numbers of the element. In the case of elements with both even mass numbers and even atomic numbers, such as ${}^{12}_{6}C$, ${}^{16}_{8}O$, and ${}^{34}_{16}S$, $I = 0$ and consequently, these elements are inactive in NMR spectroscopy [52]. Elements with odd mass numbers with odd atomic numbers (${}^{1}_{1}H$, ${}^{19}_{9}F$) or odd mass numbers with even atomic numbers (${}^{13}_{6}C$, ${}^{17}_{8}O$) have quantum numbers that are odd multiples of $\frac{1}{2}$, such as $I = \frac{1}{2}, \frac{3}{2}, \frac{5}{2}, \frac{7}{2}$, etc. [52]. Elements with even mass numbers and odd atomic numbers have quantum numbers that are integers, $I = 1, 2, 3, 4$, etc. For the purposes of this work only ^{1}H will be considered, which has $I = \frac{1}{2}$ [52]. For ^{1}H the quantum number of 1/2 means the magnetic quantum number (*m*) values are

$m_1 = +\frac{1}{2}$ and $m_2 = -\frac{1}{2}$ and there are only two possible energy states for the nucleus in the presence of a static, homogeneous magnetic field [52, 55].

An NMR instrument exposes a sample to a homogeneous magnetic field, wherein the ^{1}H nuclei in a sample have two possible orientations, parallel or antiparallel to the field [52]. The parallel spin state is slightly lower in energy. To "flip" the spin to the antiparallel state, more energy is supplied by the NMR spectrometer by electromagnetic radiation [52, 55]. If the energy applied is adequate, the nucleus is excited to the higher energy state [52]. The nucleus is said to *resonate* with the applied radiation, which is where *nuclear magnetic resonance* gets its name [52]. In general, the spin quantum numbers *I* of the nuclei determine the number of energy states expressed in a magnetic field [52].

Each nuclei in the molecule resonates at a different frequency when analyzed via NMR due to the surrounding bonds and atoms in the molecule [52]. The magnetic field required to align the nuclei of a given molecule also affects the electrons within the molecule [52]. The electrons generate their own magnetic field surrounding the nucleus, opposing the external magnetic field and causing a perceived reduction of strength [52]. This phenomenon is called shielding, and is the foundation for differentiating similar molecular groups on the basis of their surroundings [52]. NMR spectra present the differences as chemical shifts (δ) in parts per million (ppm) [52]. As no two magnets produce the same magnetic field, a reference material is typically used. The most common reference material is tetramethylsilane (TMS) as it is clearly distinguishable from most other resonances, is cost effective, and is chemically inert [52]. Typically, a sample is prepared in a deuterated solvent due to deuterium resonances appearing outside

the range of proton resonances [52]. While most commercially available solvents are not 100% deuterated, the protons that show up within the measured spectra can be used as a reference chemical shift [52]. For the purposes of this work deuterated chloroform ($CDCl_3$, $\delta_{1H} = 7.27$) was used. ^{1}H-NMR spectroscopy was used to identify chemical species and determine mole ratios of random copolymers within this work. This is discussed further in Chapter 3.

2.3 Size Exclusion Chromatography (SEC)

Size exclusion chromatography (SEC) is the most common method for obtaining a molar mass distribution for synthetic and naturally occurring polymers [56]. Although number average (M_n), weight average (M_w), and z average (M_z) molar mass relationships were known before 1960, the first characterization method to determine molar mass distribution in a single experiment was only established in 1964 [56]. John Moore of Dow Chemical Company first published his work on gel permeation chromatography (GPC), a method of SEC that built on previous work by Porath and Flodin on gel filtration chromatography (GFC) [56, 57]. While GFC is only applicable for water-soluble materials, GPC expanded the possibilities of SEC to organic solvents by using a crosslinked gel, in the case of Moore, styrene/divinylbenzene based gel [56, 57]. This allowed researchers to easily obtain molecular weight distributions and dispersities (ratio of M_w to M_n; $Đ$) for a wide range of polymers. Modern SEC is able to detect a wide range of molecular weights from monomers to ultrahigh molecular mass polymers and can be used to distinguish complex polymer blends [56].

SEC utilizes packed columns of inert gel or porous material such as modified polystyrene or glass beads to determine molar mass distribution based on elution time

through the column [56]. A stream of pure solvent is continuously fed to the column. When a sample made of diluted polymer in solution is injected into the stream the polymer begins to diffuse through the column [56]. Due to their volume, the larger polymer chains can not enter into as many pores as the smaller polymer chains [56]. This allows the larger chains to pass over a portion of the pores and travel faster through the column [56]. After exiting the column, the solvent stream is passed through a concentration-sensitive detector such as a differential refractometer [56]. Molar mass distributions are found by comparing the elution time and concentration of the sample to a calibration curve made from standards of known molar masses and $Đ$s [56]. SEC was used within this work to determine M_n, M_w, and $Đ$ for each synthesized thermoplastic polymer.

2.4 Thermogravimetric Analysis (TGA)

Thermogravimetric analysis (TGA) measures the mass of a sample as a function of time and/or temperature [58]. TGA instruments can be used to observe phenomena including decomposition, phase changes, and chemical reactions [58]. A small sample, approximately 10 mg, is loaded onto a pan made of platinum or ceramic [58]. The pan is then placed within a furnace equipped with a high resolution thermobalance that measures and records the mass of the sample continuously [58]. The atmosphere of the furnace influences the rate of change in the mass of the sample. Therefore, TGA instruments often have a purge gas consisting of inert gas such as nitrogen, helium, or argon as well as an oxidative environment such as air [58].

TGA was used in this study primarily as a means to measure degradation. Mass of the sample was plotted against temperature. The initial decomposition temperature (IDT)

was taken as the temperature at 5% mass loss of the sample ($T_{5\%}$). The temperature at the maximum rate of degradation (T_{max}) was taken as the peak of the second-order transition curve. The temperature at 50% mass loss ($T_{50\%}$) and the char content, taken as the final mass of the sample at the temperature at the end of the experiment, typically 700 °C, were also measured.

2.5 Differential Scanning Calorimetry (DSC)

Differential Scanning Calorimetry (DSC) is a widely used thermal analysis technique that is used to determine the amount of heat absorbed or emitted over a thermal transition [28, 59]. DSC is used for identifying a wide range of polymer properties including melting point (T_m), glass transition temperature (T_g), degree of crystallinity, and polymerization [28, 59]. Typically, heat flow in W g^{-1} is plotted as a function of temperature. Thermal properties can be observed as first-order or second order transitions.

The two major types of DSC instruments include power compensation DSC and heat flux DSC [28, 59]. Both methods compare about 5-10 mg of sample to a reference material, typically air. The sample and the reference are placed within aluminum pans [59]. In power compensation DSC the two pans are put into two separate furnaces equipped with a thermocouple and a power source [58, 59]. The two pans are kept at the same temperature by compensating the power supplied to each furnace [58, 59]. If the sample absorbs or releases heat, as is the case during a reaction, the heat flux is proportional to the power necessary to maintain equal temperature in each chamber [58, 59]. In the case of heat flux DSC, the two pans are placed within a single furnace equipped with two points of temperature measurement located on a thermally conductive

plate [58]. If the heat flux into the sample and the reference are equal, the temperature difference between the two points remains constant [58]. A heat flux DSC was used within this study. This is discussed further in Chapter 3.

2.6 Fourier Transform-Infrared Spectroscopy (FT-IR)

Fourier transform-infrared spectroscopy (FT-IR) is a type of vibrational spectroscopy based on the interaction of electromagnetic radiation and a material. Due to its high sensitivity, rapid speed of data collection, non-destructive nature, and extensive range of applications, FT-IR is a widely used characterization technique [60]. It has been used in both industry and research applications for routine measurements, quality control, and dynamic measurements. In the polymer industry, FT-IR is valuable for measuring degrees of polymerization [61].

The basis for infrared (IR) spectrometry is the Michelson interferometer, which directs a collimated beam of light towards a beam splitter. Of the two resulting beams, one travels without interruption and the second is varied by a movable mirror. The beams are recombined at the beam splitter, where approximately half of the light returns to the source and the other half travels through a sample and into the detector. The signal measured by the detector is then related to its spectrum through its Fourier transform [62].

IR spectroscopy is divided into far IR at 400-10 cm^{-1}, mid IR at 4,000-400 cm^{-1}, and near IR at 14,000-4,000 cm^{-1}, which can be used to detect rotational, rotational-vibrational, and harmonic vibrational motions, respectively [61]. Functional groups present within a sample can be observed by passing radiation in the form of light through a sample at a specified wavelength and measuring the fraction of energy that is absorbed

by the sample. The radiation provided causes a bond between two molecules to stretch, bend, or rotate. The resulting spectra are highly characteristic for each substance, serving as an identifiable "fingerprint" [60]. In this work, near-IR is used with a CaF_2 beam splitter to determine the extent of cure of the synthesized thermosetting polymers.

2.7 Dynamic Mechanical Analysis (DMA)

Dynamic mechanical analysis (DMA) is a technique for measuring the viscoelastic properties of a material by applying an oscillatory force or deformation to a sample and assessing the response of the sample [63]. DMA instruments effectively measure the ability of a material to store and/or dissipate energy, which correlates to properties such as hardness, strength, yield point, and impact [64]. For a perfectly elastic material, the applied force and the sample displacement have a phase angle or lag, δ, of 0º and for a purely viscous material, δ would be 90º. Most materials are viscoelastic and have a δ between 0º and 90º, which can be divided into the storage, or elastic, moduli (E') and loss, or viscous, moduli (E'') [63, 65].

Some early DMA instruments were only able to measure the ratio of the loss modulus to the storage modulus, or the tan δ [65]. Tan δ is calculated directly from the δ and is the measure of the internal friction of the material [63]. Additionally, DMA tests can study T_g, relaxation temperatures, cure or vitrification behavior, stress-relaxation behavior, and creep recovery behavior can be determined [65]. The properties of interest can be studied in a range of geometries, including tension, compression, shear, three point bend, dual cantilever, and single cantilever [65]. For the purposes of this work, single cantilever geometry was used to determine E', E'', and tan δ as a function of

temperature and the effective molecular weight between crosslinks (M_c). This is discussed further in Chapter 3.

2.8 Fracture Toughness

Fracture toughness is a mechanical test method that is used to characterize the critical strain energy release rate (G_{Ic}) and plane-strain fracture toughness (K_{Ic}). G_{Ic} represents the energy required to fracture a material and K_{Ic} represents the resistance of a material to fracture. For plastics, plane strain fracture toughness is used with either single-edge-notch bend (SENB) or compact tension (CT) geometries. SENB requires a beam shaped sample to be center-notched, cracked and loaded in a three-point bend manner pre-test, and a CT consists of a single-edge notched plate loaded in tension. Specific dimensions and test procedures are outlined in ASTM D5045-14 [66]. For this work, SENB geometry was used.

For polymers and other materials, fracture toughness can be an important parameter to measure, however, sample preparation is highly variable. The ASTM D5045-14 standard specifies the notch must be machined, then a natural crack must be generated by tapping a razor blade or a razor blade can be slid or sawn across the notch [66, 67]. Within this body of work, notches were machined on a diamond edged saw and cracks were created by sawing a single edged razor blade across the notch according to the ASTM D5045-14. The specific methods are discussed further in Chapter 3.

Chapter 3

Experimental Materials and Methods

Text and figures are reproduced and adapted with permission from A. W. Bassett, K. R. Sweet, R. M. O'Dea, A. E. Honnig, C. M. Breyta, J. H. Reilly, J. J. La Scala, T. H. Epps, III, and J. F. Stanzione, III, reference [1].

3.1 Introduction

The materials, methods, and procedures used within this body of work are detailed in the following chapter. The syntheses of random solution copolymers, random reversible addition-fragmentation chain transfer (RAFT) solution polymerized copolymers, and thermosetting resins are detailed. The characterization techniques utilized for each polymer are detailed.

3.2 Materials

Epichlorohydrin (99 %), gastrodigenin (4-hydroxybenzyl alcohol, 97 %), dichloromethane (DCM, 99.6 %), glycidyl methacrylate (oxiran-2-ylmethyl 2-methylprop-2-enoate, 97%), vanillyl alcohol (4-hydroxy-3-methoxybenzyl alcohol, 99 %), chloroform-d_3 ($CDCl_3$, 99.8 atom % D_3), and anisole (99 %) were purchased from Acros Organics. Ethyl acetate (99.9 %), hexanes (99.9 %), methanol (99.8 %), tetrahydrofuran (Optima™ THF, 99.9 %) and triethylamine (TEA, 99 %) were purchased from Fisher Scientific. Methacryloyl chloride (97 %), chloroform (99.8 %), and methyl methacrylate (MMA, 99 %) were purchased from Alfa Aesar. *N*,*N*-Dimethylformamide (DMF, 99.8 %), benzyltriethylammonium chloride (TEBAC, 99 %), poly(glycidyl methacrylate) (poly(GMA)) (M_n = 10,000-20,000 Da), 2-cyano-2-propyl benzodithioate (97 %), and methyl methacrylate (MMA, 99 %) were purchased from Sigma Aldrich.

2,2'-Azobis(2-methylpropinitrile) (AIBN, 95 %) was purchased from AstaTech. Compressed nitrogen (N_2, 99.998 %), and compressed argon (Ar, 99.999 %) were purchased from Airgas. Sodium hydroxide was purchased from VWR. 4,4′-Isopropylidenediphenol-epichlorohydrin copolymer (EPON828™, 100 %) and diethylmethlbenzenediame (EPIKURE W™, 100%) were purchased from HEXION. Vanillyl alcohol epoxy-methacrylate (VAEM) and gastrodigenin epoxy-methacrylate (GDEM) were synthesized using the procedures available in Bassett et al. with similar results [1]. All chemicals mentioned above were used without further purification.

3.3 Random Solution Polymerization

3.3.1 Solution homopolymerizations. VAEM (0.2513 g) was mixed with 1 wt% of AIBN and 3.32 mL DMF per gram of monomer. The solution was sparged with argon for approximately 10 minutes, after which the reaction vessel was sealed, and the solution was heated to 60 ºC while stirring. After 24 hours, the solution was precipitated in excess methanol. The resulting product, poly(VAEM), was then dissolved in DCM and re-precipitated in hexanes to remove any residual reactants and initiator. The procedure was repeated for GDEM to form poly(GDEM) and for MMA to form poly(MMA). A representative reaction scheme for the syntheses of the homopolymers can be seen in Figure 6.

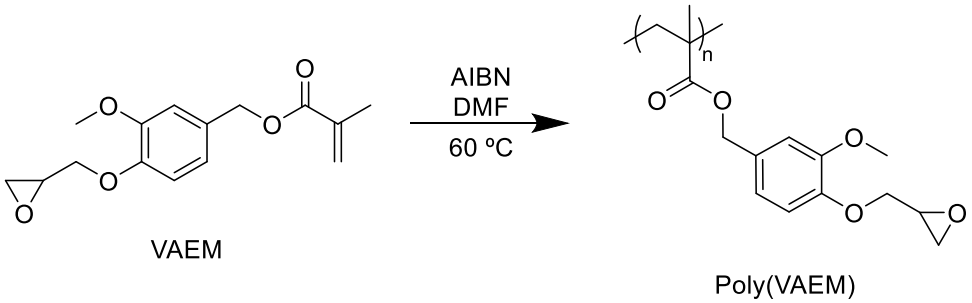

Figure 6. Representative reaction scheme for synthesis of homopolymers; solution polymerization of VAEM to prepare poly(VAEM).

3.3.2 Solution copolymerizations. A mixture of VAEM (0.274 g, 0.986 mmol) and MMA (0.230 g, 2.30 mmol) was added to a round bottom flask with AIBN (5.0 mg, 0.030 mmol) and DMF (1.67 mL, 22.8 mmol). The solution was sparged with argon for approximately 10 minutes, after which the reaction vessel was sealed, and the solution was heated to 60 ºC while stirring. After 24 hours, the solution was precipitated in excess methanol. The resulting product was then dissolved in DCM and re-precipitated in hexanes to remove any residual reactants and initiator. The resulting copolymer will be designated by its mole ratio as determined by ^{1}H-NMR spectroscopy, 31-69 poly(VAEM-co-MMA). A representative reaction scheme for the synthesis of the copolymers can be seen in Figure 7.

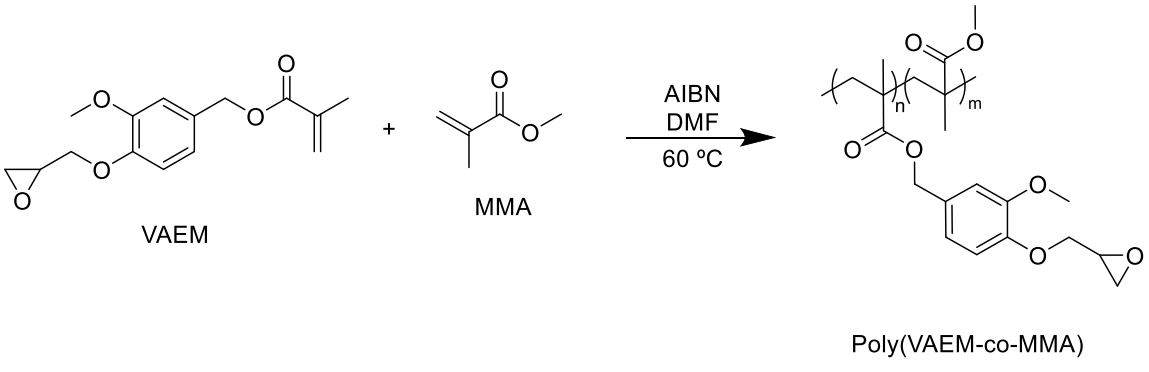

Figure 7. Representative reaction scheme for synthesis of random copolymers; solution polymerization of VAEM and MMA to prepare poly(VAEM-co-MMA).

The procedure was repeated to produce copolymers with varying monomer ratios of approximately 30, 50, and 70 mol % epoxy monomer to 70, 50, and 30 mol % MMA, respectively. The exact reactant amounts for each reaction are given in Table 1. Each reaction was completed with a total monomer to AIBN weight ratio of 100:1 and 3.32 mL DMF per gram of monomer.

Table 1

Copolymer reactant amounts used in this study

Copolymer	**Epoxy-functional Monomer Amount**		**MMA Monomer Amount**		**AIBN Amount**		**DMF Amount**	
(mol ratio)	(g)	(mmol)	(g)	(mmol)	(mg)	(mmol)	(mL)	(mmol)
53-47 poly(VAEM-co-MMA)	0.402	1.45	0.150	1.50	5.5	0.033	1.83	25.0
72-28 poly(VAEM-co-MMA)	0.502	1.80	0.090	0.90	5.9	0.036	1.83	26.9
30-70 poly(GDEM-co-MMA)	0.305	1.23	0.296	2.98	6.0	0.037	2.00	27.4
52-48 poly(GDEM-co-MMA)	0.592	2.38	0.247	2.47	8.4	0.051	2.79	38.1
70-30 poly(GDEM-co-MMA)	0.515	2.07	0.089	0.890	6.0	0.037	2.00	27.4
31-69 poly(GMA-co-MMA)	0.504	3.55	0.828	8.27	13.3	0.081	4.42	60.5
49-51 poly(GMA-co-MMA)	0.862	6.06	0.617	6.16	14.8	0.090	4.91	67.1
68-32 poly(GMA-co-MMA)	1.01	7.10	0.311	3.11	13.2	0.080	4.38	59.9

3.4 RAFT Polymerization

A mixture of 5 mol % GMA monomer and 95 mol % MMA monomer was added to a round bottom flask with a 1 mol % ratio of 2-cyano-2-propyl benzodithioate CTA, a 0.1 mol % ratio of AIBN, and a 5 mol % ratio of anisole per gram of monomer. The solution was sparged with argon for approximately 10 minutes, after which the reaction vessel was sealed, and the solution was heated to 72 ºC while stirring. After 3 hours, the solution was precipitated in excess hexanes. The resulting product, poly(GMA-co-MMA), was then dissolved in chloroform and re-precipitated in hexanes to remove any residual reactants and initiator. A representative reaction scheme for the RAFT polymerization of the GMA with MMA can be seen in Figure 8.

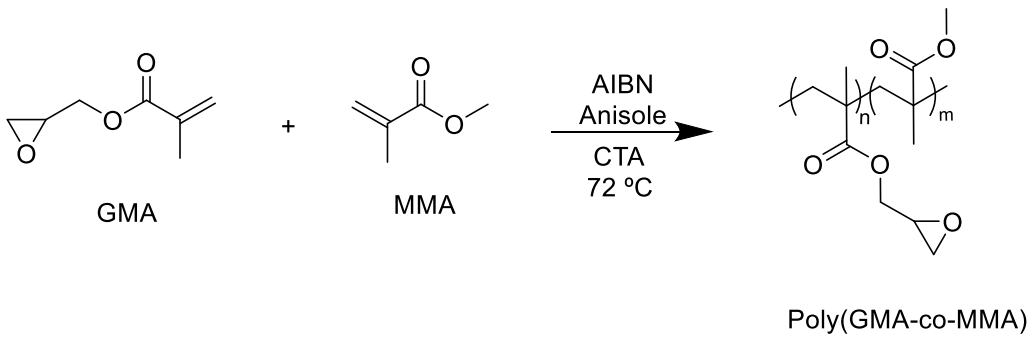

Figure 8. Reaction scheme for copolymerization of GMA and MMA.

A mixture of 5 mol % VAEM monomer and 95 mol % MMA monomer was added to a round bottom flask with a 1 mol % ratio of 2-cyano-2-propyl benzodithioate CTA, a 0.1 mol % ratio of AIBN, and an equimolar ratio of anisole per gram of monomer. The solution was sparged with argon for approximately 10 minutes, after which the reaction vessel was sealed, and the solution was heated to 72 ºC while stirring. After 3 hours, the solution was precipitated in excess hexanes. The resulting product,

poly(VAEM-co-MMA), was then dissolved in chloroform and re-precipitated in hexanes to remove any residual reactants and initiator. A representative reaction scheme for the RAFT polymerization of VAEM with MMA can be seen in Figure 9.

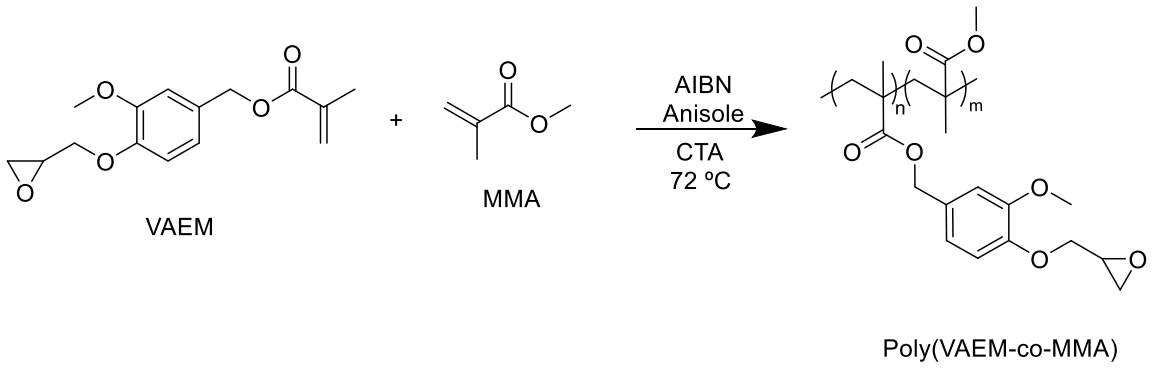

Figure 9. Reaction scheme for copolymerization of VAEM and MMA.

3.5 Characterization of Thermoplastic Polymers

All thermoplastic polymers synthesized in this work were characterized by ^{1}H-NMR spectroscopy on a Bruker 400 MHz NMR instrument (400.15 MHz, 32 scans at 298 K, relaxation delay of 1 s). The copolymer mole ratios (with respect to the total monomer reacted) were determined through the use of characteristic chemical shift peaks within each molecule and the use of Equation 3. The characteristic peaks were located at approximately 3.6 ppm, 3.25 ppm, 3.8 ppm, and 4.9 ppm for MMA, GMA, VAEM, and GDEM, respectively.

$$Mole\ Ratio\ MMA = \frac{\left(\frac{Integration}{Number\ of\ H}\right)_{MMA\ peak\ ref}}{\left(\frac{Integration}{Number\ of\ H}\right)_{MMA\ peak\ ref} + \left(\frac{Integration}{Number\ of\ H}\right)_{Comonomer\ peak\ ref}} \quad (3)$$

The number-average molecular weight (M_n), weight-average molecular weight (M_w), and dispersity ($Đ$) were obtained on a Waters Acquity Advanced Polymer Chromatography (APC) instrument with THF as the eluent (0.6 mL min^{-1}), using polystyrene standards with M_n of 537,000 Da (Đ = 1.03), 59,300 Da (Đ = 1.05), and 8,650 Da (Đ = 1.03) as a reference.

The glass transition temperatures (T_g)s of the thermoplastic polymers were measured using a TA Instruments Discovery DSC 2500. A Tzero aluminium pan was loaded with 3-6 mg of sample and sealed with a Tzero lid. Three heating and cooling cycles were performed at a rate of 10 °C min^{-1} under continuous N_2 flow (50 mL min^{-1}) with a temperature ramp range of 0-150 °C. The second and third cycles had no significant changes for all samples. The T_g was determined as the midpoint of the inflection in the second heating cycle. Three replicates of each thermoplastic were prepared and tested using this procedure.

The thermal degradation properties of the thermoplastics including initial decomposition temperature (IDT), temperature at 50% weight loss ($T_{50\%}$), temperature at maximum degradation rate (T_{max}), and char content were characterized using a TA Instruments Discovery TGA 550. A powdered sample of 4–6 mg of each polymer was loaded into a platinum pan and heated a rate of 10 ºC min^{-1} to 700 ºC in either a N_2 or air atmosphere (40 mL min^{-1} balance gas flow rate and 25 mL min^{-1} sample gas flow rate). Each polymer was run in triplicate for oxidative (air) and inert (N_2) environments.

The epoxy equivalent weights (EEWs) of the epoxy thermoplastic samples used within interpenetrating polymer networks (IPNs) were determined using ^{1}H-NMR

spectroscopy and Equation 4. In Equation 4, *E* represents the weight percent epoxide, which was determined through ^{1}H-NMR spectroscopy [16].

$$EEW = 43 \times \frac{100}{E} \tag{4}$$

3.6 Resin Formulation and Cure

Each epoxy-functional thermoplastic was individually blended in a Thinky mixer for approximately 20 min with the commercially available epoxy resin EPON828 and EPIKURE W, an amine crosslinker. The structures of EPON828 and EPIKURE W are shown in Figure 10.

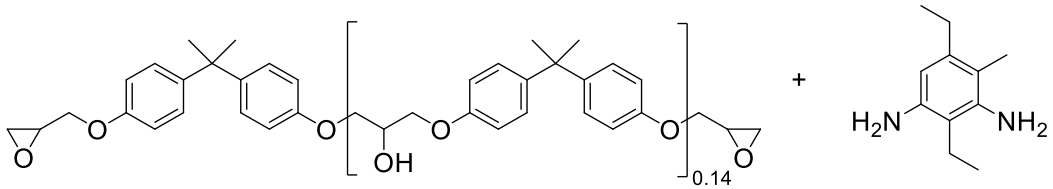

Diglycidyl ether of bisphenol A (EPON828) Diethyl toluene diamine (EPIKURE W)

Figure 10. Chemical structures of EPON828 and EPIKURE W.

The epoxy-functional thermoplastic and the EPON828 resin were loaded in a 5:95 weight ratio. The EEW of the blended resin was calculated using Equation 5, where W_{E1} and W_{E2} are the weights of the epoxies 1 and 2, respectively, and EEW_1 and EEW_2 are the epoxy equivalent weights of epoxies 1 and 2, respectively.

$$EEW_{Blend} = \frac{W_{Total}}{\frac{W_{E_1}}{EEW_{E_1}} + \frac{W_{E_2}}{EEW_{E_2}}} \tag{5}$$

A stoichiometric addition of EPIKURE W was added to the epoxy mixture by using the system parts of amine per hundred parts epoxy resin (phr) as shown in Equation 6 where AHEW (amine hydrogen equivalent weight) represents the amine hydrogen equivalent weight [68]. The AHEW of EPIKURE W is 44.57 g/eq.

$$phr = \frac{AHEW \times 100}{EEW_{Blend}} \quad (6)$$

The blended resins were poured into molds and cured at 90 ºC for 4 h and postcured at 180 ºC for 2 h. The cured resins were allowed to slowly cool to room temperature overnight. The cured resins were dark yellow to brown in color.

3.7 Resin Characterization

The T_gs of the cured resins were measured using a TA Instruments Discovery DSC 2500. A Tzero aluminium pan was loaded with 3-6 mg of sample and sealed with a Tzero lid. Three heating and cooling cycles were performed at a rate of 10 °C min^{-1} under continuous N_2 flow (50 mL min^{-1}) with a temperature ramp range of 0-250 °C. The second and third cycles had no significant changes for all samples. The T_g was determined as the midpoint of the inflection in the second heating cycle. Three replicates of each cured resin were prepared and tested using this procedure.

The thermal degradation properties of the cured resins including IDT, $T_{50\%}$, T_{max}, and char content were characterized using a TA Instruments Discovery TGA 550. A sample of 4–6 mg of each polymer was loaded into a platinum pan and heated a rate of 10 ºC min^{-1} to 700 ºC in either a N_2 or air atmosphere (40 mL min^{-1} balance gas flow rate and 25 mL min^{-1} sample gas flow rate). Each cured resin was run in triplicate for oxidative (air) and inert (N_2) environments.

Density was determined through the use of Archimedes' Principle, shown in Equation 7 [69]. A precision scale was equipped with a density kit. The dry and immersed weights were measured of each sample. Deionized water was used as the immersion liquid. Four replicates of each cured resin were prepared and tested using this procedure.

$$\frac{solid\ density}{liquid\ density} = \frac{solid\ weight, dry}{solid\ weight, dry - solid\ weight, immersed} \quad (7)$$

To determine the extents of cure of the cured resins, a Thermo Scientific Nicolet iS50 FT-IR was used. For each spectrum, 64 scans were collected in the near-IR range of 4000-8000 cm^{-1} at room temperature with 8 cm^{-1} resolution. The resulting peaks were quantified to determine the extents of cure, or the amount of oxirane and amine groups that were reacted to form the cured polymer networks. The peaks corresponding to the oxirane functional groups are visible at approximately 4530 cm^{-1}. The primary amine functionality is visible around 5000 cm^{-1} and both primary and secondary amines are visible around 6500 cm^{-1}. Hydroxyl groups formed during the reaction can be seen as a broad peak at 7000 cm^{-1}. The reference peak is visible at 5900 cm^{-1} and is not affected by the polymerization. The amine functionality was used to determine the extent of cure of the epoxy–amine network [70]. The equation used to quantify extent of cure is given by Equation 8. A typical pre- and post-cure FT-IR spectrum is shown in Figure 11.

$$X(amine) = \frac{\left(\frac{Abs_{4530\ cm^{-1}\ or\ 6500\ cm^{-1}}}{Abs_{ref}}\right)_{precure} - \left(\frac{Abs_{4530\ cm^{-1}\ or\ 6500\ cm^{-1}}}{Abs_{ref}}\right)_{postcure}}{\left(\frac{Abs_{4530\ cm^{-1}\ or\ 6500\ cm^{-1}}}{Abs_{ref}}\right)_{precure}} \quad (8)$$

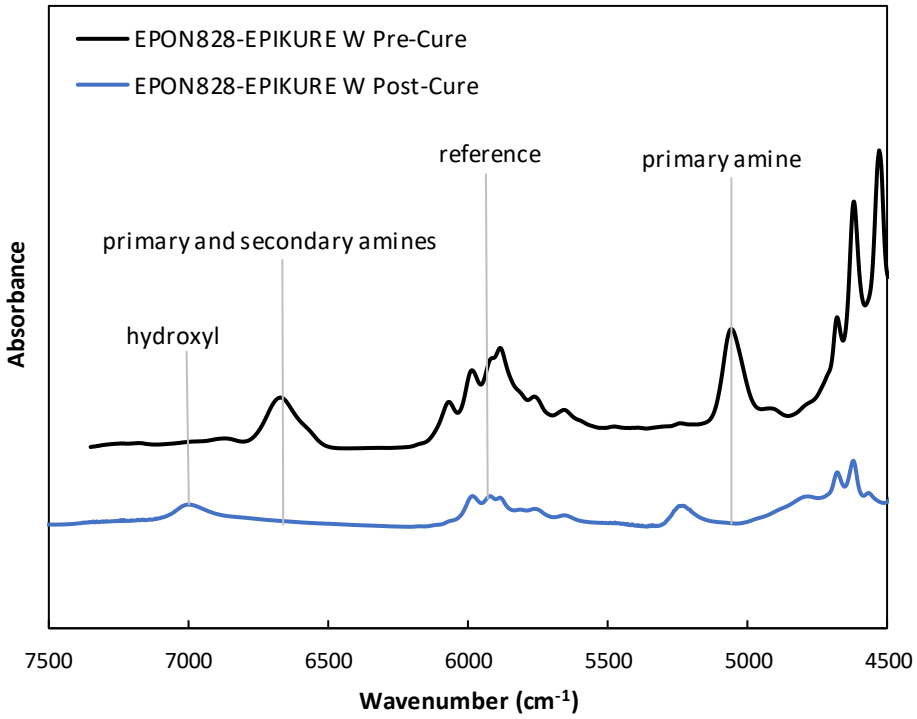

Figure 11. Representative near-IR spectrum of epoxy and amine thermosetting resin system, shown before and after cure. Vertically offset for clarity.

The viscoelastic properties of the cured resins were measured using a TA Instruments Q800 DMA. Each sample was prepared with appropriate dimensions (35 × 12 × 2.5 mm^3) and tested using a single cantilever geometry in accordance with McAninch et al. [65]. The tests were performed at a frequency of 1.0 Hz, oscillatory deflection amplitude of 7.5 μm, and a Poisson's ratio of 0.35. The heating ramp rate was 2 °C min^{-1} from 0 to 250 °C. Four replicates of each cured resin were prepared and tested using this procedure.

Fracture toughness was tested to compare the cured thermoplastic loaded epoxy-amine resins and the commercially available cured epoxy-amine resins. Three-point single edge notched bend (SENB) samples of all cured resins were prepared in

accordance with ASTM- D5045-14 at room temperature. Samples were prepared to be 44 × 10 × 4 mm^3 to ensure plane-strain. Using a diamond saw, samples were notched and then scored by sawing a single edged razor blade across the notch to generate a crack. Samples were then tested on an Instron 5966 with a 1 kN load cell and a 3-point bend flexure fixture at a cross head speed of 10 mm min^{-1}. The plane-strain fracture toughness, K_{1C}, and the critical strain energy release rate, G_{1C}, were determined upon fracture [66]. A minimum of five replicates of each cured resin were prepared and tested using this procedure.

Chapter 4

Results and Discussion

Text and figures are reproduced and adapted with permission from A. W. Bassett, K. R. Sweet, R. M. O'Dea, A. E. Honnig, C. M. Breyta, J. H. Reilly, J. J. La Scala, T. H. Epps, III, and J. F. Stanzione, III, reference [1].

4.1 Introduction

The major goal of this work was to explore the utility of the bio-based, aromatic, epoxy-functional monomers vanillyl alcohol epoxy-methacrylate (VAEM) and gastrodigenin epoxy-methacrylate (GDEM) in various polymer configurations. The only analogous commercially available epoxy-methacrylate monomer, glycidyl methacrylate (GMA), is most often copolymerized to impart tunable properties to polymeric materials. For this reason, this work began with polymerizing GMA, VAEM, GDEM and characterizing their copolymers. With the intent to use epoxy-functional thermoplastics as resin modifiers, the copolymers in this work were created with varying amounts of methyl methacrylate (MMA), a widely available and common methacrylate monomer with desirable properties. Poly(MMA) forms a homogeneous solution with the epoxy resin diglycidyl ether of bisphenol A (DGEBA) and does not react in any post-polymerization modifications of the oxirane group present on the epoxy-methacrylate monomers [49, 71, 72]. Additionally, poly(MMA) has been used to toughen epoxy resin systems [38]. The properties of poly(MMA) make MMA a beneficial comonomer for use in the epoxy-functional thermoplastic copolymers and as a resin modifier. The resulting synthesized thermoplastics were characterized via ^{1}H-NMR spectroscopy and SEC. The

effects of varying amounts of bio-based, aromatic, epoxy-functional monomers, VAEM and GDEM, and the non-aromatic GMA on the thermal properties were found using DSC and TGA and are reported within this section.

The epoxy-functional thermoplastics were then synthesized for their use in thermosetting resins through RAFT reactions. This strategy allowed for the preparation of low molecular weight (~10-20K Da) epoxy-functional thermoplastics, confirmed via ^{1}H-NMR spectroscopy and SEC. When used as resin modifiers, thermoplastic chain lengths can change the phase morphology of the cured resin, which in turn can alter the thermal and mechanical properties of the cured resin [44]. Fairly low molecular weights (~10K Da) of thermoplastics have been shown to impart increased toughness to cured epoxy resins; therefore, molecular weights of ~10-20K Da were chosen for the epoxy-functional thermoplastics [44]. The RAFT copolymers were also prepared with a 5:95 mole ratio of epoxy-functional monomer to MMA in order to distribute the epoxy functionality throughout the copolymer chains. By using copolymers with a distribution of epoxy functional groups as resin modifiers, the epoxy functionality could be utilized in the epoxy-amine crosslinking reaction without increasing the crosslink density, and in turn the brittleness, of the cured resins. The chain lengths and mole ratios were chosen in an attempt to maintain or enhance thermal properties while potentially increasing mechanical toughness.

The influence of the thermoplastic structure on a cured thermosetting resin was investigated by individually loading 5 wt% of both the non-aromatic poly(GMA-co-MMA) and the aromatic poly(VAEM-co-MMA) into EPON828 with a stoichiometric amount of EPIKURE W amine. The loading amount was chosen because low loadings

(~3 wt% of the overall resin) have been shown to impart increased toughness to cured epoxy resins [44]. When incorporated into thermosetting epoxy resins, the epoxy-functional thermoplastics created a grafted interpenetrating polymer network (IPN) through the reactive oxirane groups on the thermoplastic polymers binding to the epoxy resin. Incorporating resin modifiers into an epoxy resin typically involves deceasing the beneficial thermal properties of epoxy resins for enhanced toughness [44]. This has been the case when using a thermoplastic with no epoxy functionality, such as poly(MMA), to form a semi-IPN [44, 72]. By making a grafted IPN, it was hypothesized that the thermal integrity of the thermosetting resin could be maintained while imparting the toughness often associated with the incorporation of thermoplastic polymer into resins. For this stage, poly(GDEM-co-MMA) was not used due to the results in the first part of this study. Extents of cure of the neat and thermoplastic loaded resins were established through FT-IR spectroscopy. The thermal and mechanical properties were studied through the use of DSC, TGA, DMA, and fracture toughness.

4.2 Characterization of Random Thermoplastic Copolymers

The thermoplastic polymers were polymerized using synthesis methods adapted from Fei et al [73]. Each epoxy-functional monomer was polymerized in varying mole ratio amounts with MMA. MMA was chosen due to its low cost and commercial availability, methacrylate structure, and the ability of poly(MMA) to form a homogeneous solution with DGEBA [72]. Poly(MMA) has also previously been found to toughen epoxy resin systems [38]. The resulting thermoplastics were white solids at 25 ºC. Poly(GMA), a white solid at 25 ºC, was purchased from Sigma-Aldrich and used as a reference. The structures of the homopolymers and copolymers are shown in Figure 12.

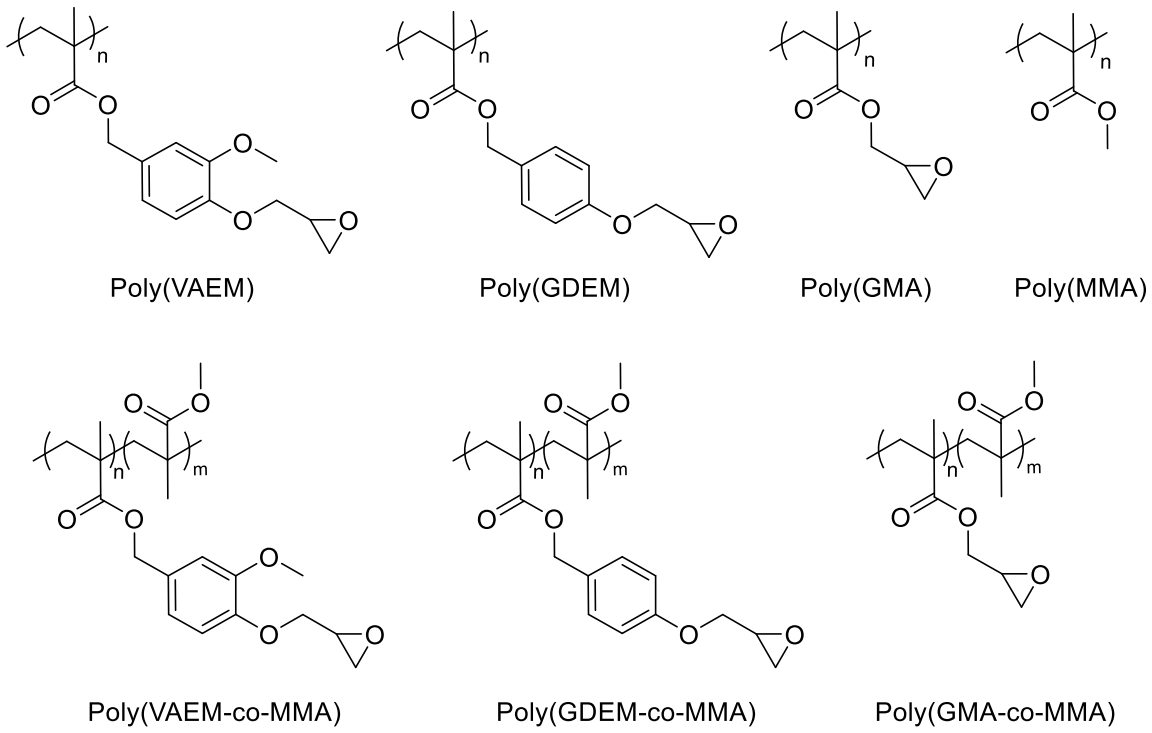

Figure 12. Solution polymerized thermoplastic polymers prepared in this study.

The presence of the epoxy group on the pendant chain was confirmed via ^{1}H-NMR spectroscopy for each thermoplastic polymer. The ^{1}H-NMR spectra of poly(VAEM) and 53-47 poly(VAEM-co-MMA) are shown in Figure 13 and Figure 14, respectively. The ^{1}H-NMR spectra for poly(GMA), poly(GDEM), and the copolymers of poly(VAEM-co-MMA), poly(GMA-co-MMA), and poly(GDEM-co-MMA) are provided in Appendix A. The reference peak located at 4.2 ppm on the spectrum was set to an integration of 1. The protons present on the epoxy are labeled as 5 and 6 shown at 3.3 ppm and 2.6–2.8 ppm, respectively. Each epoxy proton peak integrated to 1, indicating the preservation of three protons on the epoxy ring.

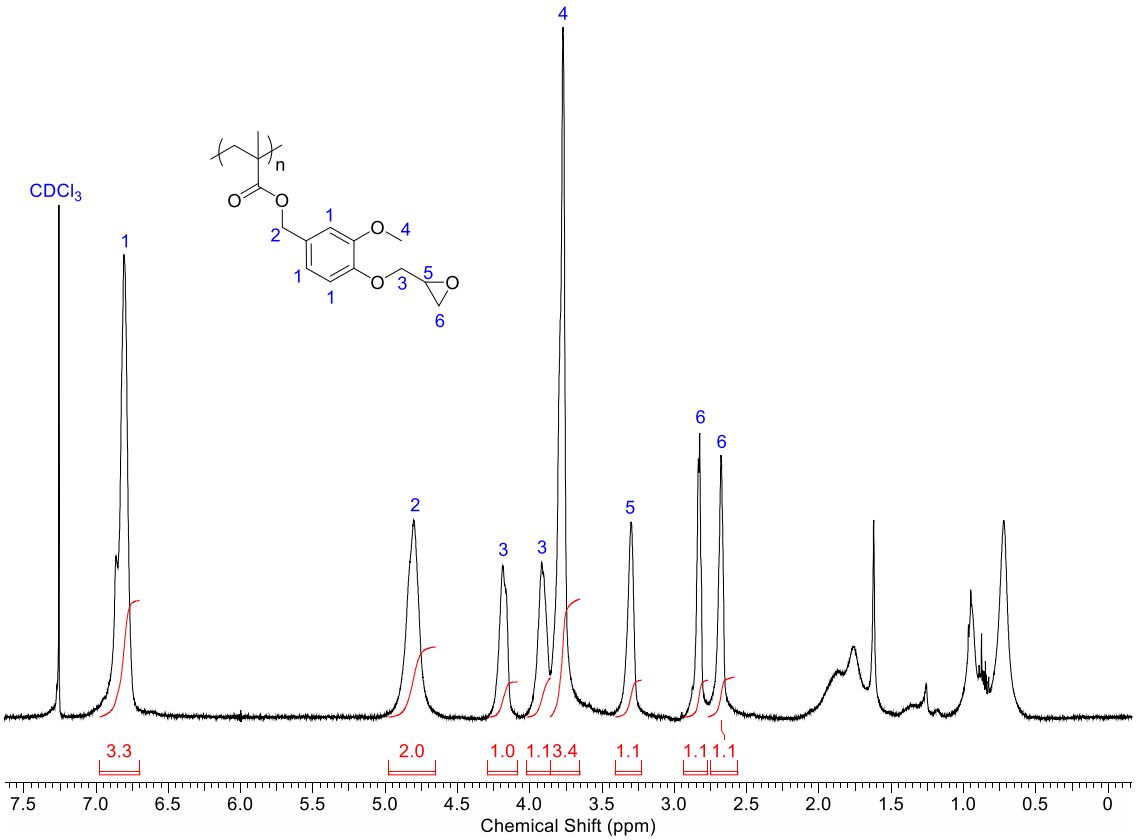

Figure 13. ^{1}H-NMR spectrum with partial peak assignments and associated integrations for poly(vanillyl alcohol epoxy-methacrylate) (poly(VAEM)). Unidentified peaks correspond to the polymer backbone.

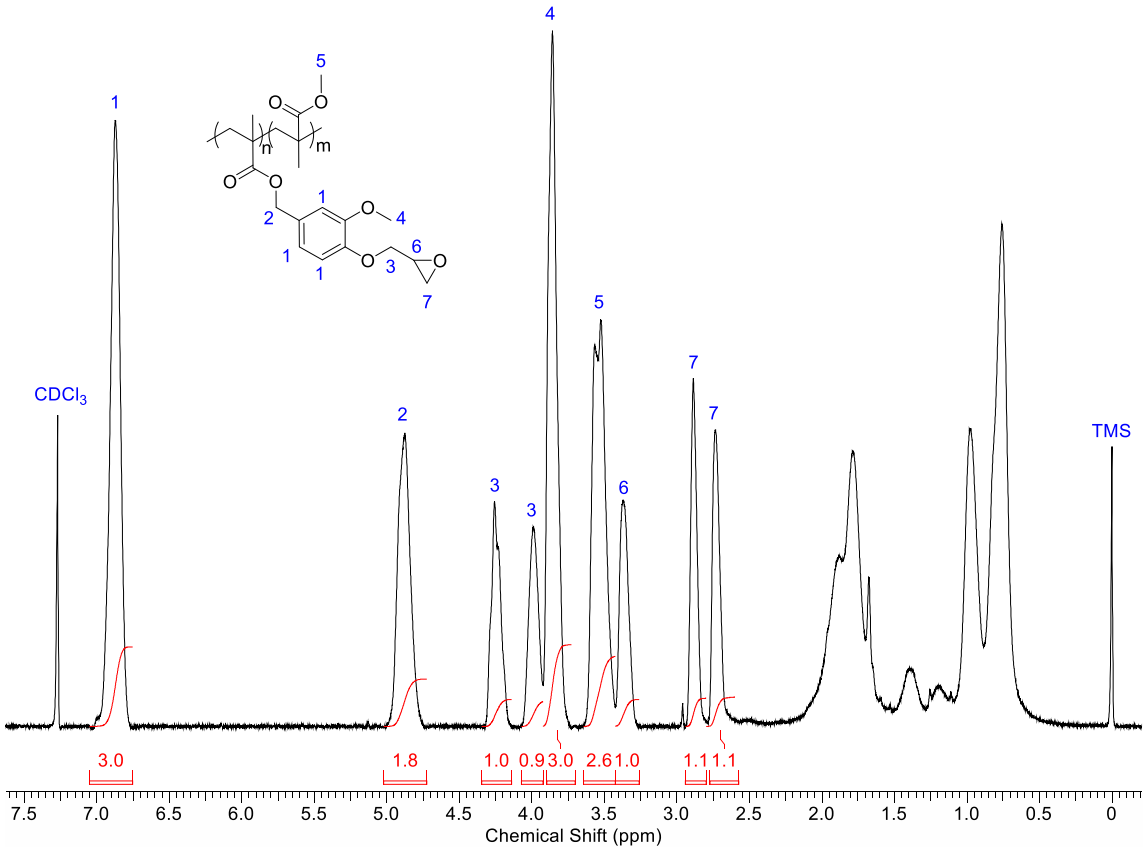

Figure 14. ^{1}H-NMR spectrum with partial peak assignments and associated integrations for 53-47 poly(vanillyl alcohol epoxy-methacrylate-co-methyl methacrylate) (53-47 poly(VAEM-co-MMA)). Unidentified peaks correspond to the polymer backbone.

The mole ratios of each polymer were determined through the use of ^{1}H-NMR spectroscopy, the results of which are found in Table 2. Deviations of final mole ratios of the copolymers from the mole ratios of reactants is likely due to the kinetics specific to each reaction mixture. An exploration of reaction kinetics is beyond the scope of this work. The molecular weight distributions and T_gs of each polymer were determined using APC and DSC, respectively. The resulting data are shown in Table 2, APC and DSC traces are provided in Appendices C and D, respectively. The M_ns of the prepared thermoplastics range from approximately 14,000 Da to 63,000 Da with the majority

falling at approximately 40,000-50,000 Da. Generally, the higher molecular weight monomers produced higher molecular weight polymers, although there is no clear trend based on the mole ratio of monomer added. The dispersities of the prepared thermoplastic polymers spans from approximately 1.4 to 3.3. The wide range of values for both the molecular weights and dispersities are likely because the polymers were prepared via solution free-radical polymerization, which provides no control over molecular weight or dispersity [27, 74, 75].

Table 2

Characterization details of random copolymers synthesized within the mole ratio study

	MMA	M_n	M_w	**Đ**	T_g
	(mol %)[a]	(Da)	(Da)		(°C)
	100	14,300	20,400	1.43	112 ± 2
GMA	**MMA**	M_n	M_w	**Đ**	T_g
(mol %)[a]	(mol %)[a]	(Da)	(Da)		(°C)
31	69	42,300	112,600	2.66	111 ± 2
49	51	24,400	54,100	4.51	101 ± 2
68	32	15,100	46,000	3.29	93 ± 3
100	0	39,500	101,900	2.58	66 ± 1
GDEM	**MMA**	M_n	M_w	**Đ**	T_g
(mol %)[a]	(mol %)[a]	(Da)	(Da)		(°C)
30	70	58,600	115,400	1.97	99 ± 1
52	48	42,800	87,300	2.04	77 ± 1
70	30	47,300	86,500	1.83	70 ± 1
100	0	46,600	152,300	3.26	62 ± 1
VAEM	**MMA**	M_n	M_w	**Đ**	T_g
(mol %)[a]	(mol %)[a]	(Da)	(Da)		(°C)
31	69	46,600	97,000	2.08	90 ± 2
53	47	52,100	95,000	1.82	76 ± 2
72	28	63,100	115,800	1.83	55 ± 2
100	0	52,700	88,500	1.68	60 ± 5

[a] Determined using ^{1}H-NMR spectroscopy.

The T_g values for the synthesized homopolymers were consistent with previous studies [1, 71]. The copolymer T_g values fall between the two corresponding homopolymers, consistent with the general trend of the Fox equation [76]. The T_gs of the copolymers show an increasing trend with increasing mole percent of MMA, with the exception of 72-28 poly(VAEM-co-MMA), which falls within the error of poly(VAEM). The T_gs of the thermoplastics as a function of mole percent MMA and Fox equations for each pair of monomers are found in Figure 15 [76]. The copolymers, in particular poly(GMA-co-MMA), deviated from the Fox equation. As the copolymers did not achieve similar M_ns and $Đ$s to the corresponding homopolymers in all instances, the T_gs fell outside of the predicted values. If similar M_ns and $Đ$s were achieved by all the thermoplastics, it is likely the copolymers would fall closer to the predicted values [76].

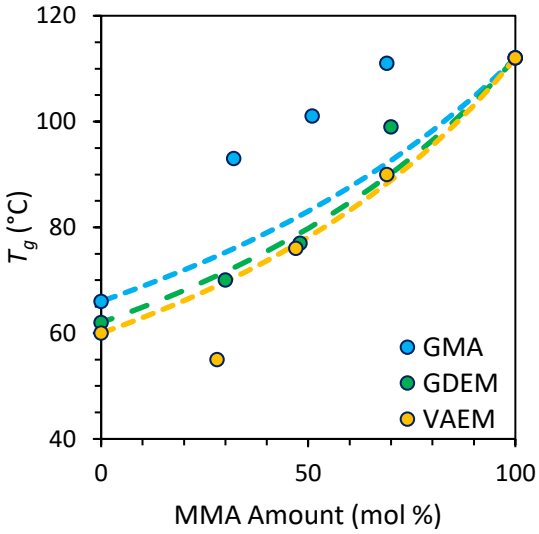

Figure 15. Glass transition temperatures of thermoplastic polymers as a function of MMA amount with Fox equations for each copolymer represented by dashed lines.

The thermogravimetric properties of each polymer were analyzed using TGA in both inert (N_2) and oxidative (air) atmospheres. The representative thermograms of each polymer tested in N_2 are shown in Figure 16-Figure 18. The thermograms and first derivatives of each polymer tested in air are available in Appendix B. The IDT, $T_{50\%}$, T_{max}, and char content average values are listed in Table 3 for both N_2 and air atmospheres.

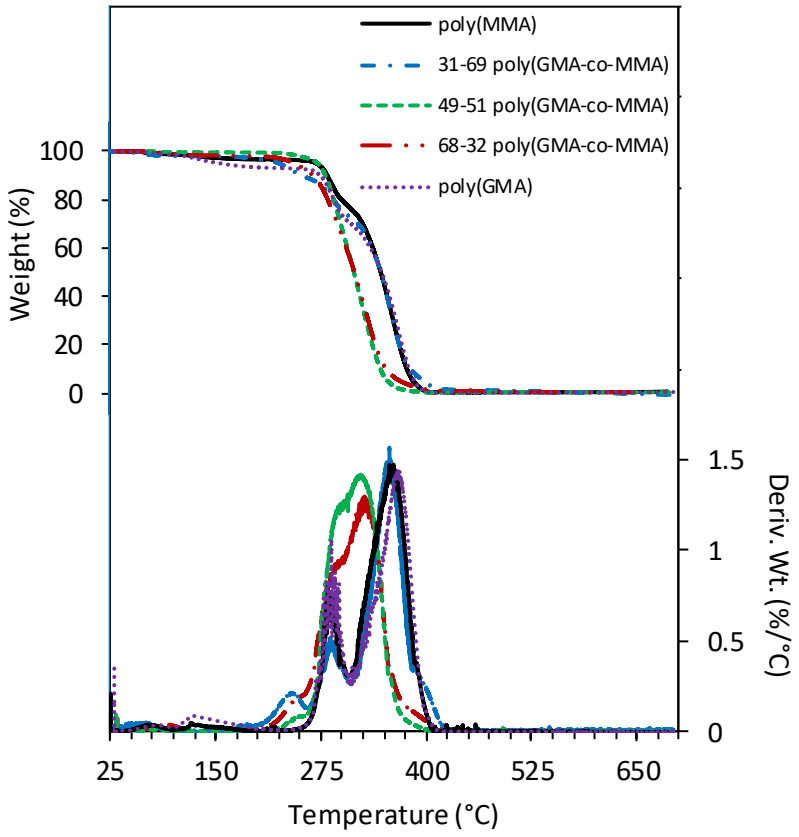

Figure 16. Representative TGA thermograms and the respective first derivatives of poly(GMA), poly(MMA), and their respective copolymers in N_2.

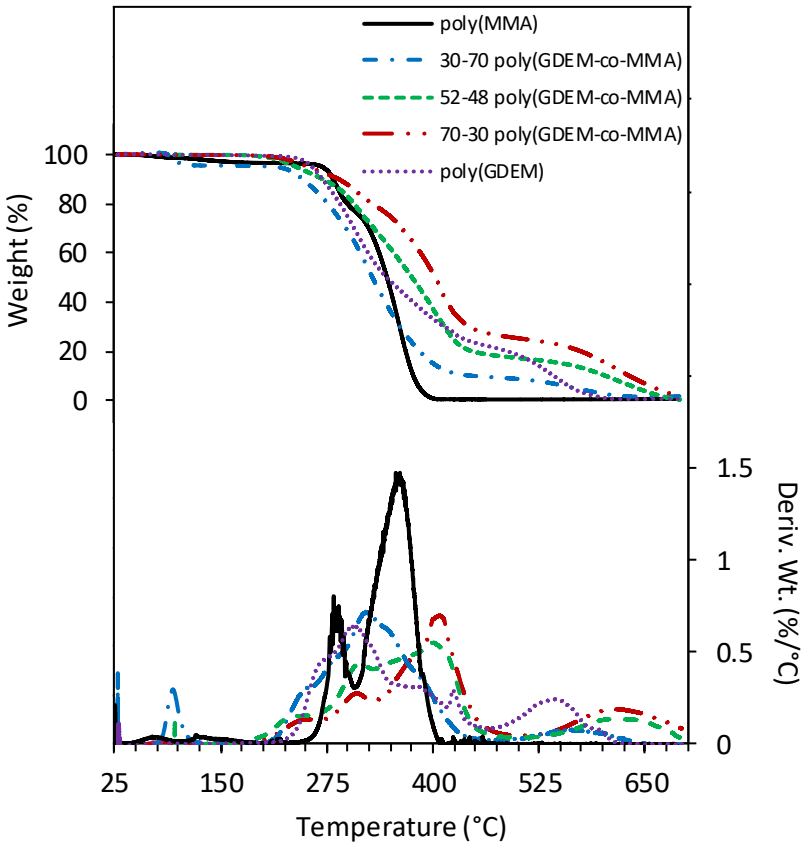

Figure 17. Representative TGA thermograms and the respective first derivatives of poly(GDEM), poly(MMA), and their respective copolymers in N_2.

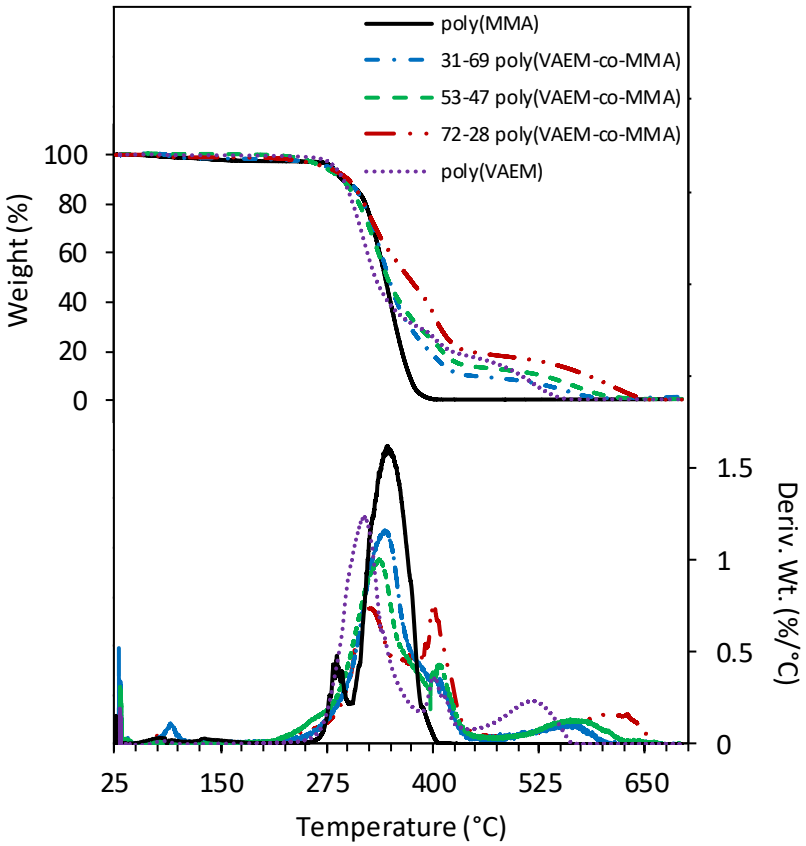

Figure 18. Representative TGA thermograms and the respective first derivatives of poly(VAEM), poly(MMA), and their respective copolymers in N_2.

Table 3

Thermogravimetric analysis data of copolymers synthesized within the mole ratio study

Polymer	N_2				Air			
	IDT (°C)	T_{50} (°C)	T_{max} (°C)	Char wt%	IDT (°C)	T_{50} (°C)	T_{max} (°C)	Char wt%
poly(MMA)	271 ± 2	350 ± 6	367 ± 7	0.3 ± 0.5	281 ± 1	344 ± 1	344 ± 1	0.4 ± 0.1
31-69 poly(GMA-co-MMA)	231 ± 8	346 ± 1	357 ± 2	0.3 ± 0.4	273 ± 1	309 ± 1	301± 1	0.4 ± 0.1
49-51 poly(GMA-co-MMA)	270 ± 2	314 ± 1	323 ± 1	0.4 ± 0.0	267 ± 3	293 ± 1	287 ± 1	0.5 ± 0.6
68-32 poly(GMA-co-MMA)	239 ± 23	326 ± 15	334 ± 23	0.1 ± 0.1	256 ± 1	293 ± 3	294 ± 3	0.3 ± 0.2
poly(GMA)	236 ± 11	327 ± 2	278 ± 2	0.7 ± 0.4	248 ± 1	309 ± 1	287 ± 1	0.4 ± 0.2
30-70 poly(GDEM-co-MMA)	201 ± 21	328 ± 1	322 ± 1	1.3 ± 0.5	207 ± 24	325 ± 4	313 ± 2	0.8 ± 0.1
52-48 poly(GDEM-co-MMA)	235 ± 5	374 ± 1	400 ± 5	0.4 ± 0.2	172 ± 87	372 ± 7	398 ± 1	0.4 ± 0.3
70-30 poly(GDEM-co-MMA)	252 ± 1	401 ± 1	406 ± 1	0.8 ± 0.8	261 ± 1	405 ± 6	405 ± 1	0.9 ± 0.1
poly(GDEM)	261 ± 1	365 ± 6	307 ± 1	0.1 ± 0.1	260 ± 1	398 ± 5	294 ± 1	0.3 ± 0.3
31-69 poly(VAEM-co-MMA)	266 ± 8	350 ± 1	351 ± 1	1.7 ± 1.0	279 ± 5	341 ± 9	323 ± 9	3.0 ± 2.5
53-47 poly(VAEM-co-MMA)	265 ± 7	347 ± 2	334 ± 6	0.9 ± 0.5	270 ± 12	348 ± 5	331 ± 3	1.6 ± 0.9
72-28 poly(VAEM-co-MMA)	270 ± 6	371 ± 1	388 ± 18	1.1 ± 1.0	278 ± 5	387 ± 2	395 ± 1	0.1 ± 0.1
poly(VAEM)	288 ± 1	335 ± 1	330 ± 1	0.2 ± 0.1	287 ± 3	335 ± 5	320 ± 2	0.4 ± 0.1

The prepared homopolymers exhibited thermal stabilities similar to those found in literature, with the highest overall thermal stability in poly(MMA) and significantly higher thermal stabilities in poly(VAEM) and poly(GDEM) compared to poly(GMA). Poly(GDEM) and poly(VAEM) had significantly higher IDT values than poly(GMA), likely due to the added aromaticity in the pendant chain enhancing thermal stability [77]. Between poly(GDEM) and poly(VAEM), the placement and number of methoxy moieties had minimal effects on thermal stability. Similar thermal degradation trends are noted for $T_{50\%}$ and T_{max} data, and the char content was similar for all of the homopolymers in both atmospheres.

The copolymer thermal properties are similar to their respective homopolymers. 31-69 poly(GMA-co-MMA) has similar thermal stability to poly(MMA). With increasing GMA, the thermal stability remains below that of poly(MMA) as well as below that of a majority of the copolymers containing VAEM and GDEM. For 30-70 poly(GDEM-co-MMA), the thermal stability is lower than that of poly(MMA) and poly(GDEM). However, with increasing GDEM content, the thermal properties of the copolymers increase. A similar trend is seen for the copolymers containing VAEM. Copolymerizing GDEM or VAEM with MMA shows improved thermal stability as compared to copolymerizing with GMA, likely due to the added aromaticity in the pendant chain enhancing thermal stability [77]. Similar char contents were found for all copolymers in both atmospheres. Moving forward, poly(GDEM) and its copolymers were not used as its thermal properties were similar to those of the poly(VAEM) polymers and both contain aromaticity. The next sections focus on comparing the non-aromatic poly(GMA-co-MMA) to the aromatic poly(VAEM-co-MMA).

4.3 Characterization of RAFT Thermoplastic Polymers

The thermoplastic polymers were polymerized in varying molar masses using synthesis methods adapted from Fei et al. and Holmberg et al [73, 78]. The resulting thermoplastics were solid at 25 ºC. The red color of the 2-cyano-2-propyl benzodithioate CTA was imparted to the thermoplastics, resulting in a light pink color. The structures of the polymers, with the omission of the CTA, are shown in Figure 19.

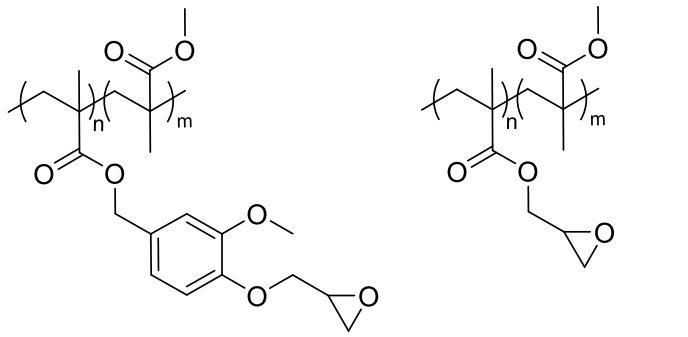

Figure 19. RAFT solution polymerized thermoplastics prepared in this study.

The mole ratios of each polymer were determined through the use of ^{1}H-NMR spectroscopy, the results of which are found in Table 4. Deviations of final mole ratios of the copolymers from the mole ratios of reactants is likely due to the kinetics specific to each reaction mixture. An exploration of reaction kinetics is beyond the scope of this work. The molecular weights and T_gs of each polymer were determined using APC and DSC, respectively. The resulting data are shown in Table 4, with APC and DSC traces provided in Appendices C and D, respectively.

Table 4

Characterization details of RAFT solution polymerized thermoplastic polymers

GMA (mol %)[a]	**MMA** (mol %)[a]	M_n (Da)	M_w (Da)	**Đ**	T_g (°C)
6.0	94.0	12,200	15,000	1.23	90 ± 2
VAEM (mol %)[a]	**MMA** (mol %)[a]	M_n (Da)	M_w (Da)	**Đ**	T_g (°C)
7.7	92.3	16,400	19,600	1.16	83 ± 1

[a] Determined using ^{1}H-NMR spectroscopy.

The T_gs of both thermoplastics were lower than what is expected when compared to the results in Table 2 and the Fox equation. This is likely due to the lower M_n values of the RAFT synthesized polymers [28]. The difference in T_g between the poly(GMA-co-MMA) and poly(VAEM-co-MMA) is approximately 7 °C with the higher value T_g corresponding to poly(GMA-co-MMA). When comparing poly(GMA-co-MMA) and poly(VAEM-co-MMA) thermoplastics from Table 2 of both similar M_n values and composition, an analogous relationship is shown.

The synthesized thermoplastics contain several reactive groups on each polymer chain, an estimated 7-11 epoxies per chain based on ^{1}H-NMR spectroscopy. The chains are anticipated to have approximately evenly spaced oxirane groups due to the controlled nature of RAFT reactions [25, 31]. By synthesizing the polymers in a random reaction rather than as a block copolymer, the oxirane groups can be located throughout the polymer chains rather than in a group at one point on the chain. This allows the chains to form a unique network conformation when reacted in an epoxy-amine resin and is

expected to affect properties of that resin. By making the chains low molecular weight, the polymer chains can form short, branching regions within a bigger thermoset network. This was expected to impact the thermomechanical properties of the cured resins. The impact of these polymers on a cured resin is discussed further in section 4.4.

The thermogravimetric properties of each polymer were analyzed using TGA in both inert (N_2) and oxidative (air) atmospheres. Representative thermograms of each polymer tested in N_2 are shown in Figure 20. The thermograms and first derivatives of each polymer tested in air are available in Appendix B. The IDT, $T_{50\%}$, T_{max}, and char content average values are listed in Table 5 for both N_2 and air atmospheres.

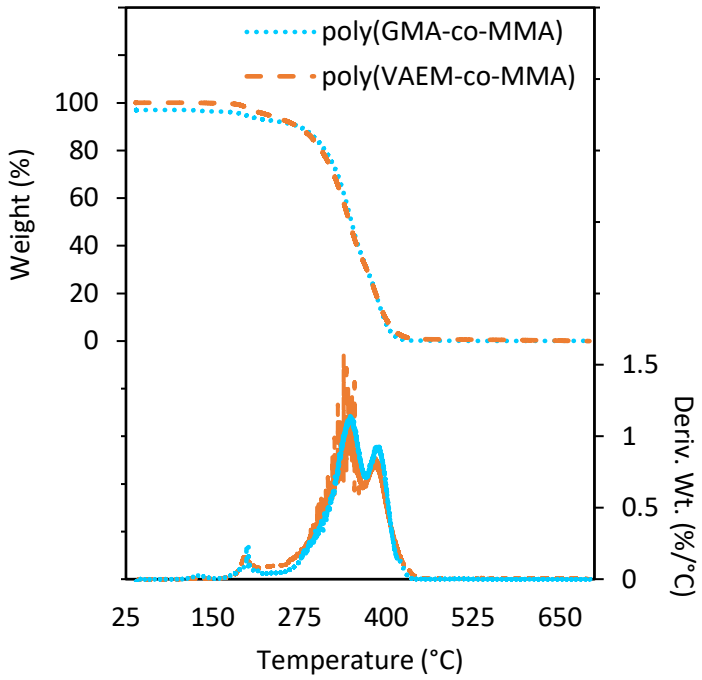

Figure 20. Representative TGA thermograms and the respective first derivatives of the RAFT polymerized poly(GMA-co-MMA) and poly(VAEM-co-MMA) in N_2.

Table 5

Thermogravimetric analysis data of RAFT solution polymerized thermoplastic polymers

	N_2				Air			
Polymer	**IDT** (°C)	**T_{50}** (°C)	**T_{max}** (°C)	**Char** wt%	**IDT** (°C)	**T_{50}** (°C)	**T_{max}** (°C)	**Char** wt%
poly(GMA-co-MMA)	250 ± 3	353 ± 1	347 ± 1	0.15 ± 0.10	271 ± 1	346 ± 2	343 ± 2	0.01 ± 0.01
poly(VAEM-co-MMA)	226 ± 6	346 ± 2	340 ± 1	0.01 ± 0.01	249 ± 1	348 ± 3	339 ± 8	0.01 ± 0.01

The thermal stabilities of the RAFT polymerized poly(GMA-co-MMA) and poly(VAEM-co-MMA) are similar to the results shown in Table 3. The IDT, T_{50}, T_{max}, and char values of poly(GMA-co-MMA) and poly(VAEM-co-MMA) were similar to one another, indicating the aromaticity of VAEM did not have a significant impact on the thermal stabilities at 5 mol% loading. The RAFT copolymers showed some thermal property differences when compared to the random solution polymerized copolymers, as shown in section 4.2, likely due in part to the CTA. As the CTA was not removed from the RAFT synthesized polymers, it could contribute to the overall polymer properties. This effect is likely minimal, as the CTA remains only as an end group on the thermoplastic copolymers.

4.4 Interpenetrating Polymer Networks

This section explores the incorporation of the thermoplastic copolymers into IPNs. By curing the thermoplastics with the amine crosslinker in the epoxy-amine system, the polymer chains have the potential to react with both the epoxy-functional thermoplastics and/or EPON828. The following section details the impacts of the thermoplastic polymers on the thermomechanical properties of the cured resins.

The epoxy equivalent weights (EEWs) of each epoxy used in this study and the amine hydrogen equivalent weight (AHEW) of EPIKURE W are shown in Table 6. The EEWs of the epoxy resins were used to prepare the neat and thermoplastic loaded polymers as described in section 3.6. The neat EPON828-EPIKURE W was a viscous liquid resin with a clear, orange-brown appearance before cure, imparted from the EPIKURE W. The cured neat resin had a clear yellow appearance. The thermoplastic loaded resins were opaque, viscous liquids with suspended thermoplastic particles and a

dark orange color pre-cure, imparted from both the EPIKURE W and the pink color of the RAFT polymerized thermoplastics. The post-cured thermoplastic loaded resins had a slightly darker yellow color than the neat resin and a clear appearance.

Table 6

Epoxy and amine hydrogen equivalent weights of resin components

Epoxy Resin Component	**EEW** (g/eq)	**AHEW** (g/eq)	**MW** (g mol^{-1})	**n**[a] (Da)
EPON828	186.70	-	340.41286 + [284.3496]n	0.12
poly(GMA-co-MMA)	1745.70[b]	-	12,200	-
poly(VAEM-co-MMA)	1488.17[b]	-	16,400	-
EPIKURE W	-	44.57	178.27	-

[a] Average repeat unit based on EEW and MW.

[b] Determined using ^{1}H-NMR spectroscopy.

The extents of cure of each resin are shown in Table 7. The values were determined through near-IR by comparing pre-cured resin spectra to post-cured resin spectra as described in Chapter 3. The near-IR analysis indicates the final extents of cure were similar for all three resin systems. The extents of cure are calculated based on the conversion of amine groups. There is no way to measure which epoxy component of the resin system (either the oxirane groups of EPON828 or those of the thermoplastics) have cured in part or fully. The resulting values indicate the addition of 5 wt% thermoplastic polymer has little effect on the overall extent of cure of the resin.

Table 7

Epoxy equivalent weight of resin components

Epoxy Resin System	Extent of Cure (%)
Neat	86 ± 1
5 wt% poly(GMA-co-MMA)	86 ± 2
5 wt% poly(VAEM-co-MMA)	84 ± 1

The thermogravimetric properties of each polymer were analyzed using TGA in both inert (N_2) and oxidative (air) atmospheres. Representative thermograms of each polymer tested in N_2 are shown in Figure 21. The thermograms and first derivatives of each polymer tested in air are available in Appendix B. The IDT, $T_{50\%}$, T_{max}, and char content average values are listed in Table 8 for both N_2 and air atmospheres.

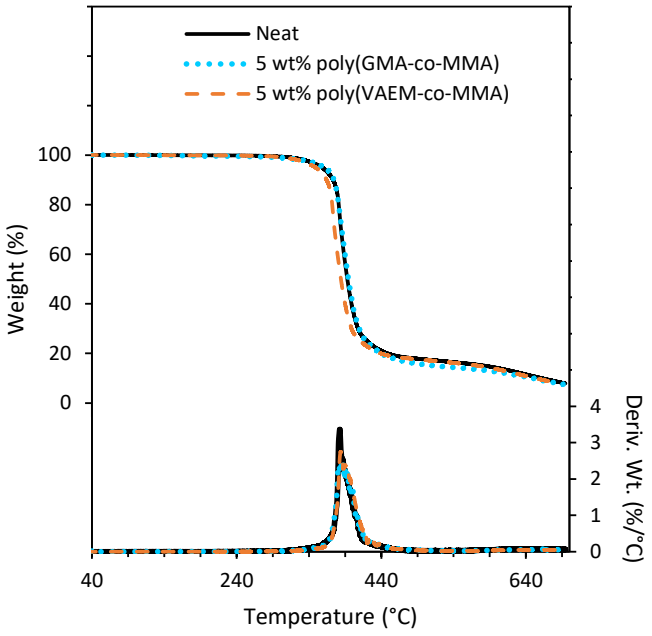

Figure 21. Representative TGA thermograms and the respective first derivatives of the cured thermosetting resins in N_2.

Table 8

Thermogravimetric analysis data of thermosetting epoxy resins in N_2 and air

	N_2				Air			
Epoxy Resin System	**IDT** (°C)	**T_{50}** (°C)	**T_{max}** (°C)	**Char** wt%	**IDT** (°C)	**T_{50}** (°C)	**T_{max}** (°C)	**Char** wt%
Neat	363 ± 6	393 ± 1	384 ± 3	8.9 ± 1.4	366 ± 2	388 ± 2	380 ± 1	0.02 ± 0.02
5 wt% poly(GMA-co-MMA)	362 ± 1	394 ± 1	385 ± 3	7.5 ± 0.18	363 ± 2	393 ± 1	383 ± 1	0.08 ± 0.05
5 wt% poly(VAEM-co-MMA)	366 ± 4	397 ± 2	382 ± 2	8.1 ± 0.66	356 ± 3	392 ± 1	384 ± 1	0.05 ± 0.03

The cured resins loaded with the epoxy-functional thermoplastic exhibited low or no statistical differences in IDT, T_{50}, T_{max} or char content in a N_2 atmosphere compared to the cured neat resin or each other. This indicates the thermal stability of the cured resins was maintained with the addition of the thermoplastic copolymer.

The thermomechanical properties were measured using DMA to quantitate the viscoelastic behavior of the cured resins. Table 9 shows the properties measured and calculated via DMA. The E' and E'' thermograms are shown in Figure 22 and the tan δ thermogram is shown in Figure 23. The glassy E' of the poly(GMA-co-MMA) loaded EPON828-EPIKURE W and poly(VAEM-co-MMA) loaded EPON828-EPIKURE W are higher than that of the neat resin by 0.2 and 0.3 GPa, respectively, although the error overlaps with that of the cured neat resin. This indicates some enhanced stiffness with the addition of thermoplastic copolymers to the resin, which could in turn correlate to better mechanical performance [44]. While the difference is not statistically significant in these samples, additional thermoplastic loading could potentially provide more enhancement of the glassy E'.

The poly(GMA-co-MMA) and poly(VAEM-co-MMA) loaded EPON828-EPIKURE W cured resins displayed secondary transitions, T_g^{β}, corresponding to movement of the chain segments of the thermoplastic within the thermoset. The T_g^{β} peak is lower than that of the thermoplastic T_g values from DSC as shown in Table 4, however the DMA was run at 2 ºC min^{-1} while the DSC was run at 10 ºC min^{-1}. This difference in ramp rates likely accounts for the different T_g values. The DSCs of the cured resins of poly(GMA-co-MMA) and poly(VAEM-co-MMA) loaded EPON828-EPIKURE W did not show a T_g^{β}; however, this is likely due to the low loading of the thermoplastic. DMA

tests have also been shown to be more sensitive than DSC [58]. The presence of a secondary transition indicates that the poly(GMA-co-MMA) and poly(VAEM-co-MMA) loaded EPON828-EPIKURE W cured resins are two-phase systems. Two-phase epoxy systems typically produce T_gs that are closer to one another than the T_gs of the individual species, which is seen in these systems through the lowering of the loss modulus and tan δ peaks [44].

The T_gs of the cured resins, taken as the peak of the E″, were 168 ± 8 °C, 161 ± 1 °C, and 161 ± 1 °C for the neat, poly(GMA-co-MMA) loaded EPON828-EPIKURE W, and poly(VAEM-co-MMA) loaded EPON828-EPIKURE W, respectively. Glass transition is often linked to the crosslink density of resins, where increased distance between crosslinks corresponds to decreased T_g. The effective molecular weight between crosslinks (M_c) values of the thermoplastic loaded cured resins show a significant increase when compared to the neat cured resin as expected. This indicates that as thermoplastic is loaded into the system, there is more free volume between the crosslinks and, subsequently, the T_g lowers [79, 80]. While the T_g of the neat cured resin was higher, it was within error of the thermoplastic loaded cured resins indicating there was minimal impact of thermoplastic loading on T_g. There was no significant difference in E″ between poly(GMA-co-MMA) and poly(VAEM-co-MMA) loading.

Similar results were shown in the peak of the tan δ. The neat cured resin was higher than that of the thermoplastic loaded cured resins at 179 ± 8 °C compared to 172 ± 2 °C of poly(GMA-co-MMA) loaded EPON828-EPIKURE W and 173 ± 1°C of poly(VAEM-co-MMA) loaded EPON828-EPIKURE W. The values were not statistically different from one another; however, the neat cured resin showed a higher tan δ,

indicating a minimal lowering of tan δ with the addition of thermoplastic polymer. The tan δ of the poly(VAEM-co-MMA) loaded EPON828-EPIKURE W cured resin appeared 1 °C higher than poly(GMA-co-MMA) loaded EPON828-EPIKURE W cured resin, likely due to the aromatic content imparted from the VAEM in the side group of the thermoplastic; however, the differences between the copolymer loaded cured resins was minimal at this loading amount.

The T_gs from the DMA thermograms were consistent with those found via DSC, where the neat cured resin has a T_g of 172 ± 2 °C, the poly(GMA-co-MMA) loaded EPON828-EPIKURE W cured resin has a T_g of 160 ± 2 °C, and the poly(VAEM-co-MMA) loaded EPON828-EPIKURE W cured resin has a T_g of 162 ± 2 °C. By adding 5 wt% thermoplastic to the resin system, the T_g values decreased approximately 10 °C, consistent with the DMA results. There was no statistically significant difference between the T_gs from DSC of the two thermoplastic loaded cured resins; however, that of the poly(VAEM-co-MMA) loaded EPON828-EPIKURE W cured resin was approximately 2 °C higher. This is likely due to the aromatic content imparted from the VAEM in the side group of the thermoplastic. The DSC thermograms for each of the cured resins are shown in Appendix D.

The M_c values are 551 ± 22 g mol^{-1} for the poly(GMA-co-MMA) loaded EPON828-EPIKURE W cured resin and 567 ± 27 g mol^{-1} for the poly(VAEM-co-MMA) loaded EPON828-EPIKURE W cured resin. This is to be expected, as the M_c values are at minimum that of the neat resin at 475 ± 39 g mol^{-1}, and at maximum that of the distance between the epoxy groups in the epoxy-functional thermoplastics, a value that can be estimated as the EEWs of the copolymers [~ 1746 g mol^{-1} for poly(GMA-co-

MMA) and ~ 1488 g mol^{-1} for poly(VAEM-co-MMA)]. At the low thermoplastic loading of 5 wt%, the M_c values of the cured resins are expected to be closer to that of the neat resin than the pure thermoplastic copolymers, which is supported through the values established using DMA.

The poly(GMA-co-MMA) loaded EPON828-EPIKURE W and poly(VAEM-co-MMA) loaded EPON828-EPIKURE W cured resins exhibited higher densities than that of the neat cured resin, with the poly(VAEM-co-MMA) loaded EPON828-EPIKURE W cured resin exhibiting a statistically significant increase in density. The increase is likely due to packing of the thermoplastic polymer chains at room temperature, creating a denser material. Additionally, the crosslinking of the epoxy groups within thermoplastic chains could contribute to the difference between the poly(GMA-co-MMA) loaded EPON828-EPIKURE W and the poly(VAEM-co-MMA) loaded EPON828-EPIKURE W cured resins, similar to the backbiting phenomenon experienced in some thermoplastic reactions such as RAFT polymerization [28]. The VAEM repeat units are longer than the GMA repeat units, which could allow for more internal bonding within thermoplastic chains. Overall, the changes in density were minimal indicating the thermoplastic polymers had a marginal impact on resin density.

Table 9

Dynamic mechanical analysis and density data of the cured thermosetting epoxy resins

Epoxy Resin System	*E′* @ 25 °C (GPa)	T_g^{β} (°C)	Peak of *E″* (°C)	Peak of Tan δ (°C)	eff. M_c (g mol^{-1})	ρ @ 25 °C (g cm^{-3})
Neat	2.2 ± 0.3	-	168 ± 8	179 ± 8	475 ± 39	1.162 ± 0.002
5 wt% poly(GMA-co-MMA)	2.4 ± 0.1	46 ± 1	161 ± 1	172 ± 2	551 ± 22	1.163 ± 0.002
5 wt% poly(VAEM-co-MMA)	2.5 ± 0.1	48 ± 2	161 ± 1	173 ± 1	567 ± 27	1.166 ± 0.001

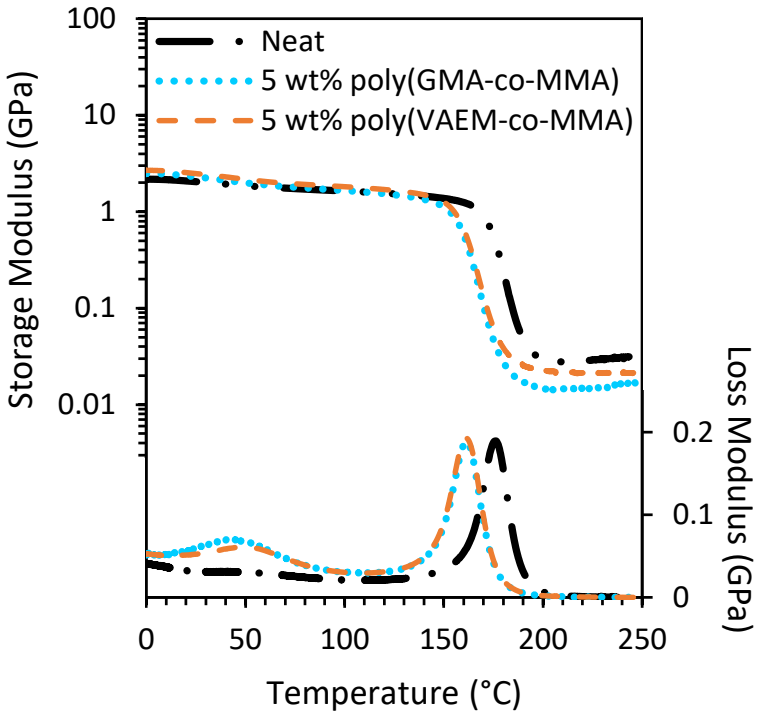

Figure 22. Representative DMA thermograms of the storage and loss moduli of thermosetting polymers loaded with thermoplastic.

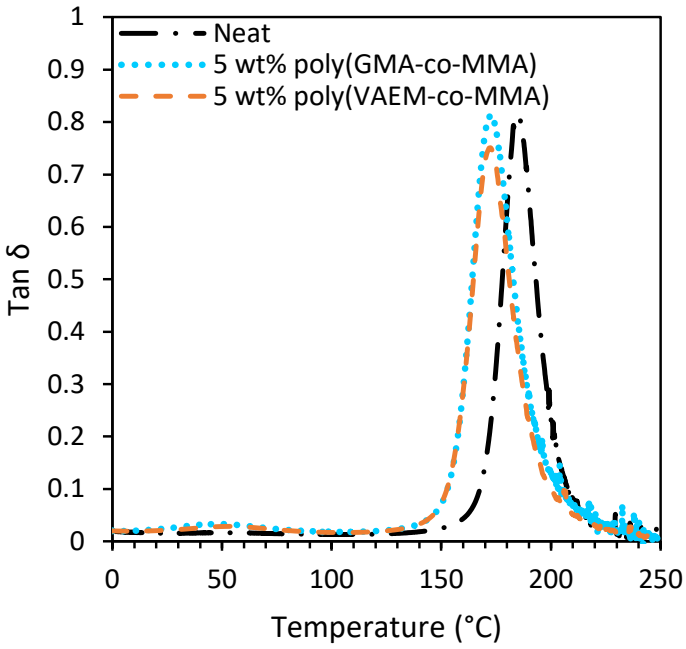

Figure 23. Representative DMA thermograms of the tan δ of thermosetting polymers loaded with thermoplastic.

To determine the extent of structural differences between neat and thermoplastic loaded cured resins, fracture toughness was conducted. Critical strain energy release rate, G_{1C}, and plane-strain fracture toughness, K_{1C}, were evaluated and are shown in Table 10. All samples displayed linear load and deformation increased until the point of fracture, indicating brittle behavior [81]. Representative load displacement curves are shown in Figure 24 for all thermosetting resins.

The poly(GMA-co-MMA) and poly(VAEM-co-MMA) loaded cured resins showed no statistical difference in either G_{1C} or K_{1C} when compared to neat cured resin, indicating minimal effects of the incorporation of 5 wt% of epoxy-functional thermoplastics. Despite the marginal differences, the poly(GMA-co-MMA) loaded EPON828-EPIKURE W cured resin showed the highest G_{1C} and K_{1C} values at 205 J m^{-2}

and 0.755 MPa $m^{1/2}$, respectively. The second highest was the poly(VAEM-co-MMA) loaded EPON828-EPIKURE W cured resin with a G_{1C} of 187 J m^{-2} and a K_{1C} of 0.725 MPa $m^{1/2}$, followed by the neat cured resin with a G_{1C} of 183 J m^{-2} and a K_{1C} of 0.684 MPa $m^{1/2}$. This indicates that the addition of the thermoplastics did impart some toughness to the overall resin. While the results were not statistically different from one another at this loading of thermoplastic, higher loading amounts of poly(GMA-co-MMA) and poly(VAEM-co-MMA) could provide an increased toughening effect.

Table 10

Fracture toughness results of thermosetting epoxy resins

Epoxy Resin System	**G_{1C}** J m^{-2}	**K_{1C}** MPa $m^{1/2}$
Neat	183 ± 40	0.684 ± 0.036
5 wt% poly(GMA-co-MMA)	205 ± 72	0.755 ± 0.084
5 wt% poly(VAEM-co-MMA)	187 ± 56	0.725 ± 0.073

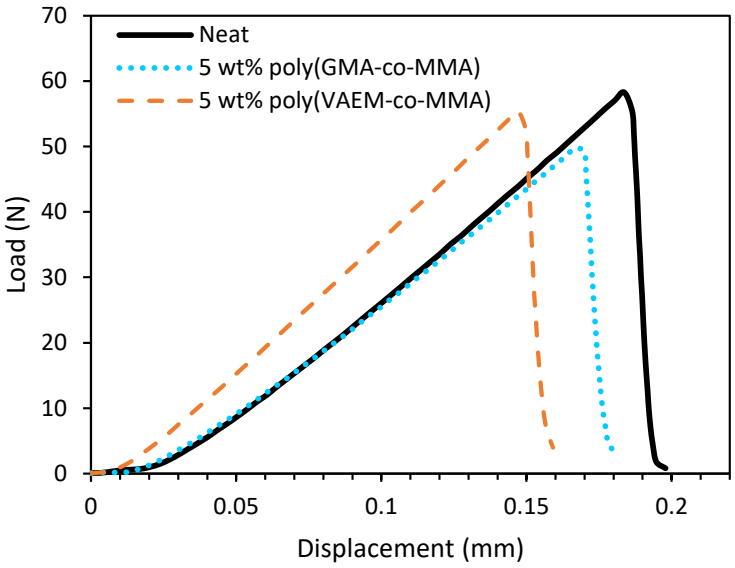

Figure 24. Representative load displacement curves of thermosetting polymers loaded with thermoplastic.

Chapter 5

Conclusions and Future Work

5.1 Conclusions

This thesis focused on creating and evaluating epoxy-functional thermoplastic polymers from aromatic, bio-derived monomers, then formulating the resulting thermoplastics into thermosetting epoxy resin interpenetrating polymer networks (IPNs) for their use in the automotive, aerospace, and additive manufacturing industries. Epoxy-functional thermoplastic copolymers were hypothesized to maintain or enhance thermal properties and significantly increased mechanical toughness when synthesized and incorporated into IPNs. The epoxy-methacrylate monomers vanillyl alcohol epoxy-methacrylate (VAEM) and gastrodigenin epoxy-methacrylate (GDEM) were homopolymerized to form poly(VAEM) and poly(GDEM) and randomly copolymerized in varying ratios with the common comonomer methyl methacrylate (MMA) to form poly(VAEM-co-MMA) and poly(GDEM-co-MMA) thermoplastics. Glycidyl methacrylate (GMA), a non-aromatic, commercially available epoxy-methacrylate monomer, was similarly polymerized for comparison. The structures and mole ratios of each synthesized polymer were confirmed via ^{1}H-NMR spectroscopy. Each polymer was evaluated via SEC, the majority of which had M_n values within the range of 40-50,000 Da and dispersities of approximately 1.4-3.3. The T_g values ranged from 60-111 °C, of which poly(MMA) had the highest overall value. The thermal properties of the polymers were evaluated via TGA, where the use of aromatic monomers GDEM and VAEM resulted in comparable thermal stabilities to GMA when copolymerized. The VAEM

copolymers showed the most improved thermal stability when compared to poly(MMA) and GMA copolymers.

Next, random copolymers poly(VAEM-co-MMA) and poly(GMA-co-MMA) were synthesized via reversible addition-fragmentation chain transfer (RAFT) polymerization to form low molecular weight epoxy-functional thermoplastics for use as performance additives in thermosetting resins. The thermoplastic polymers had M_ns of approximately 12,200 Da and 16,400 Da, respectively, and 7-11 epoxy groups per chain. The structures and mole ratios of each synthesized polymer were confirmed via ^{1}H-NMR spectroscopy. The T_gs were 90 °C for poly(GMA-co-MMA) and 83 °C for poly(VAEM-co-MMA). The thermal stabilities were similar to one another.

Poly(GMA-co-MMA) and poly(VAEM-co-MMA) were separately formulated at 5 wt% into an epoxy resin system containing EPON828 and EPIKURE W and cured thermally to produce IPNs. The extents of cure for all the resin systems were approximately 85%. The resulting thermosets were compared to the neat cured resin and evaluated for thermal and mechanical properties using DSC, TGA, DMA, and fracture toughness. The cured resins exhibited comparable thermal stabilities to one another with IDT values of 362-366 °C, T_{50} values of 393-397 °C and T_{max} values of 382-385 °C in N_2, with similar values in air. The char content for all the cured resins was approximately 8 wt% in N_2 and 0.04 wt% in air.

The viscoelastic and fracture properties of the cured resins showed minimal differences; however, they indicate a step towards the desired advancements. The poly(VAEM-co-MMA) and poly(GMA-co-MMA) loaded EPON828-EPIKURE W cured resins showed higher glassy storage moduli than the neat cured resin, indicating some

enhanced stiffness due to the thermoplastic modifiers at the 5 wt% loading of the thermoplastic copolymers. There was a reduction in T_g of about 7 °C with the addition of the thermoplastic copolymers, and a similar reduction in the peak of the tan δ; however, this was not found to be statistically different than the neat cured resin. The poly(VAEM-co-MMA) loaded cured resin had the highest effective molecular weight between crosslinks, followed by the poly(GMA-co-MMA) loaded cured resin, indicating the addition of thermoplastic modifiers increased the free volume of the resin systems. For fracture toughness, the poly(GMA-co-MMA) loaded cured resin had the highest G_{1C} and K_{1C} values at 205 J m^{-2} and 0.755 MPa $m^{1/2}$, respectively, followed by the poly(VAEM-co-MMA) loaded cured resin, indicating a toughening effect on the resin through the addition of the epoxy-functional thermoplastics. In total, the incorporation of the epoxy-functionalized copolymers into the resin system exhibited maintained thermal properties and progress towards increased mechanical toughness when compared to the commercial resin system, indicating advancement towards the ultimate goal of high performance polymer networks for commercial and military applications.

5.2 Recommendations for Future Work

The further improvement of the IPNs within this work is not only desirable, but crucial for their use in high performance applications. While the poly(VAEM-co-MMA) and poly(GMA-co-MMA) loaded EPON828-EPIKURE W cured resins showed some benefits in toughness and stiffness with maintained thermal properties, to expand into the automotive, aerospace, and the additive manufacturing industries the properties need to show more than marginal enhancement. Recent advancements in AM in particular have shown that epoxy resins can be modified for higher speed printing, strength and

toughness enhancement, and maintenance of thermal properties [35, 82-85]. For the systems in this work to bridge the gaps in the advanced materials space, further changes in formulation and studies of structure-property relationships are needed.

The first steps towards improving the IPNs would likely involve changing the concentration or molecular weight of the copolymers. While typical thermoplastic loading is usually less than 10 wt% in epoxy-thermoplastic blends, mechanical improvements including toughening of the epoxy system have also been shown at 15 wt% or more [38, 86, 87]. Increasing the loading of the copolymers is a fairly minor modification to the procedure followed within this work and could provide the increased toughening effect desired for the cured resins. Studies have also investigated at the effects of increased thermoplastic chain length on thermal and mechanical properties. The work of Rico et al. has shown that changing the chain length can have significant impacts on phase morphology. In the study, increasing chain length was found to decrease miscibility in poly(MMA)-modified diglycidyl ether of bisphenol A (DGEBA) systems, which in turn impacts thermal and mechanical properties such as T_g and toughness [38, 44, 87]. A similar effect could be seen if the molecular weight of the copolymers were changed. Morphology studies have been performed on a wide variety of systems; however, the specific impacts differ vastly based on the thermoplastic used [44]. To better understand how the concentration and/or molecular weight of the copolymers impacts the cured resins, a phase morphology study using an instrument such as a scanning electron microscope (SEM) would be useful. This could be performed in conjunction with thermal and mechanical tests.

While increasing concentration or molecular weight could enhance the epoxy resin system, the epoxy-functional thermoplastics explored in this work may not behave like those typically used to toughen epoxy systems due to their ability to react in the thermoset curing stage. Studies have been completed with reactive thermoplastics containing poly(GMA); however, those typically employ a block copolymer configuration or reactive end groups [50, 87, 88]. For block copolymers, the cure can cause polymerization induced phase separation (PIPS), which has been shown to provide a toughening effect through the creation of distinct domains within the thermoset. PIPS can also occur with a non-reactive thermoplastic additive if two or more distinct blocks arrange into thermodynamically favorable domains during polymerization [13, 89]. Using a thermoplastic with reactive end groups can form similar phase separation [50]. Without distinct blocks or reactive end groups in the random copolymers of poly(GMA-co-MMA) and poly(VAEM-co-MMA) in this work, distinct domains are unlikely to occur in the same manner or provide a similar toughening effect.

Most IPNs do experience some form of phase separation; however, predicting morphology can be difficult as it is dependent on the kinetics of polymerization and crosslinking. Phase morphology can be an inaccurate method of predicting thermal and mechanical properties, and extensive testing is often necessary [90]. While properties can not be easily predicted, the systems in this study could have similar morphology influences as other IPN systems. IPNs typically experience more miscibility with increased distance between crosslinks or blocks [5, 41]. This system would experience these effects by increasing the space between the oxirane crosslinking sites. This could change phase morphology, and in turn impact the thermal and mechanical properties of

the network. Additionally, by increasing the distance between oxiranes on the thermoplastic polymers, the aliphatic content in the epoxy network would increase. This could inadvertently provide more benefits, as in general, aliphatic content provides a toughening effect to epoxy networks [91]. By tuning the distance between the oxirane groups, the networks have potential to boost toughness and maintain the current thermal properties.

Another way to increase fracture toughness or thermal stability would be to exchange the MMA in the system for another comonomer. This work primarily focused on working with copolymers of MMA; however, mechanical and thermal properties can be adjusted through the comonomer used. As T_gs of copolymers are one of the easiest to predict properties, an increase in T_g could be reasonably expected by using a comonomer with a higher T_g than MMA and a decrease of T_g when using a comonomer with a lower T_g than MMA [76]. The thermal properties of a polymer are typically related to its structure, where those with higher aromatic content typically show more thermal stability than those with more aliphatic content [77]. It is also possible that adding a monomer with more aliphatic content than MMA could increase the fracture toughness [91]. By exploring the different comonomers available, the properties of the IPN system could be altered for different applications.

A wide variety of comonomers can easily be used in place of MMA in the current synthesis and are readily available. The aromatic monomer phenyl methacrylate has a T_g of approximately 127 °C when homopolymerized and could help increase the thermal stability of the thermoplastics [92]. Other aromatic monomers such as the lignin-derived methacrylate monomers syringyl methacrylate, vanillin methacrylate, guaiacol

methacrylate, cresol methacrylate, and 4-ethylguaiacol methacrylate have shown T_gs in the range of approximately 110-200 °C and were thermally stable to approximately 300 °C when homopolymerized. While these monomers are not currently commercially available, using a bio-based, aromatic comonomer would significantly increase the bio-based content and thermal properties of the thermoplastic polymers [78, 93].

In terms of aliphatic monomers, bio-based options are readily available. *N*-butyl acrylate is commercially available, can be produced from bio-based feedstocks, and contains an aliphatic, four-carbon chain that could provide the toughening effect needed [94]. Another aliphatic monomer, lauryl methacrylate, is derived from lauryl alcohol found in natural fatty acids and has a long 12-carbon chain. Lauryl methacrylate has been explored for its use as a reactive diluent in vinyl ester resins and may serve well to increase toughness through the long side chain. The low T_g of -65 °C could impact the overall thermal stability of the thermoplastic, but could be balanced with other aspects of a thermosetting resin formula if lauryl methacrylate provides a significant toughening effect [80]. Other bio-based monomers include furfuryl methacrylate (FM), made from the polysaccharide-derived furfuryl alcohol, glucose-6-acrylate-1,2,3,4-tetraacetate (GATA), a glucose-based monomer, and the commercially available isobornyl methacrylate (IBOMA), derived from the compound isoborneol found in several flower and tree species [80, 95-97]. The wide range of comonomers available expand the possibilities for the properties of the IPN system. A figure of the potential comonomers is shown in Figure 25.

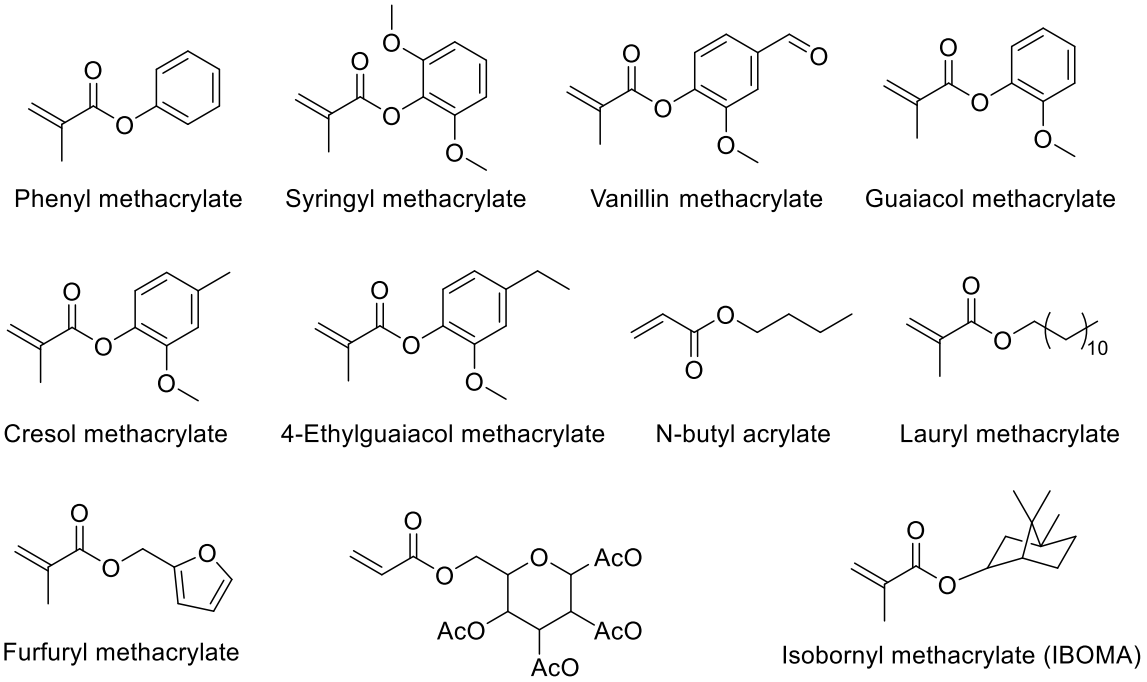

Figure 25. Potential comonomers for thermoplastic copolymers.

Homo- or copolymers of epoxy-functional monomers have many potential applications beyond their use as resin modifiers. The oxirane group allows for further post-polymerization modification including functionalization using amines, thiols, carboxylic acids, and water [12]. These types of modifications can be used to create complex polymer networks such as amphiphilic copolymers, star polymers, graft copolymers, and hydrogels [12, 98, 99]. Poly(GMA) and its copolymers have been used in many such network configurations; however, the use of aromatic epoxy-functional thermoplastics such as poly(VAEM) and poly(GDEM) could be used to enhance the thermal properties of these materials. The wide range of polymer structures allow poly(GMA) to be utilized in gene delivery, polymer scaffolds, self-healing materials, automotive coatings, protective finishes, and adhesives, among many other applications

[12, 13]. By using the aromatic epoxy-functional thermoplastics poly(VAEM) and poly(GDEM) as alternatives to poly(GMA), the applications of epoxy-functional thermoplastics can be further expanded.

References

[1] A. W. Bassett *et al.*, "Dual-functional, aromatic, epoxy-methacrylate monomers from bio-based feedstocks and their respective epoxy-functional thermoplastics," *Journal of Polymer Science,* 2020.

[2] R. Geyer, J. R. Jambeck, and K. L. Law, "Production, use, and fate of all plastics ever made," *Science Advances,* vol. 3, no. 7, 2017.

[3] M. N. Subramanian, *Polymer Blends and Composites: Chemistry and Technology*. Hoboken, NJ: John Wiley & Sons, Incorperated, 2017.

[4] J. A. Carioscia, J. W. Stansbury, and C. N. Bowman, "Evaluation and Control of Thiol-ene/Thiol-epoxy Hybrid Networks," *Polymer (Guildf),* vol. 48, no. 6, pp. 1526-1532, Mar 8 2007.

[5] L. H. Sperling, "Interpenetrating Polymer Networks - an Overview," (in English), *Interpenetrating Polymer Networks,* vol. 239, pp. 3-38, 1994.

[6] J. J. La Scala, J. A. Orlicki, C. Winston, E. J. Robinette, J. M. Sands, and G. R. Palmese, "The use of bimodal blends of vinyl ester monomers to improve resin processing and toughen polymer properties," (in English), *Polymer,* vol. 46, no. 9, pp. 2908-2921, Apr 15 2005.

[7] J. Kim, H. Oh, and E. Kim, "A dual-functional monomer having an epoxy and methacrylate group for holographic recording," *Journal of Materials Chemistry,* vol. 18, no. 40, 2008.

[8] M. Kumar, S. Mohanty, S. K. Nayak, and M. Rahail Parvaiz, "Effect of glycidyl methacrylate (GMA) on the thermal, mechanical and morphological property of biodegradable PLA/PBAT blend and its nanocomposites," *Bioresour Technol,* vol. 101, no. 21, pp. 8406-15, Nov 2010.

[9] (2018). *How is Glycidyl Methacrylate (GMA) used and what are the key benefits?* Available: https://dowac.custhelp.com/app/answers/detail/a_id/4249/~/gma---applications-and-benefits

[10] P. Jiang, Y. Shi, P. Liu, and Y. Cai, "Synthesis of well-defined glycidyl methacrylate based block copolymers with self-activation and self-initiation behaviors via ambient temperature atom transfer radical polymerization," *Journal of Polymer Science Part A: Polymer Chemistry*, vol. 45, no. 14, pp. 2947-2958, 2007.

[11] P. K. Kuroishi, M. J. Bennison, and A. P. Dove, "Synthesis and post-polymerisation modification of an epoxy-functional polycarbonate," *Polymer Chemistry*, vol. 7, no. 46, pp. 7108-7115, 2016.

[12] Ezzah M. Muzammil, A. Khan, and M. C. Stuparu, "Post-polymerization modification reactions of poly(glycidyl methacrylate)s," *RSC Advances*, vol. 7, no. 88, pp. 55874-55884, 2017.

[13] X. Luo, R. Ou, D. E. Eberly, A. Singhal, W. Viratyaporn, and P. T. Mather, "A thermoplastic/thermoset blend exhibiting thermal mending and reversible adhesion," *ACS Appl Mater Interfaces*, vol. 1, no. 3, pp. 612-20, Mar 2009.

[14] B. G. Harvey *et al.*, "Renewable thermosetting resins and thermoplastics from vanillin," *Green Chemistry*, vol. 17, no. 2, pp. 1249-1258, 2015.

[15] M. Fache, B. Boutevin, and S. Caillol, "Epoxy thermosets from model mixtures of the lignin-to-vanillin process," *Green Chemistry*, vol. 18, no. 3, pp. 712-725, 2016.

[16] E. D. Hernandez, A. W. Bassett, J. M. Sadler, J. J. La Scala, and J. F. Stanzione, III, "Synthesis and Characterization of Bio-based Epoxy Resins Derived from Vanillyl Alcohol," *ACS Sustainable Chemistry & Engineering*, vol. 4, no. 8, pp. 4328-4339, 2016.

[17] F. G. Calvo-Flores and J. A. Dobado, "Lignin as Renewable Raw Material," *ChemSusChem*, 10.1002/cssc.201000157 vol. 3, no. 11, pp. 1227-1235, 2010.

[18] T. S. Junko Hayashia, Shigeyoshi Deguchia, Qing Linb, Syunji Horiea, Shizuko Tsuchiyaa, Shingo Yanoa, Kazuo Watanabea, Fumio Ikegamia, "Phenolic compounds from Gastrodia rhizome and relaxant effects of related compounds on isolated smooth muscle preparation," *Phytochemistry*, vol. 59, pp. 513-519, 2001.

[19] S. Y. Huang, G. Q. Li, J. G. Shi, and S. Y. Mo, "Chemical constituents of the rhizomes of Coeloglossum viride var. bracteatum," *J Asian Nat Prod Res*, vol. 6, no. 1, pp. 49-61, Mar 2004.

[20] M. Fache, E. Darroman, V. Besse, R. Auvergne, S. Caillol, and B. Boutevin, "Vanillin, a promising biobased building-block for monomer synthesis," *Green Chem.*, vol. 16, no. 4, pp. 1987-1998, 2014.

[21] E. A. Baroncini, S. K. Yadav, G. R. Palmese, and J. F. Stanzione, III, "Recent advances in bio-based epoxy resins and bio-based epoxy curing agents," (in English), *Journal of Applied Polymer Science*, vol. 133, no. 45, Dec 5 2016.

[22] M. Biron, "Thermoplastics and Thermoplastic Composites (2nd Edition)," ed: Elsevier, 2013.

[23] Y. K. B. C. John Chiefari, Frances Ercole, Julia Krstina, Justine Jeffery, Tam P. T. Le, Roshan T. A. Mayadunne, Gordon F. Meijs, Ezio Rizzardo, San H. Thang, "Living Free-Radical Polymerization by Reversible Addition- Fragmentation Chain Transfer: The RAFT Process," *Macromolecules*, vol. 31, no. 16, pp. 5559-5562, 1998.

[24] A. B. L. Charles L. McCorkmic, "Aqueous RAFT Polymerization: Recent Developments in Synthesis of Functional Water-Soluble (Co)polymers with Controlled Structures," *Accounts of Chemical Research*, vol. 37, no. 5, pp. 312-325, 2004.

[25] D. J. Keddie, G. Moad, E. Rizzardo, and S. H. Thang, "RAFT Agent Design and Synthesis," *Macromolecules*, vol. 45, no. 13, pp. 5321-5342, 2012.

[26] G. Moad, Y. K. Chong, A. Postma, E. Rizzardo, and S. H. Thang, "Advances in RAFT polymerization: the synthesis of polymers with defined end-groups," *Polymer*, vol. 46, no. 19, pp. 8458-8468, 2005.

[27] S. Perrier, "50th Anniversary Perspective: RAFT Polymerization—A User Guide," *Macromolecules*, vol. 50, no. 19, pp. 7433-7447, 2017.

[28] R. J. Young and P. A. Lovell, *Introduction to Polymers*, Third Edition ed. Boca Raton, FL: Taylor & Francis Group, LLC, 2011.

[29] G. Moad, E. Rizzardo, and S. H. Thang. *A Micro Review of Reversible Addition/Fragmentation Chain Transfer (RAFT) Polymerization*. Available: https://www.sigmaaldrich.com/technical-documents/articles/crp-guide/micro-review-of-reversible-addition-fragmentation-chain-transfer-raft-polymerization.html

[30] W. Meiser, J. Barth, M. Buback, H. Kattner, and P. Vana, "EPR Measurement of Fragmentation Kinetics in Dithiobenzoate-Mediated RAFT Polymerization," *Macromolecules*, vol. 44, no. 8, pp. 2474-2480, 2011.

[31] G. Moad, "Mechanism and Kinetics of Dithiobenzoate-Mediated RAFT Polymerization - Status of the Dilemma," *Macromolecular Chemistry and Physics*, vol. 215, no. 1, pp. 9-26, 2014.

[32] B. Klumperman, E. T. van den Dungen, J. P. Heuts, and M. J. Monteiro, "RAFT-Mediated Polymerization-A Story of Incompatible Data?," *Macromol Rapid Commun*, vol. 31, no. 21, pp. 1846-62, Nov 1 2010.

[33] S. Thomas, C. Sinturel, and R. Thomas, *Micro and Nanostructured Epoxy/Rubber Blends*. John Wiley & Sons, Incorporated, 2014.

[34] I. Gibson, *Additive Manufacturing Technologies Rapid Prototyping to Direct Digital Manufacturing*. Boston, MA: Springer US, 2010.

[35] K. B. Manning *et al.*, "Self Assembly–Assisted Additive Manufacturing: Direct Ink Write 3D Printing of Epoxy–Amine Thermosets," *Macromolecular Materials and Engineering*, vol. 304, no. 3, p. 1800511, 2019/03/01 2019.

[36] T. J. Horn and O. L. A. Harrysson, "Overview of current additive manufacturing technologies and selected applications," (in English), *Science Progress*, vol. 95, no. 3, p. 255, Sep 2012

[37] R. Mezzenga, L. Boogh, and J.-A. E. Manson, "A Thermodynamic Model for Thermoset Polymer Blends with Reactive Modifiers," *Journal of Polymer Science: Part B: Polmer Physics*, vol. 38, pp. 1893-1902, 2000.

[38] M. Rico, J. Lopez, B. Montero, R. Bouza, and F. J. Diez, "Influence of the molecular weight of a modifier on the phase separation in an epoxy thermoset modified with a thermoplastic," *European Polymer Journal*, vol. 58, pp. 125-134, 2014.

[39] A. M. Tomuta, X. Fernandez-Francos, F. Ferrando, X. Ramis, and A. Serra, "Enhanced chemical reworkability of DGEBA thermosets cured with rare earth triflates using aromatic hyperbranched polyesters (HBP) and multiarm star HBP-b-poly(ε-caprolactone) as modifiers," *Polymers for Advanced Technologies*, vol. 24, pp. 962-970, 2013.

[40] E. S. Rodriguez, V. G. Falchi, L. Asaro, I. A. Zucchi, and R. J. J. Williams, "Toughening an epoxy network by the addition of an acrylic triblock copolymer and halloysite nanotubes," *Composites Communications*, vol. 12, pp. 86-90, 2019.

[41] L. H. Sperling and R. Hu, "Interpenetrating Polymer Networks," in *Polymer Blends Handbook*, L. A. Utracki and C. A. Wilkie, Eds. Dordrecht: Springer Netherlands, 2014, pp. 677-724.

[42] L. H. Sperling and V. Mishra, "The Current Status of Interpenetrating Polymer Networks," *Polymers for Advanced Technologies*, vol. 7, pp. 197-208, 1996.

[43] L. H. Sperling, *Interpenetrating Polymer Networks and Related Materials*. New York: Plenum Press, 1981.

[44] J. Parameswaranpillai, N. Hameed, J. Pionteck, and E. M. Woo, "Handbook of Epoxy Blends." Springer International Publishing, 2017, p.^pp. Pages.

[45] W. Rungswang, K. Kato, M. Kotaki, and S. Chirachanchai, "Size-controllable nanospheres prepared by blending a thermoset monomer in confined morphology with thermoplastic elastomer," *Polymer*, vol. 53, no. 6, pp. 1167-1171, 2012.

[46] Y. Zhang, R. Foos, K. Landfester, and A. Taden, "Themoset-thermoplastic hybrid nanoparticles and composite coatings," *Polymer*, vol. 55, no. 10, pp. 2305-2315, 2014.

[47] J. Lopez, C. Ramirez, M. J. Abrad, L. Barral, J. Cano, and F. J. Diez, "Blends of Acrylonitrile-Butadiene-Styrene with an Epoxy/Cycloaliphatic Amine Resin: Phase-Separation Behavior and Morphologies," *Journal of Applied Polymer Science*, vol. 85, pp. 1277-1286, 2002.

[48] I. A. Zucchi, M. J. Galante, and R. J. J. Williams, "Comparison of morphologies and mechanical properties of crosslinked epoxies modified by polystyrene and poly(methyl methacrylate)) or by the corresponding block copolymer polystyrene-b-poly(methyl methacrylate)," *Polymer,* vol. 46, pp. 2603-2609, 2005.

[49] M. J. Galante, P. A. Oyanguren, K. Andromaque, P. M. Frontini, and R. J. J. Williams, "Blends of epoxy/amine thermosets with a high-molar-mass poly(methyl methacrylate)," *Polymer International,* vol. 48, pp. 642-648, 1999.

[50] V. Rebizant, V. Abetz, F. Tournilhac, F. Court, and L. Leibler, "Reactive Tetrablock Copolymers Containing Glycidyl Methacrylate. Synthesis and Morphology Control in Epoxy-Amine Networks," *Macromolecules,* vol. 36, pp. 9889-9896, 2003.

[51] E. D. Becker, "A Breif History of Nuclear Magnetic Resonance," *Analytical Chemistry,* vol. 65, no. 6, 1993.

[52] M. Balci, *Basic 1H-13C-NMR Spectroscopy*, First edition ed. Amsterdam, The Netherlands: Elsevier B.V., 2005.

[53] K. Hashi *et al.*, "Achievement of 1020MHz NMR," *J Magn Reson,* vol. 256, pp. 30-33, Jul 2015.

[54] A. Prasad, *Imperial Technoscience: Transnational Histories of MRI in the United States, Britain, and India*. United States of America: MIT Press, 2014.

[55] S. Hirsch, J. Braun, and I. Sack, *Magnetic Resonance Elastography*. Germany: Wiley-VCH, 2017.

[56] A. M. Striegel, S. Fanali, P. R. Haddad, C. F. Poole, and M.-L. Riekkola, Eds. *Liquid Chromatography Fundamentals and Instrumentation*, Second Edition ed. Cambridge, MA, United States: Elsevier, 2017.

[57] J. C. Moore, "Gel Permeation Chromatography. I. A New Method for Molecular Weight Distribution of High Polymers," *Journal of Polymer Science Part A,* vol. 2, pp. 835-843, 1964.

[58] G. W. Ehrenstein, G. Riedel, and P. Trawiel, *Thermal Analysis of Plastics: Theory and Practice*. Cincinnati, Ohio: Hanser Gardner Publications, Inc., 2004.

[59] Q. Guo, *Polymer Morphology: Principles, Characterization, and Processing*. Hoboken, NJ, United States: John Wiley & Sons, Inc., 2016.

[60] O. J. Rees, *Fourier Transform Infrared Spectroscopy: Developments, Techniques and Applications*. New York: Nova Science Publishers, Inc, 2010.

[61] H. Wang, X.-Z. Yuan, and H. Li, *PEM Fuel Cell Durability Handbook*. Boca Raton, FL: CRC Press, 2012.

[62] P. R. Griffths, "Fourier Transform Infrared Spectrometry," *Science*, vol. 222, no. 4621, pp. 297-302, Oct. 21, 1983 1983.

[63] R. Clavier, *Characterization Analysis of Polymers*. Hoboken, New Jersey: John Wiley & Sons, 2008.

[64] V. Shah, *Handbook of Plastics Testing Technology*, Second Edition ed. John Wiley & Sons, Inc., 1998.

[65] I. M. McAninch, G. R. Palmese, J. L. Lenhart, and J. J. La Scala, "DMA testing of epoxy resins: The importance of dimensions," *Polymer Engineering & Science*, vol. 55, no. 12, pp. 2761-2774, 2015.

[66] *Standard Test Methods for Plane-Strain Fracture Toughness and Strain Energy Release Rate of Plastic Materials*, 2014.

[67] I. M. McAninch, J. J. La Scala, G. R. Palmese, and E. J. Robinette, "Thin film initiation of cracks for fracture toughness measurements in epoxy resins," *Journal of Applied Polymer Science*, vol. 134, no. 1, pp. 44364-44364, 2016.

[68] F. Hu, S. K. Yadav, J. J. La Scala, J. M. Sadler, and G. R. Palmese, "Preparation and Characterization of Fully Furan-Based Renewable Thermosetting Epoxy-Amine Systems," *Macromolecular Chemistry and Physics*, vol. 216, no. 13, pp. 1441-1446, 2015.

[69] F. R. Foulkes, *Physical Chemistry for Engineering and Applied Sciences*. Boca Raton, FL: CRC Press, 2013.

[70] A. W. Bassett, A. E. Honnig, J. J. La Scala, and J. F. Stanzione, III, "Network toughening of additively manufactured, high glass transition temperature materials via sequentially cured, interpenetrating polymers," *Polymer International,* vol. n/a, no. n/a, 2020.

[71] U. Ali, K. Juhanni Bt. Abd Karim, and N. A. Buang, "A Review of the Properties and Applications of Poly(Methyl Methacrylate) (PMMA)," *Polymer Reviews,* vol. 55, pp. 678-705, 2015.

[72] S. Ritzenthaler, E. Girard-Reydet, and J. P. Pascault, "Influence of epoxy hardener on miscibility of blends of poly(methyl methacrylate) and epoxy networks," *Polymer,* vol. 41, no. 16, pp. 6375-6386, 2000/07/01/ 2000.

[73] X. Fei, Y. Shi, and Y. Cao, "Synthesis of photosensitive poly(methyl methacrylate-co-glycidyl methacrylate) for optical waveguide devices," *Applied Physics A,* vol. 100, no. 2, pp. 409-414, 2010.

[74] J. Chiefari *et al.*, "Living free-radical polymerization by reversible addition-fragmentation chain transfer: The RAFT process," (in English), *Macromolecules,* vol. 31, no. 16, pp. 5559-5562, Aug 11 1998.

[75] D. T. Gentekos, L. N. Dupuis, and B. P. Fors, "Beyond Dispersity: Deterministic Control of Polymer Molecular Weight Distribution," (in English), *Journal of the American Chemical Society,* vol. 138, no. 6, pp. 1848-1851, Feb 17 2016.

[76] J. R. Fried, *Polymer Science & Technology*, Second Edition ed. Upper Saddle River, NJ: Pearson Education, Inc., 2003.

[77] B. G. Harvey *et al.*, "Synthesis and characterization of a renewable cyanate ester/polycarbonate network derived from eugenol," *Polymer,* vol. 55, no. 20, pp. 5073-5079, 2014.

[78] A. L. Holmberg, N. A. Nguyen, M. G. Karavolias, K. H. Reno, R. P. Wool, and T. H. Epps, "Softwood Lignin-Based Methacrylate Polymers with Tunable Thermal and Viscoelastic Properties," *Macromolecules,* vol. 49, no. 4, pp. 1286-1295, 2016.

[79] A. W. Bassett *et al.*, "Synthesis and characterization of molecularly hybrid bisphenols derived from lignin and CNSL: Application in thermosetting resins," *European Polymer Journal,* vol. 111, pp. 95-103, 2019/02/01/ 2019.

[80] S. Cousinet, A. Ghadban, E. Fleury, F. Lortie, J.-P. Pascault, and D. Portinha, "Toward replacement of styrene by bio-based methacrylates in unsaturated polyester resins," *European Polymer Journal*, vol. 67, pp. 539-550, 2015/06/01/ 2015.

[81] I. M. McAninch, G. R. Palmese, J. L. Lenhart, and J. J. La Scala, "Characterization of epoxies cured with bimodal blends of polyetheramines," *Journal of Applied Polymer Science*, vol. 130, no. 3, pp. 1621-1631, 2013/11/05 2013.

[82] N. S. Hmeidat, J. W. Kemp, and B. G. Compton, "High-strength epoxy nanocomposites for 3D printing," *Composites Science and Technology*, vol. 160, pp. 9-20, 2018/05/26/ 2018.

[83] X. Kuang, Z. Zhao, K. Chen, D. Fang, G. Kang, and H. J. Qi, "High-Speed 3D Printing of High-Performance Thermosetting Polymers via Two-Stage Curing," *Macromolecular Rapid Communications*, vol. 39, no. 7, p. 1700809, 2018/04/01 2018.

[84] M. G. B. Odom, C. B. Sweeney, D. Parviz, L. P. Sill, M. A. Saed, and M. J. Green, "Rapid curing and additive manufacturing of thermoset systems using scanning microwave heating of carbon nanotube/epoxy composites," *Carbon*, vol. 120, pp. 447-453, 2017/08/01/ 2017.

[85] A. Bassett, "Hybrid Monomers & Resins for High-Performance Thermosetting Polymers, Thermoplastics, & Additive Manufacturing," J. Stanzione, J. La Scala, J. Banning, K. Dahm, and F. Haas, Eds., ed: ProQuest Dissertations Publishing, 2020.

[86] M. G. Prolongo, C. Arribas, C. Salom, and R. M. Masegosa, "Dynamic Mechanical Properties and Morphology of Poly(benzyl methacrylate)/Epoxy Thermoset Blends," *Polymer Engineering & Science*, vol. 50, no. 9, pp. 1820-1830, 2010.

[87] J. H. Hodgkin, G. P. Simon, and R. J. Varley, "Thermoplastic Toughening of Epoxy Resins: A Critical Review," *Polymers for Advanced Technologies*, vol. 9, pp. 3-10, 1998.

[88] M. Naguib *et al.*, "Non-reactive and reactive block copolymers for toughening of UV-cured epoxy coating," *Progress in Organic Coatings*, vol. 85, pp. 178-188, 2015.

[89] Y. Lui, "Polymerization-Induced Phase Separation and Resulting Thermomechanical Properties of Thermosetting/Reactive Nonlinear Polymer Blends: A Review," *Journal of Applied Polymer Science,* vol. 127, no. 5, pp. 3279-3292, 2013.

[90] S. Thomas *et al.*, *Micro- and Nano-structured Interpenetrating Polymer Networks: From Design to Applications*. Hoboken, NJ: John Wiley & Sons Inc., 2016.

[91] T. Liu, Y. Nie, L. Zhang, R. Chen, Y. Meng, and X. Li, "Dependence of epoxy toughness on the backbone structure of hyperbranched polyether modifiers," *RSC Advances,* vol. 5, pp. 3408-3416, 2014.

[92] S. C. Pilcher and W. T. Ford, "Poly(phenyl methacrylate) and poly(1-naphthyl methacrylate) prepared in microemulsions," *Journal of Polymer Science Part A: Polymer Chemistry,* vol. 39, no. 4, pp. 519-524, 2001/02/15 2001.

[93] A. L. Holmberg, K. H. Reno, N. A. Nguyen, R. P. Wool, and T. H. Epps, 3rd, "Syringyl Methacrylate, a Hardwood Lignin-Based Monomer for High-Tg Polymeric Materials," *ACS Macro Lett,* vol. 5, no. 5, pp. 574-578, May 17 2016.

[94] A. Niesbach, N. Fink, P. Lutze, and A. Górak, "Design of reactive distillation processes for the production of butyl acrylate: Impact of bio-based raw materials," *Chinese Journal of Chemical Engineering,* vol. 23, no. 11, pp. 1840-1850, 2015/11/01/ 2015.

[95] K. C. Wong, K. S. Ong, and C. L. Lim, "Compositon of the essential oil of rhizomes of kaempferia galanga L," *Flavour and Fragrance Journal,* vol. 7, no. 5, pp. 263-266, 1992/10/01 1992.

[96] S. K. Yadav, K. M. Schmalbach, E. Kinaci, J. F. Stanzione, and G. R. Palmese, "Recent advances in plant-based vinyl ester resins and reactive diluents," *European Polymer Journal,* vol. 98, pp. 199-215, 2018/01/01/ 2018.

[97] M. Nasiri and T. M. Reineke, "Sustainable glucose-based block copolymers exhibit elastomeric and adhesive behavior," *Polymer Chemistry,* 10.1039/C6PY00700G vol. 7, no. 33, pp. 5233-5240, 2016.

[98] N. V. Tsarevsky, S. A. Bencherif, and K. Matyjaszewski, "Graft Copolymers by a Combination of ATRP and Two Different Consecutive Click Reactions," *Macromolecules*, vol. 40, no. 13, pp. 4439-4445, 2007/06/01 2007.

[99] N. Orakdogen and B. Sanay, "Poly(Hydroxypropyl methacrylate-co-glycidyl methacrylate): Facile synthesis of well-defined hydrophobic gels containing hydroxy-functional methacrylates," *Polymer Degradation and Stability*, vol. 144, pp. 251-263, 2017/10/01/ 2017.

Appendix A

^{1}H-NMR Spectra

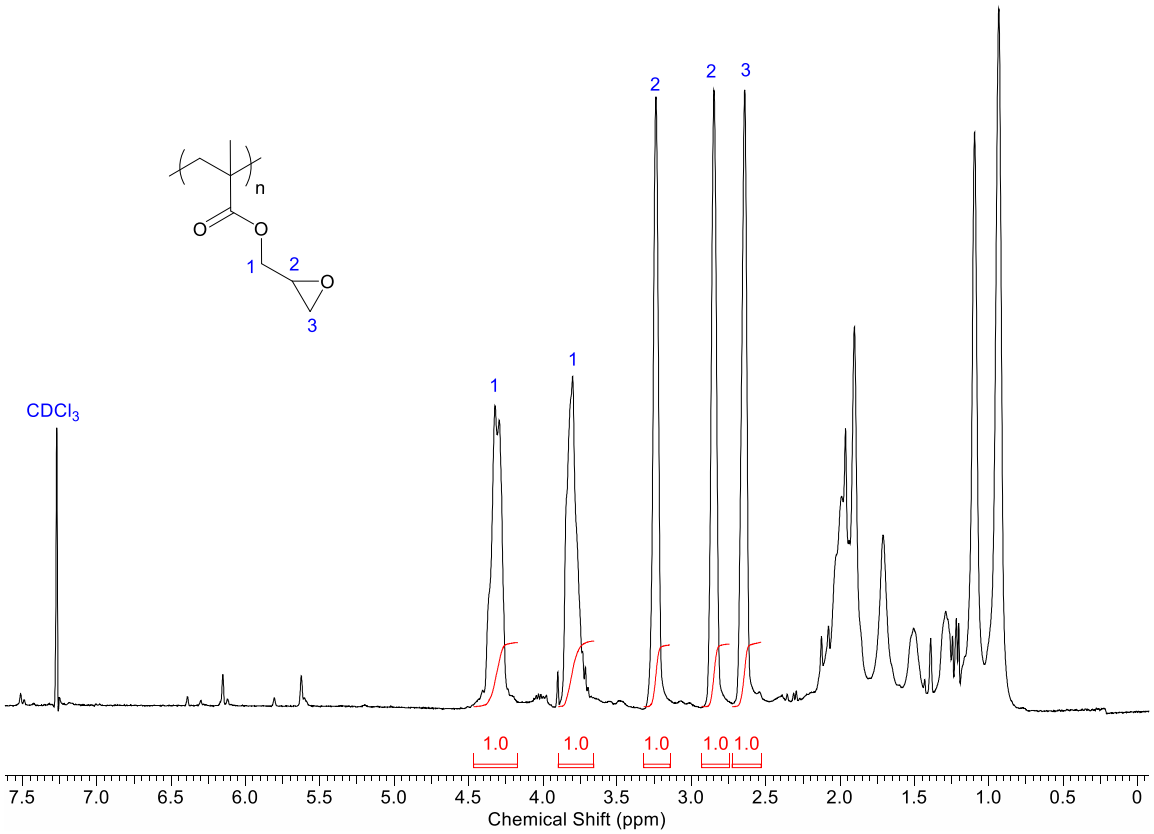

Figure A1. ^{1}H-NMR spectrum with partial peak assignments and associated integrations for poly(glycidyl methacrylate) (poly(GMA)). Unidentified peaks correspond to the polymer backbone.

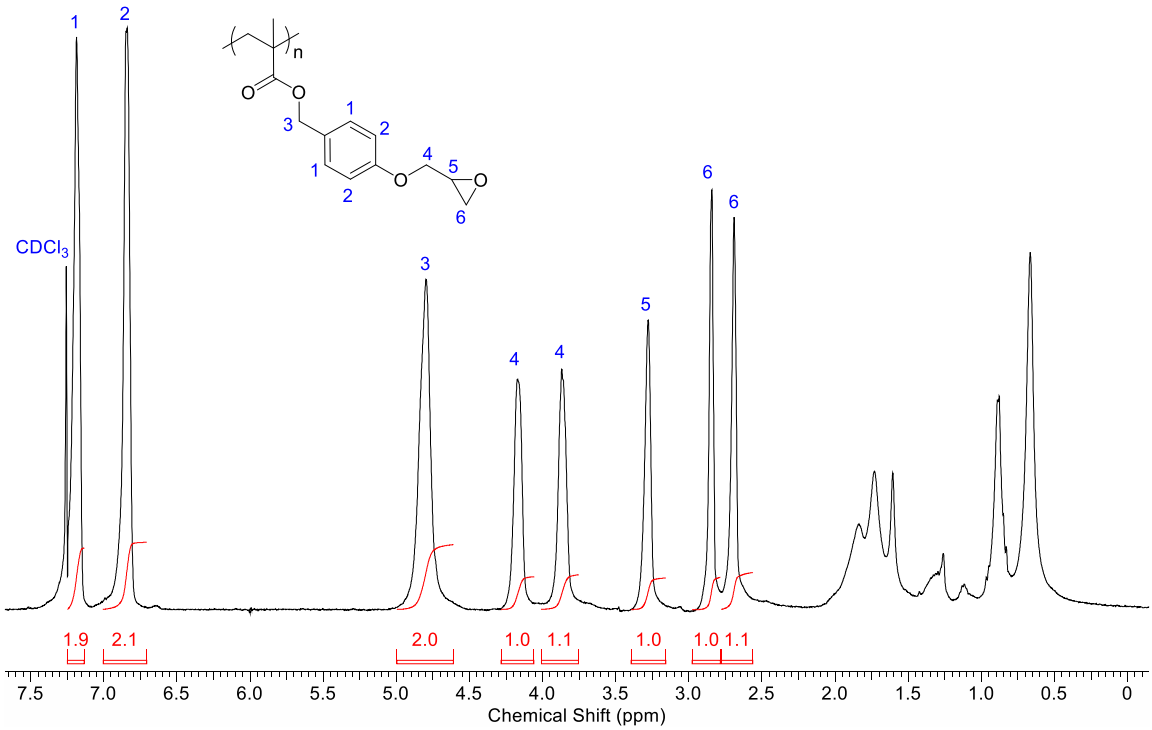

Figure A2. ^{1}H-NMR spectrum with partial peak assignments and associated integrations for poly(gastrodigenin epoxy-methacrylate) (poly(GDEM)). Unidentified peaks correspond to the polymer backbone.

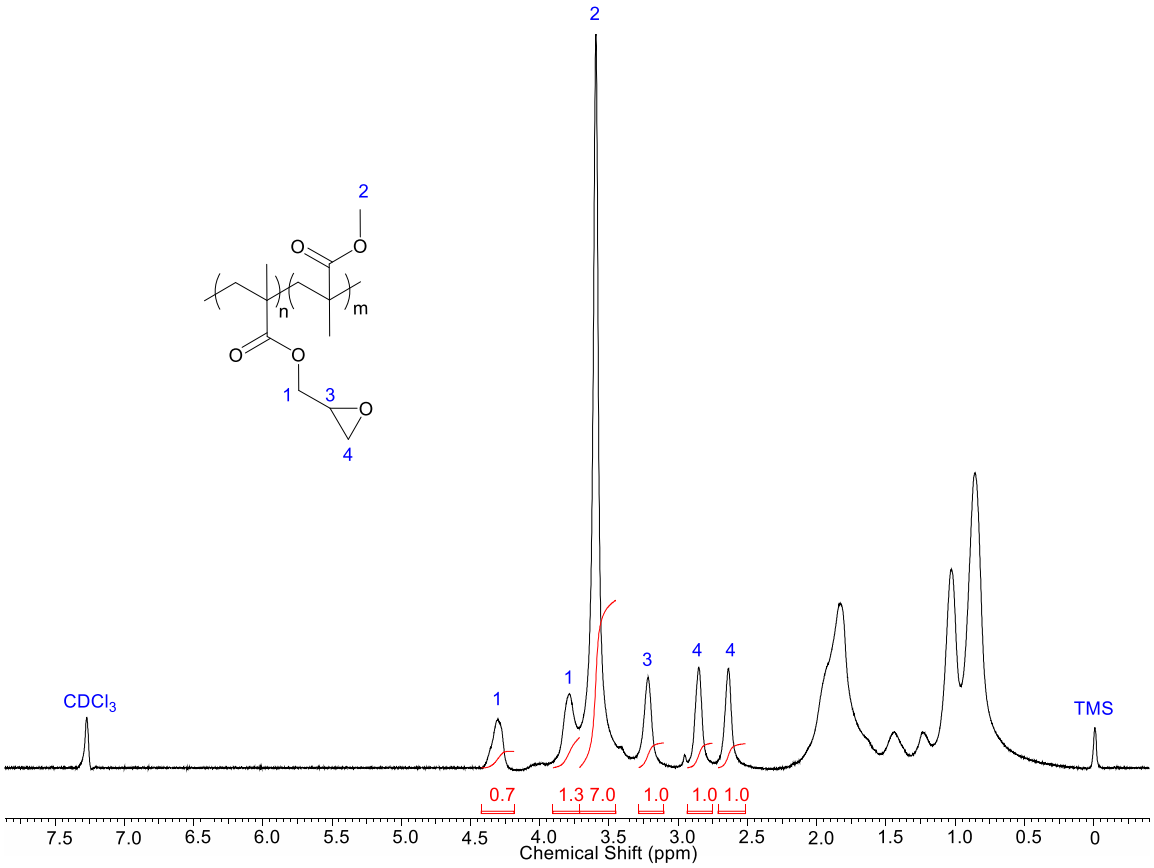

Figure A3. ^{1}H-NMR spectrum with partial peak assignments and associated integrations for poly(glycidyl methacrylate-co-methyl methacrylate) 30:70 (poly(GMA-co-MMA)). Unidentified peaks correspond to the polymer backbone.

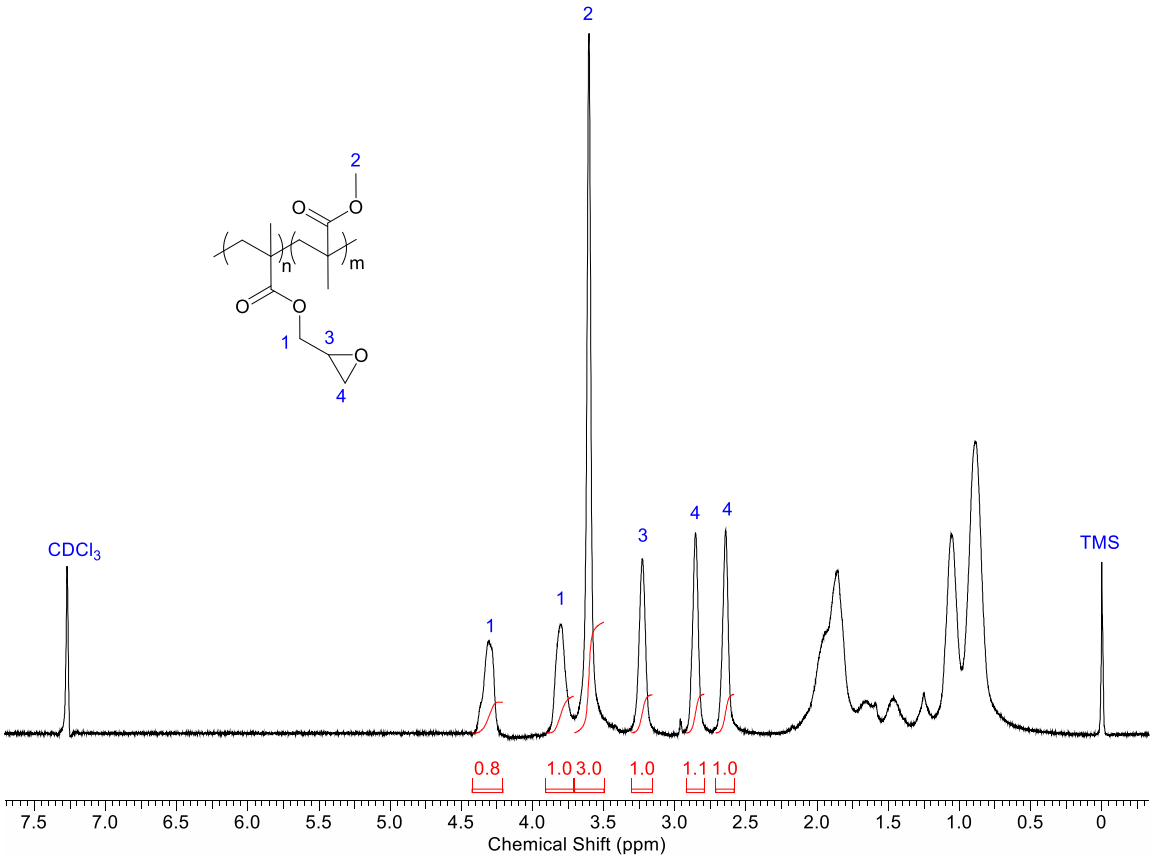

Figure A4. ^{1}H-NMR spectrum with partial peak assignments and associated integrations for poly(glycidyl methacrylate-co-methyl methacrylate) 50:50 (poly(GMA-co-MMA)). Unidentified peaks correspond to the polymer backbone.

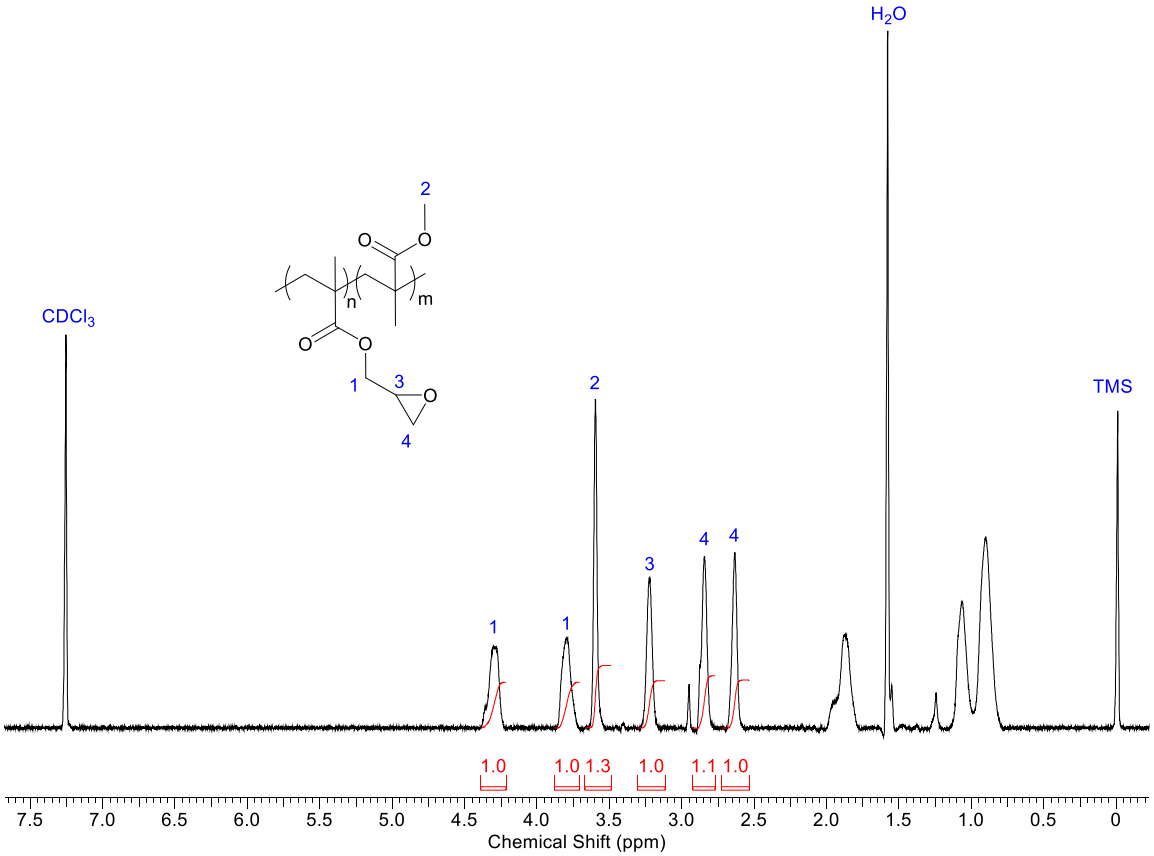

Figure A5. ^{1}H-NMR spectrum with partial peak assignments and associated integrations for poly(glycidyl methacrylate-co-methyl methacrylate) 70:30 (poly(GMA-co-MMA)). Unidentified peaks correspond to the polymer backbone.

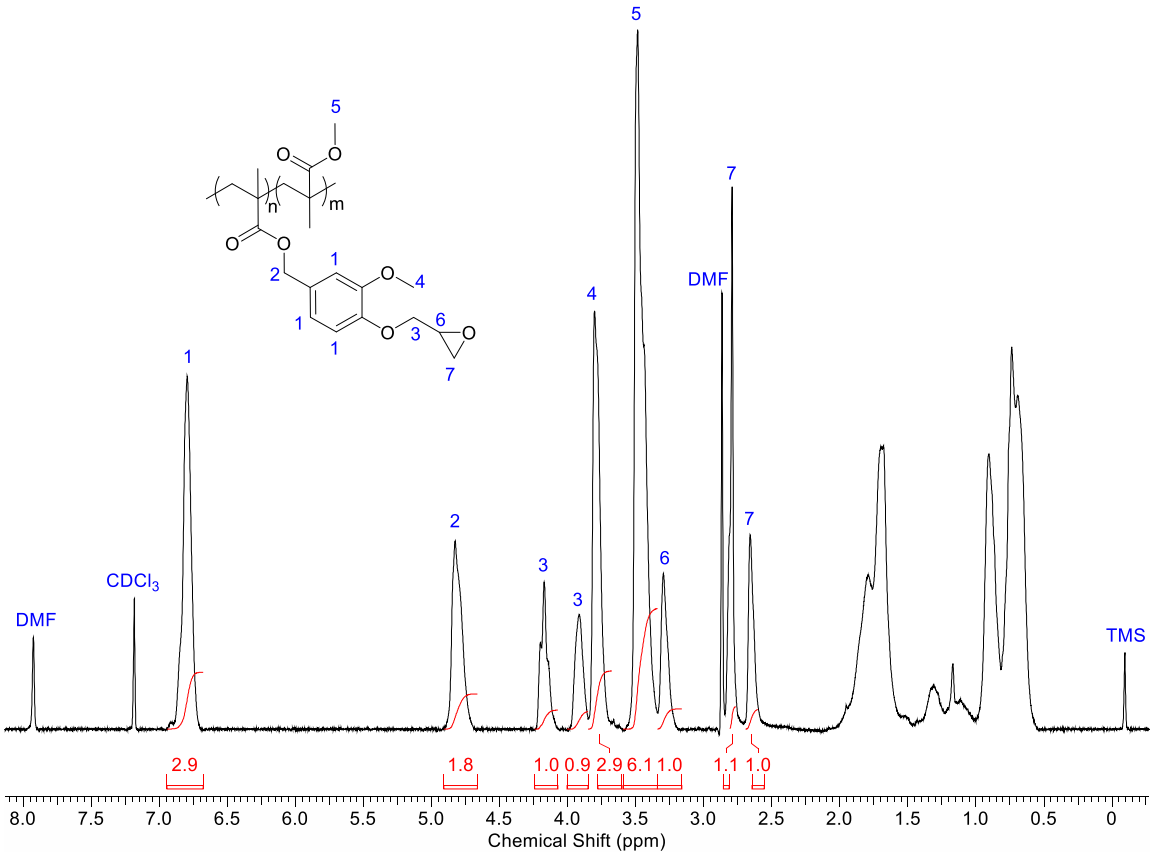

Figure A6. ^{1}H-NMR spectrum with partial peak assignments and associated integrations for poly(vanillyl alcohol epoxy-methacrylate-co-methyl methacrylate) 50:50 (poly(VAEM-co-MMA)). Unidentified peaks correspond to the polymer backbone.

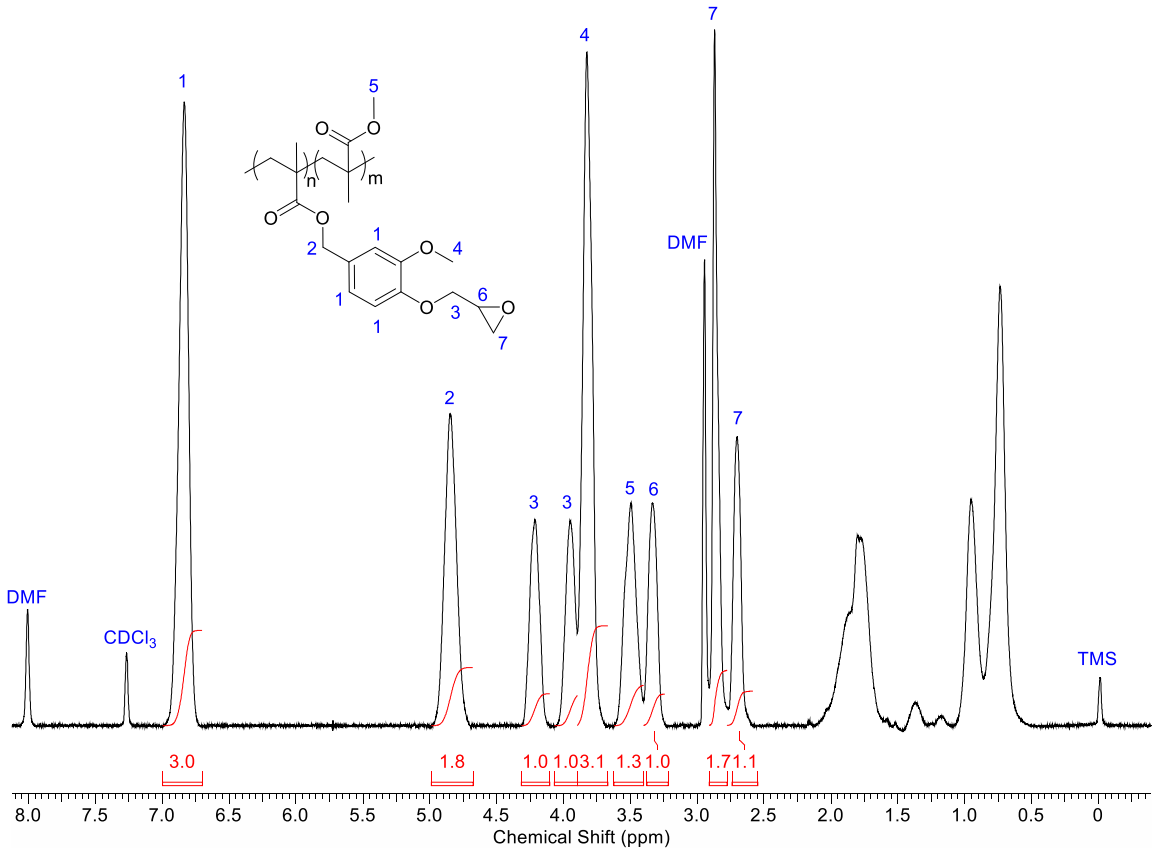

Figure A7. ^{1}H-NMR spectrum with partial peak assignments and associated integrations for poly(vanillyl alcohol epoxy-methacrylate-co-methyl methacrylate) 70:30 (poly(VAEM-co-MMA)). Unidentified peaks correspond to the polymer backbone.

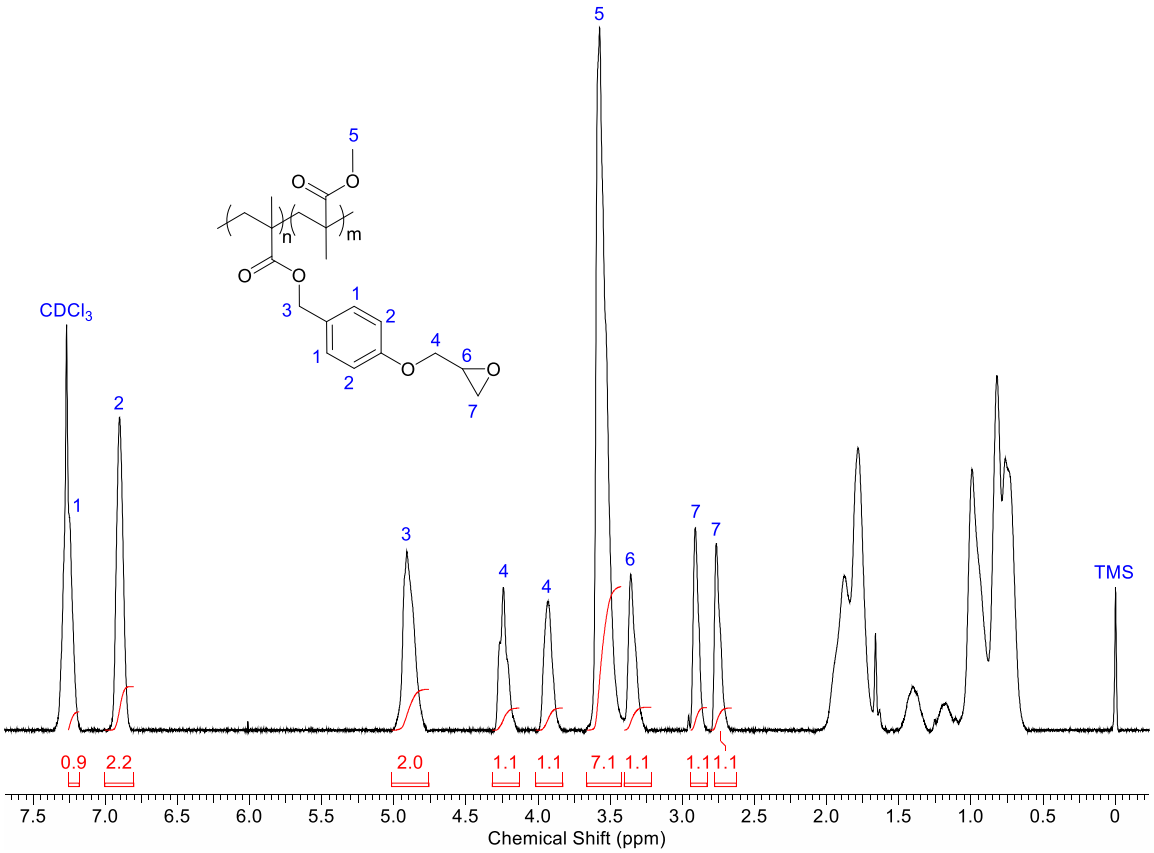

Figure A8. ^{1}H-NMR spectrum with partial peak assignments and associated integrations for poly(gastrodigenin epoxy-methacrylate-co-methyl methacrylate) 30:70 (poly(GDEM-co-MMA)). Unidentified peaks correspond to the polymer backbone.

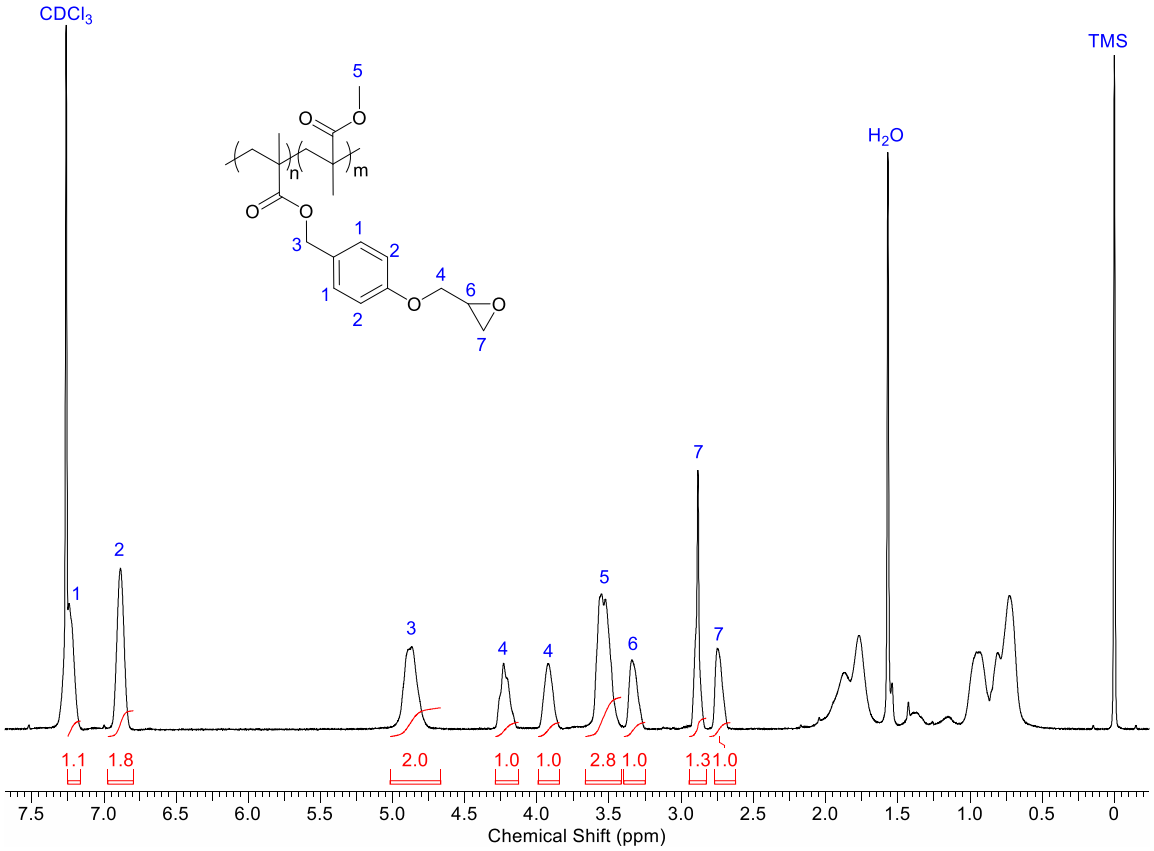

Figure A9. ^{1}H-NMR spectrum with partial peak assignments and associated integrations for poly(gastrodigenin epoxy-methacrylate-co-methyl methacrylate) 50:50 (poly(GDEM-co-MMA)). Unidentified peaks correspond to the polymer backbone.

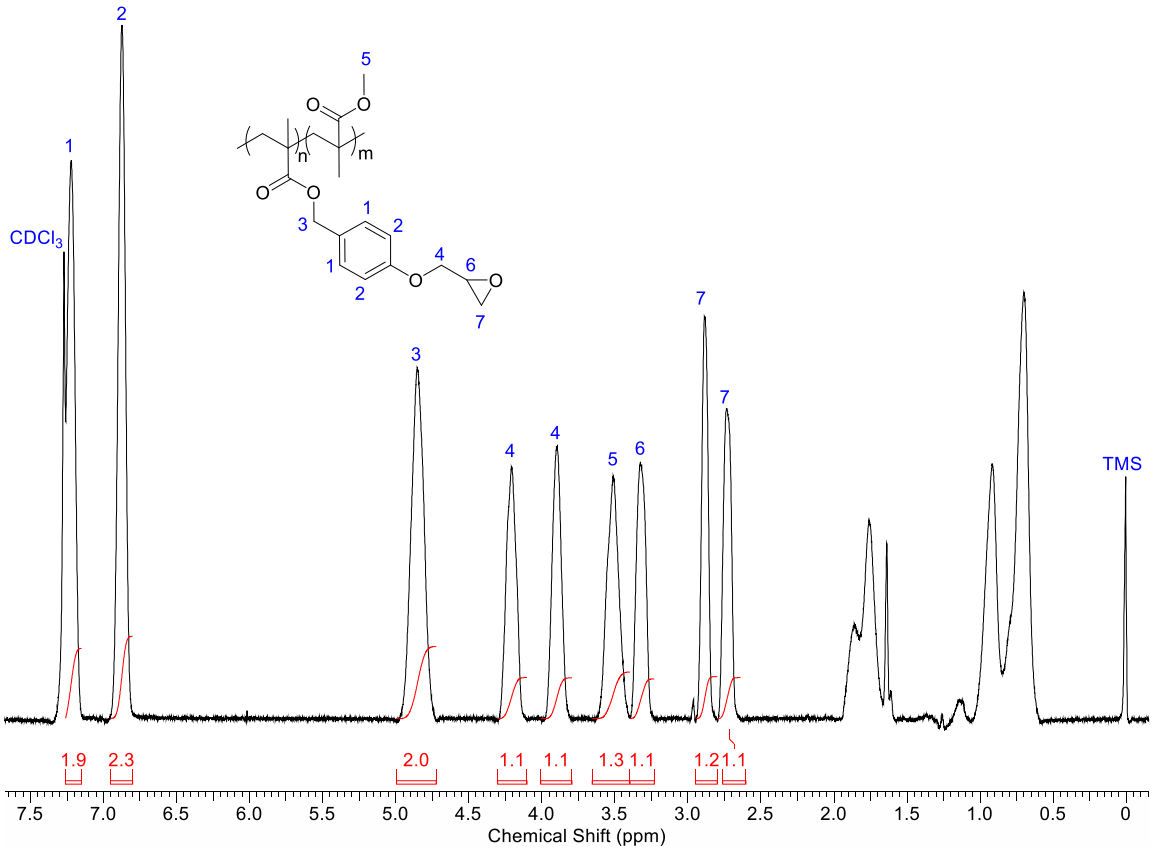

Figure A10. ^{1}H-NMR spectrum with partial peak assignments and associated integrations for poly(gastrodigenin epoxy-methacrylate-co-methyl methacrylate) 70:30 (poly(GDEM-co-MMA)). Unidentified peaks correspond to the polymer backbone.

Appendix B

TGA Thermograms

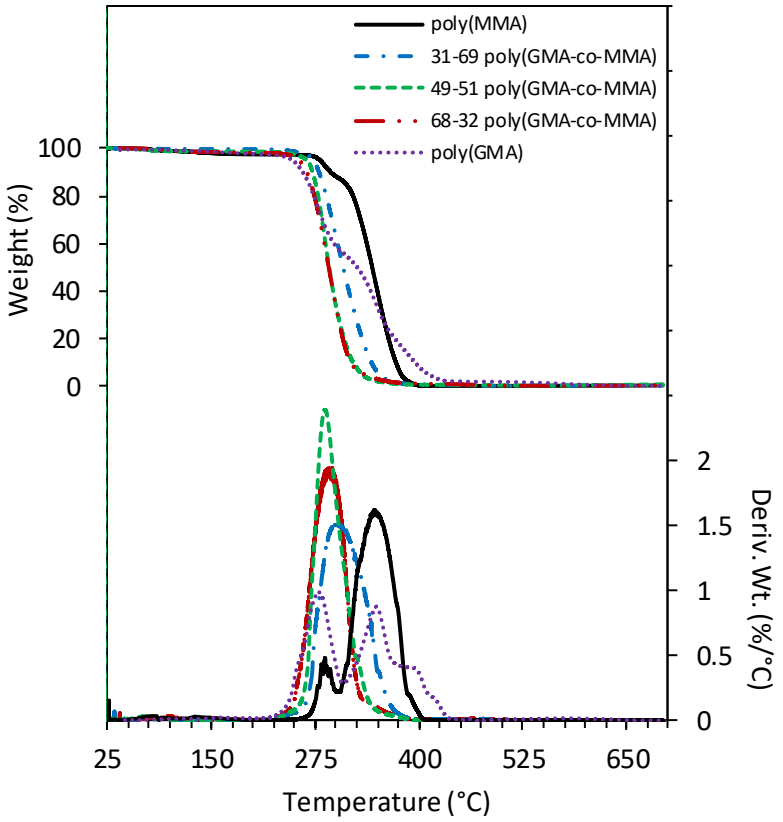

Figure B1. Representative TGA thermograms and the respective first derivatives of poly(GMA), poly(MMA), and their respective copolymers in air.

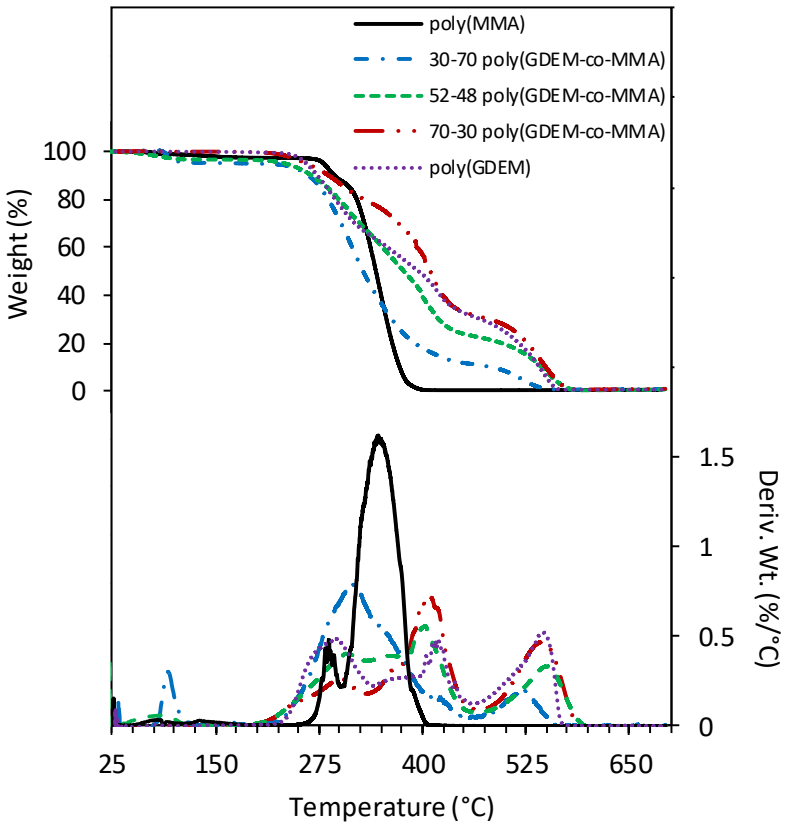

Figure B2. Representative TGA thermograms and the respective first derivatives of poly(GDEM), poly(MMA), and their respective copolymers in air.

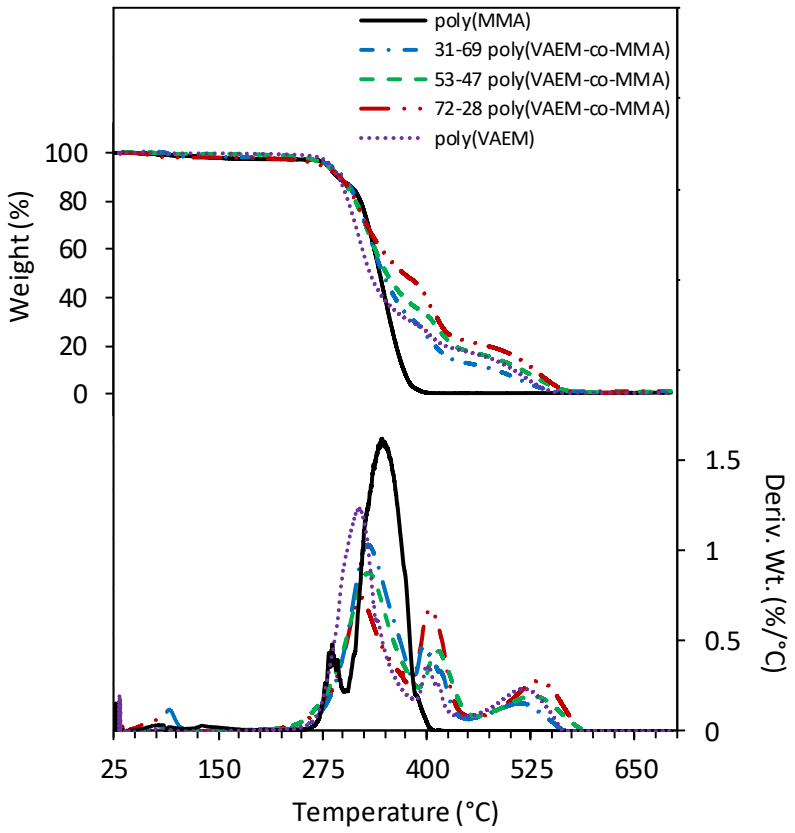

Figure B3. Representative TGA thermograms and the respective first derivatives of poly(VAEM), poly(MMA), and their respective copolymers in air.

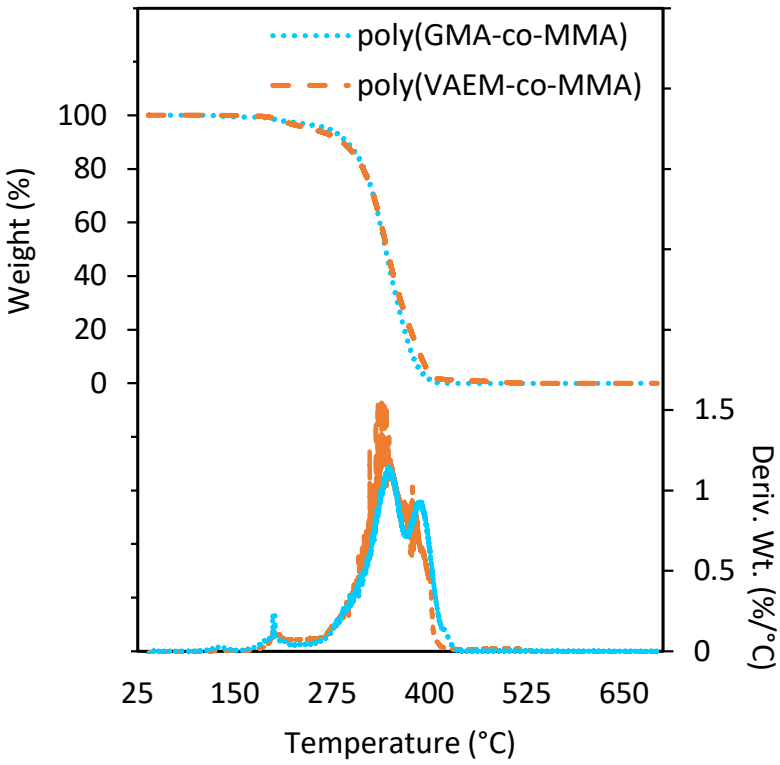

Figure B4. Representative TGA thermograms and the respective first derivatives of the RAFT polymerized thermoplastics in air.

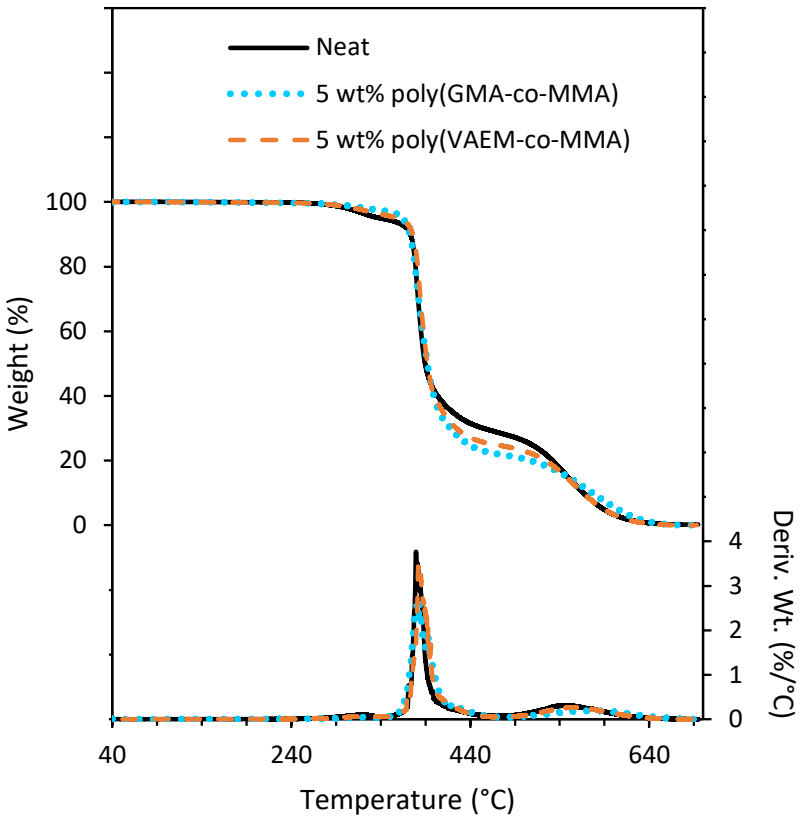

Figure B5. Representative TGA thermograms and the respective first derivatives of the cured thermosetting resins in air.

Appendix C

APC Chromatograms

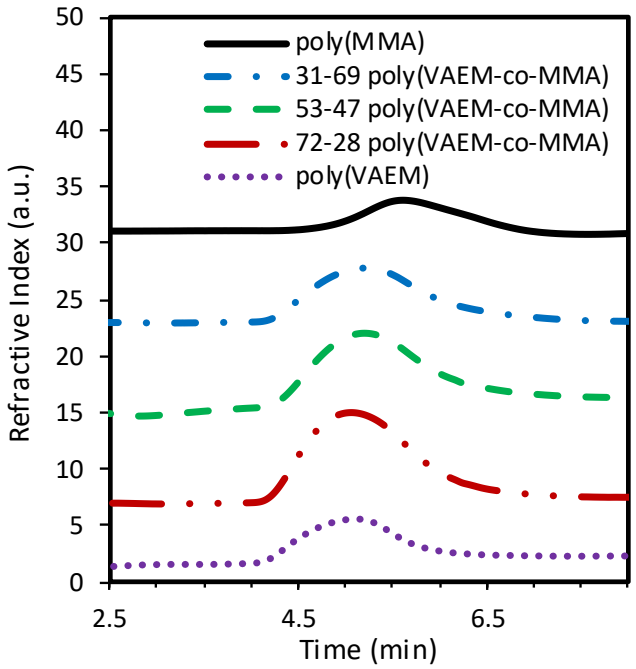

Figure C1. APC chromatograms of poly(VAEM), poly(MMA), and their respective copolymers. Vertically offset for clarity.

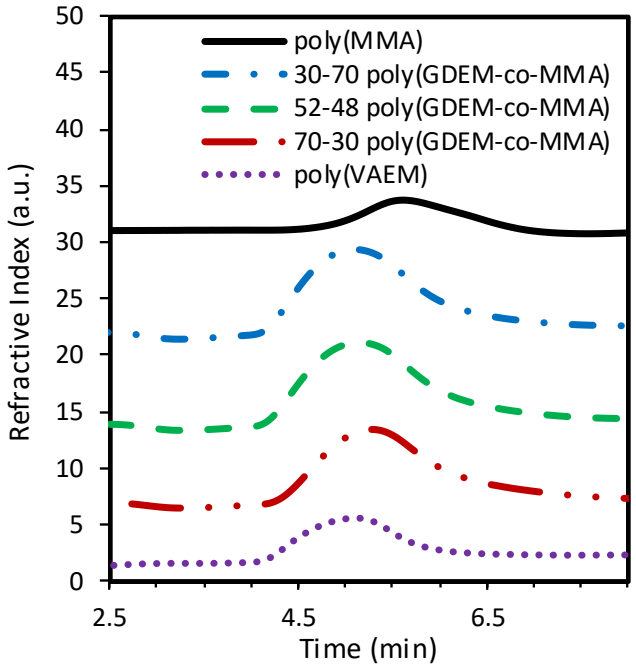

Figure C2. APC chromatograms of poly(GDEM), poly(MMA), and their respective copolymers. Vertically offset for clarity.

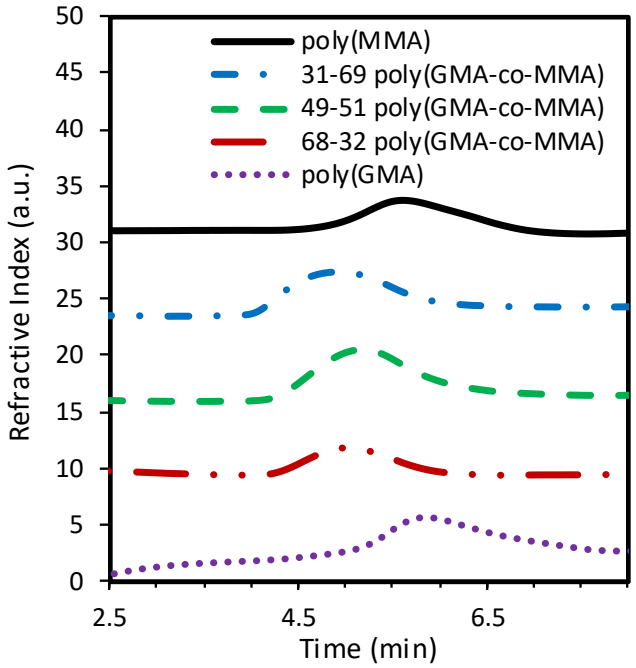

Figure C3. APC chromatograms of poly(GMA), poly(MMA), and their respective copolymers. Vertically offset for clarity.

Appendix D

DSC Thermograms

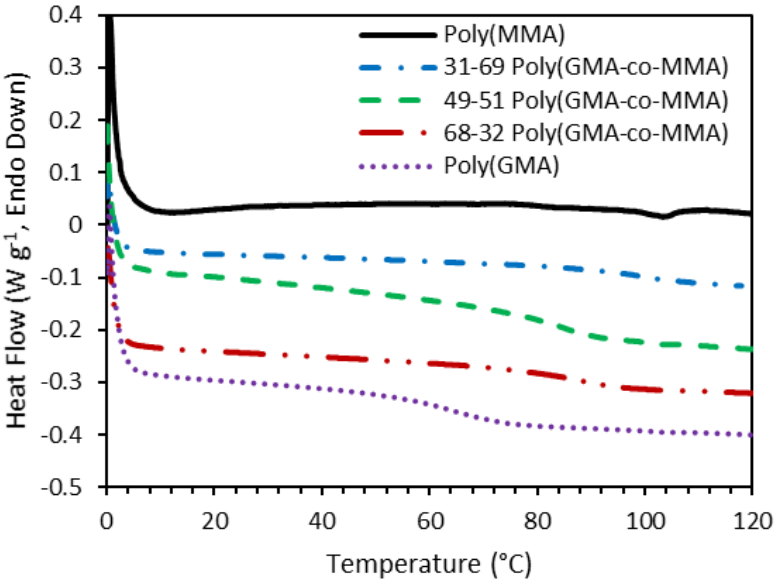

Figure D1. Representative DSC chromatograms of poly(GMA), poly(MMA), and their respective copolymers. Vertically offset for clarity.

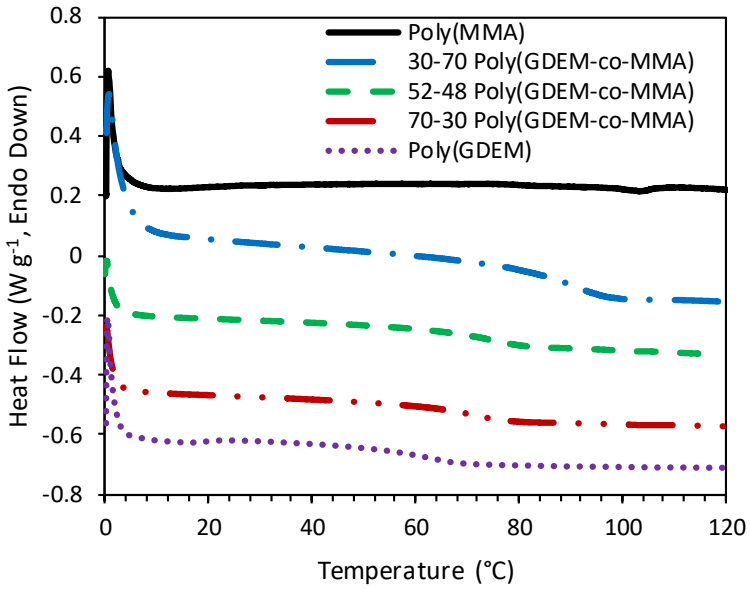

Figure D2. Representative DSC chromatograms of poly(GDEM), poly(MMA), and their respective copolymers. Vertically offset for clarity.

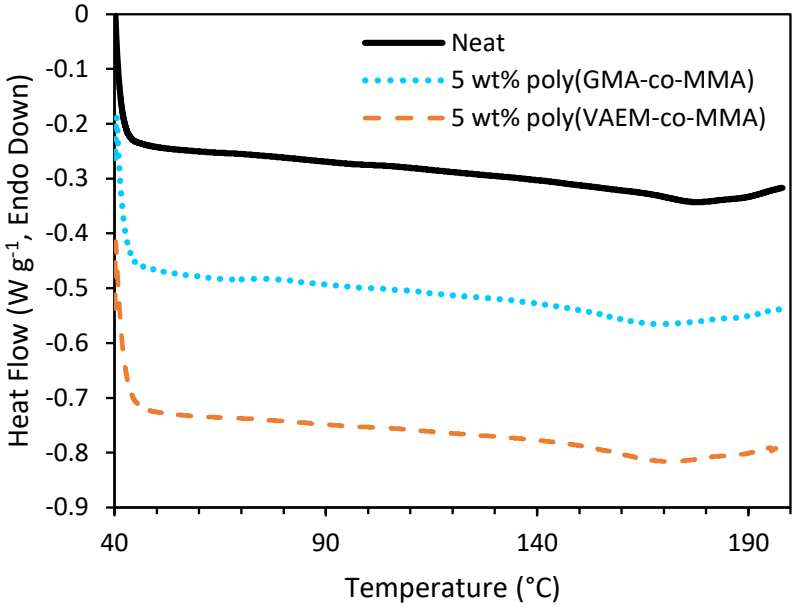

Figure D3. Representative DSC thermograms of the thermosetting polymers loaded with the thermoplastic copolymers. Vertically offset for clarity.

Appendix E

Near-IR Spectra

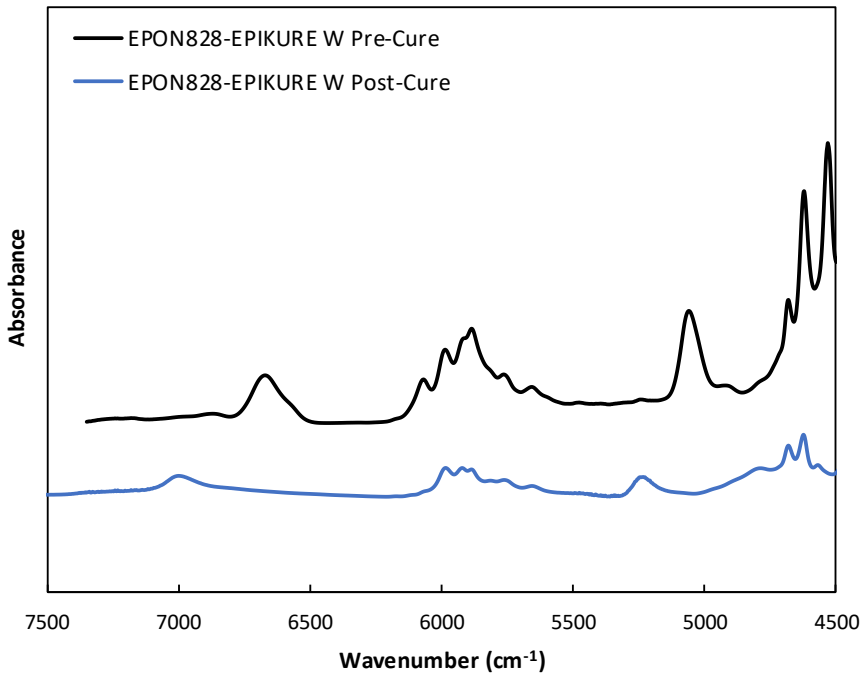

Figure E1. Representative near-IR spectrum of EPON828-EPIKURE W neat resin pre- and post-cure. Vertically offset for clarity.

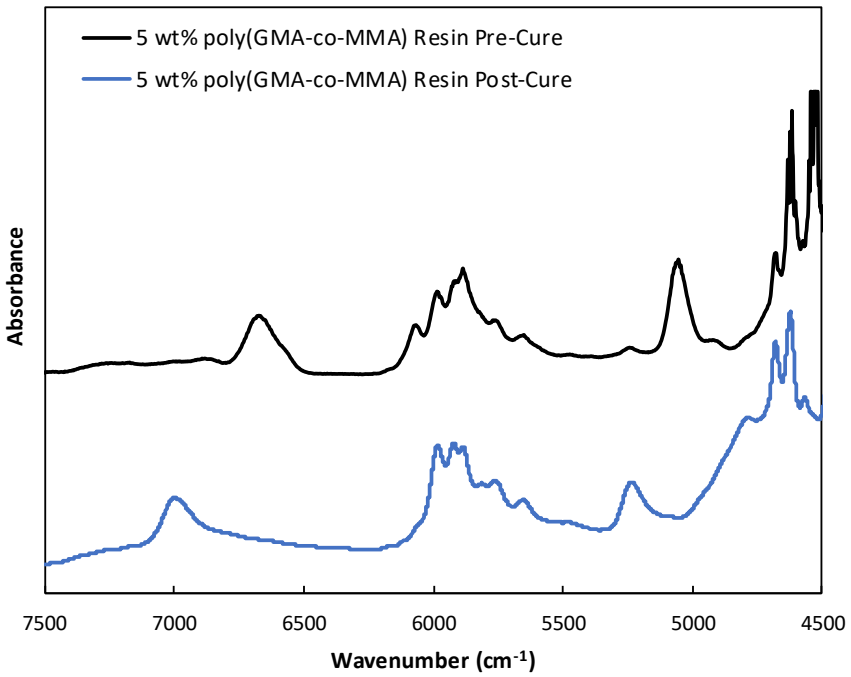

Figure E2. Representative near-IR spectrum of poly(GMA-co-MMA) loaded EPON828-EPIKURE W resin pre- and post-cure. Vertically offset for clarity.

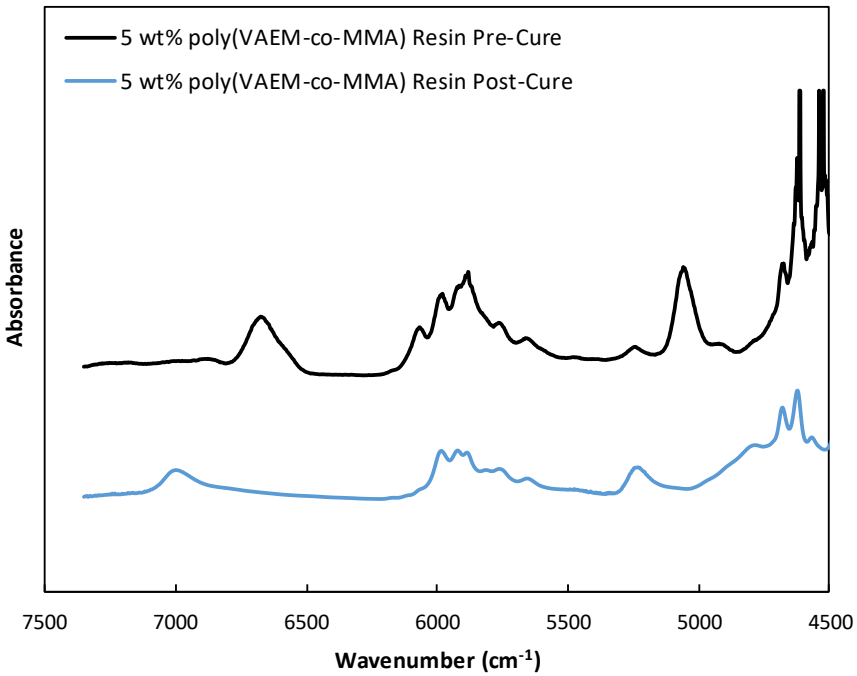

Figure E3. Representative near-IR spectrum of poly(VAEM-co-MMA) loaded EPON828-EPIKURE W resin pre- and post-cure. Vertically offset for clarity.

Appendix F

List of Acronyms, Abbreviations, and Symbols

3D printing	Three-dimensional printing
ABCP	AB-crosslinked polymers
AHEW	Amine hydrogen equivalent weight
AM	Additive manufacturing
APC	Advanced polymer chromatography
ATRP	Atom transfer radical polymerization
CT	Compact tension
CTA	Chain transfer agent
Đ	Dispersity
DCM	Dichloromethane
DGEBA	Diglycidyl ether of bisphenol A
DMA	Dynamic mechanical analysis
DMF	*N*,*N*-Dimethylformamide
DSC	Differential scanning calorimetry
E′	Storage modulus
E″	Loss modulus
EEW	Epoxy equivalent weight
FT-IR	Fourier transform-infrared
G_{1C}	Critical strain energy release rate
GD	Gastrodigenin
GDEM	Gastrodigenin epoxy-methacrylate

GFC	Gel filtration chromatography
GMA	Glycidyl methacrylate
GPC	Gel permeation chromatography
IDT	Initial decomposition temperature at 5% weight loss
IPN	Interpenetrating polymer network
K_{1C}	Critical-stress-intensity factor
LAM	Less activated monomers
M_c	Molecular weight between crosslinks
M_n	Number average molecular weight
M_w	Weight average molecular weight
M_z	Z average molecular weight
MAM	More activated monomers
MMA	Methyl methacrylate
MRI	Magnetic resonance imaging
N_2	Nitrogen
Near-IR	Near-infrared
NMR	Nuclear magnetic resonance
NMP	Nitroxide mediated polymerization
PIPS	Polymerization induced phase separation
RAFT	Reversible addition-fragmentation chain transfer
RDRP	Reversible-deactivation radical polymerizations
SIN	Simultaneous interpenetrating networks
SEC	Size exclusion chromatography

SENB	Single edge notched bend
$T_{5\%}$	Temperature at 5% weight loss
$T_{50\%}$	Temperature at 50% weight loss
T_g	Glass transition temperature
T_m	Melting temperature
T_{max}	Temperature at maximum decomposition rate
Tan δ	Tan delta
TEA	Triethylamine
TEBAC	Benzyltriethylammonium chloride
TGA	Thermogravimetric analysis
TGAP	Triglycidyl p-aminophenol
TGDDM	Tetraglycidyl diamino diphenyl methane
THF	Tetrahydrofuran
TMS	Tetramethylsilane
UV	Ultra violet
VA	Vanillyl alcohol
VAEM	Vanillyl alcohol epoxy-methacrylate
ρ	Density

Appendix G

Licensing Agreement

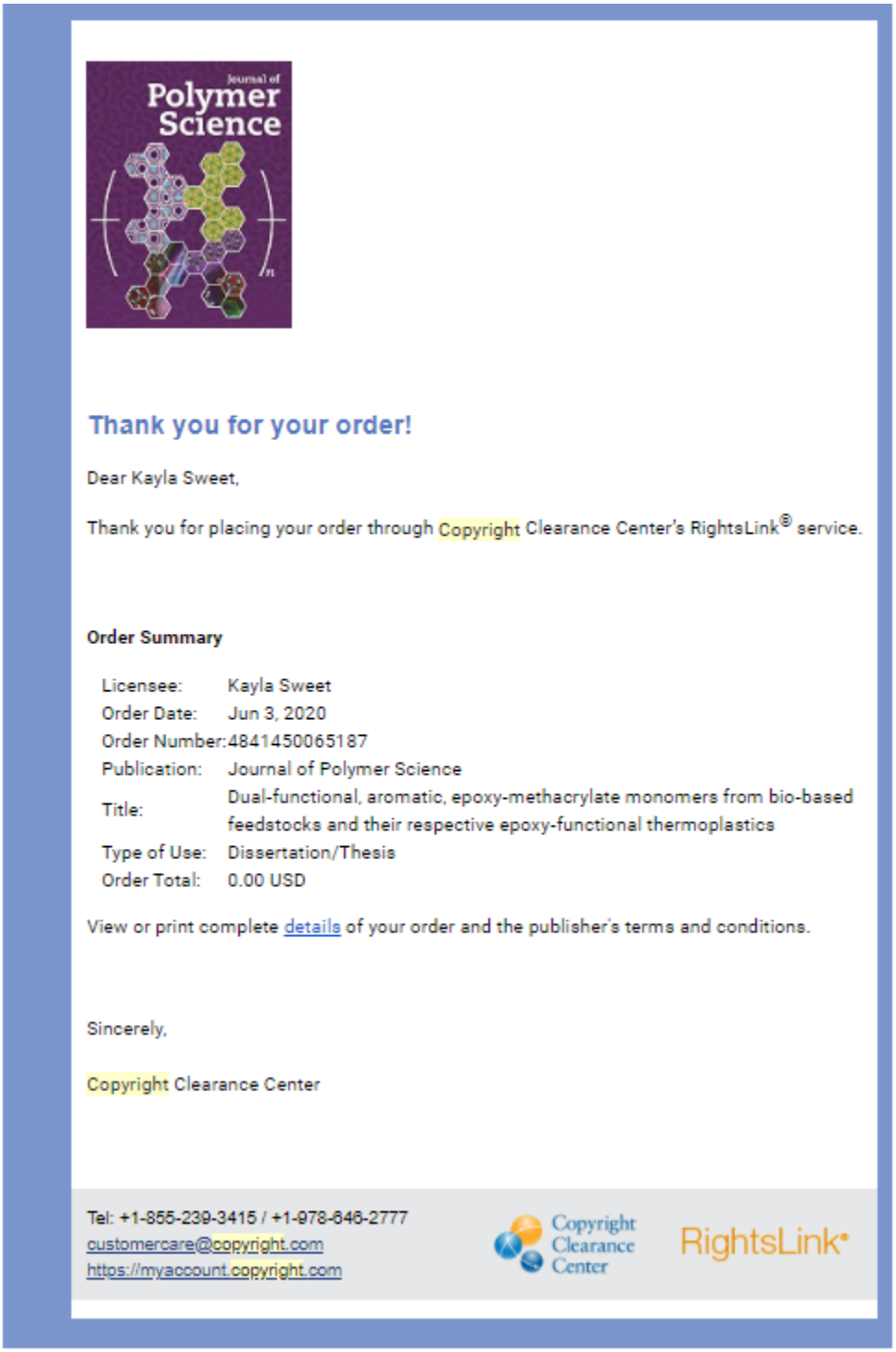

Thank you for your order!

Dear Kayla Sweet,

Thank you for placing your order through Copyright Clearance Center's RightsLink® service.

Order Summary

Licensee:	Kayla Sweet
Order Date:	Jun 3, 2020
Order Number:	4841450065187
Publication:	Journal of Polymer Science
Title:	Dual-functional, aromatic, epoxy-methacrylate monomers from bio-based feedstocks and their respective epoxy-functional thermoplastics
Type of Use:	Dissertation/Thesis
Order Total:	0.00 USD

View or print complete details of your order and the publisher's terms and conditions.

Sincerely,

Copyright Clearance Center

Tel: +1-855-239-3415 / +1-978-646-2777
customercare@copyright.com
https://myaccount.copyright.com

Copyright Clearance Center RightsLink®